Alma Mater Studiorum · Università di Bologna

Dipartimento di Fisica e Astronomia "Augusto Righi"
Corso di Laurea in Fisica

Path-Integral Molecular Dynamics using machine learned potentials for hydrogen diffusion

Relatore:
Prof. Cesare Franchini

Correlatore:
MSc. Luca Leoni

Presentata da:
Federico Mastroforti

Anno Accademico 2024/2025

Abstract

La maggior parte delle simulazioni atomistiche tratta i nuclei come particelle classiche che seguono le equazioni di Hamilton e rispettano la statistica di Boltzmann, poiché è impraticabile risolvere l'equazione di Schrödinger nucleare anche in approssimazione di Born–Oppenheimer. Questa semplificazione fallisce però nei sistemi contenenti idrogeno, anche a temperatura ambiente, dove i nuclei leggeri manifestano zero-point motion, tunneling e altri effetti quantistici.

In questa tesi adottiamo il formalismo path-integral in tempo immaginario, che mappa esattamente i nuclei quantistici su ring-polymer classici, consentendo di includere rigorosamente gli effetti quantistici nucleari (NQEs) in simulazioni di fasi condensate. Dopo aver introdotto le basi teoriche e la discretizzazione dell'integrale di cammino, esaminiamo le strategie numeriche per campionare lo spazio delle fasi esteso. Deriviamo e confrontiamo termostati stocastici (Langevin e Generalized Langevin Equation) e deterministici (Nosé–Hoover e catene di Nosé–Hoover), illustrando ergodicità, relazioni fluctuation–dissipation ed efficienza nel campionamento canonico (NVT).

Per un'applicazione pratica, eseguiamo simulazioni PIMD NVT di para-idrogeno a temperature criogeniche con il driver i-PI. Calcoliamo le radial-distribution functions (RDF), mediate sulle bead, su un intervallo di temperature e confrontiamo diversi protocolli di termostatizzazione, con dati pubblicati per valutare l'impatto degli NQEs sulle correlazioni strutturali.

Infine, con un focus su applicazioni di stoccaggio di idrogeno, studiamo la RDF di idrogeno dissolto in un cristallo hcp di magnesio a 300 K. Dalla mean-square displacement (MSD) dell'idrogeno ricaviamo una stima dell'ordine di grandezza del coefficiente di diffusione, confrontandola con i valori in letteratura.

Abstract

The vast majority of atomistic simulations treat nuclei as classical point particles evolving under Hamilton's equations and obeying Boltzmann statistics, since solving the nuclear Schrödinger equation, even within the Born–Oppenheimer approximation, is impractical. While often acceptable, this simplification fails dramatically for hydrogen-containing systems, even at room temperature, because light nuclei exhibit zero-point motion, tunneling, and other quantum effects. In this thesis, we show how the imaginary-time path-integral formalism maps quantum nuclei onto classical ring-polymer beads, enabling rigorous inclusion of nuclear quantum effects (NQEs) in complex condensed-phase simulations.

After introducing the theoretical foundations and discretization of the path-integral representation, we review numerical strategies for sampling the resulting extended phase space. We derive and compare stochastic thermostats (Langevin and Generalized Langevin Equation) and deterministic schemes (Nosé–Hoover and Nosé–Hoover chains), highlighting their ergodicity, fluctuation–dissipation relations, and efficiency in canonical (NVT) sampling.

To demonstrate a practical application, we perform NVT path-integral molecular dynamics of para-hydrogen at cryogenic temperatures using the universal i-PI engine. By computing bead-averaged radial distribution functions (RDF) across a range of temperatures and employing various thermostat protocols, we benchmark our results against published data to assess the impact of NQEs on structural correlations.

Finally, addressing a technologically relevant case, hydrogen storage, we study the RDF of hydrogen dissolved in an hcp magnesium crystal at 300 K. From the short-time mean-square displacement (MSD) of hydrogen atoms, we estimate their diffusion coefficient's order of magnitude and compare it with literature values.

Contents

1 | Path integral molecular dynamics

1.1. Introduction

To introduce the Path-Integral Molecular Dynamics (PIMD) formalism, we begin with the simplest nontrivial example: a single particle of coordinate q_1 evolving under the influence of a potential $V(q_1)$. Here, q_1 may be regarded either as a scalar (for one-dimensional motion) or as a vector in $\mathbb{R}^3$. Once the PIMD description of this one-particle system is established, the method can be extended in a straightforward manner to N distinguishable particles interacting via an arbitrary potential $V(q_1, q_2, \ldots, q_N)$.

The Hamiltonian that describes this simple system is given by:

$$H = \frac{p^2}{2m} + V(q_1) \tag{1.1}$$

where p is the momentum of the particle.

It is well established that the path-integral formulation of quantum mechanics enables one to express every physical observable as an exponential average of the appropriate action functional over all paths connecting two points in phase space, analogous to how the principle of stationary action determines the classical trajectory by minimizing the action over a trial path [7, 10].

Moreover, it allows us to express the partition function of this system as:

$$Z = \mathrm{Tr}\, e^{-\beta \hat{H}} \tag{1.2}$$

where $\beta = \frac{1}{k_B T}$.

We will show in the following paragraphs that the path-integral formulation allows us to

rewrite the above expression exactly as:

$$Z = \oint \mathcal{D}[q(\tau)] e^{-\frac{1}{\hbar}\int_0^{\beta\hbar}\left[\frac{1}{2}m\dot{q}(\tau)^2 + V(q(\tau))\right]\mathrm{d}\tau} \tag{1.3}$$

where the symbol $\oint \mathcal{D}[q(\tau)]$ is a functional integral over all the possible closed paths in configuration space, weighed with the exponential of an action-like integral over the path.

In the final part of this chapter, we will show how this form can be computed approximately and how this formalism is useful for incorporating nuclear quantum effects (NQE) in molecular dynamics.

1.2. Immaginary path integrals

As stated previously, the partition function can be written in the form:

$$Z = \int \mathrm{d}q_1 \, \langle q_1 | \, e^{-\beta\hat{H}} \, | q_1 \rangle \tag{1.4}$$

By definition, the Hamiltonian has the following form $\hat{H} = \hat{V} + \hat{T}$. Unfortunately, we cannot split the exponential operator $e^{-\beta\hat{H}}$ as the product $e^{-\beta\hat{V}}e^{-\beta\hat{T}}$ since the operators $\hat{V}$ and $\hat{T}$ do not commute[1]. However, there is the possibility of splitting the operator approximately relying on the so called "Trotter Splitting" [27, 29]:

$$e^{-\beta\hat{H}} = \left(e^{-\beta\hat{H}/P}\right)^P \approx \left(e^{-\beta_P\hat{V}/2}e^{-\beta_P\hat{T}}e^{-\beta_P\hat{V}/2}\right)^P + \mathcal{O}\left(\beta_P^2\right) \tag{1.5}$$

which becomes exact in the limit $P \to \infty$, and where we have defined the quantity $\beta_P = \frac{\beta}{P}$.

As shown in Appendix A.1, by substituting the Trotter splitting approximation into the formula and introducing $P-1$ closure relations of the type $\int \mathrm{d}q_j \, |q_j\rangle \langle q_j|$, by redistributing the P terms of the Trotter splitting to the closure relations, we can obtain the following expression:

$$\begin{aligned} Z \approx Z_P = \int \mathrm{d}q_1 \ldots \, \mathrm{d}q_P \Big[& \langle q_1 | \, e^{-\beta_P V(q_1)/2} e^{-\beta_P \hat{T}} e^{-\beta_P V(q_2)/2} \, | q_2 \rangle \ldots \\ & \ldots \langle q_P | \, e^{-\beta_P V(q_P)/2} e^{-\beta_P \hat{T}} e^{-\beta_P V(q_1)/2} \, | q_1 \rangle \Big] . \end{aligned} \tag{1.6}$$

The potential-energy operator acting on its own eigenvectors simply produces the corresponding eigenvalue, so those terms reduce to a constant factor and may be pulled outside

[1] If two operators do not commute with each other, then every function of those operators will also fail to commute

the brackets.

Consequently, we need only evaluate the remaining terms shown below:

$$\begin{aligned}\langle q_i|\, e^{-\beta_P \hat{T}}\, |q_j\rangle &= \int \mathrm{d}p\, \langle q_i|\, e^{-\beta_P \hat{T}} |p\rangle\, \langle p \mid q_j\rangle = \\ &= \frac{1}{2\pi\hbar} \int \mathrm{d}p e^{-\beta_P p^2/2m} e^{\mathrm{i}p(q_i-q_j)/\hbar} = \\ &= \frac{1}{2\pi\hbar}\sqrt{\frac{2\pi m}{\beta_P}} e^{-\frac{1}{2}\beta_P m\omega_P^2 (q_i-q_j)^2}\end{aligned} \tag{1.7}$$

where we have used $\langle p \mid q\rangle = e^{-\mathrm{i}pq/\hbar}/\sqrt{2\pi\hbar}$ and where we have introduced the variable $\omega_P = 1/\beta_P\hbar$.

By plugging this result into the previous one we get:

$$Z_P = \left(\frac{m}{2\pi\hbar^2\beta_P}\right)^{P/2} \int \mathrm{d}q_1 \ldots\ \mathrm{d}q_P e^{-\beta_P \sum_{i=1}^{P}\left[V(q_i)+\frac{1}{2}m\omega_P^2(q_i-q_{i+1})^2\right]} \tag{1.8}$$

where cyclic boundary conditions are implied in the sum, $i + P \equiv i$.

Let us therefore set aside the overall prefactor—which, notably, is independent of the configuration—and focus solely on the exponent. One immediately observes that this exponent closely resembles that of a discretized Feynman path integral, except that the usual factor $\frac{i}{\hbar\Delta t}$ appearing in front of the summation is replaced by β_p .

By making the substitutions $\beta = P\frac{1}{\Delta\tau\,\hbar}$ and $\tau = i\,t$, which imply $\omega_P = \frac{1}{\tau_{i+1}-\tau_i}$, we recover exactly the discretised form of the single-particle path integral in imaginary time τ. Now, in the limit $\Delta\tau \to 0$ (so that $\Delta\tau$ becomes $\delta\tau$) and replacing the sum by an integral, one obtains:

$$\frac{1}{\hbar}\int_0^{\beta\hbar} \mathrm{d}\tau \left[V(q(\tau)) + \frac{1}{2}m\dot{q}(\tau)^2\right] \tag{1.9}$$

Notice that making the interval in imaginary time smaller and smaller implies adding more and more complete relations into the expression of the partition function, so that the differential $dq_1 dq_2$... becomes a $D[q(\tau)]$ and the integral becomes a closed integral over all possible closed paths in configuration space.[2]

Let us now focus on the discretized partition function. It looks like a classical partition function of a cyclic polymer composed of P atoms, each of which is subject to the potential

[2] they are closed path because of the recurrence law $P + i = i$

V and the harmonic interaction with its two neighbors. Remember that V is the only real potential that the real particle feels. The other harmonic potential that the ring polymer beads feels is fictitious. This isomorphism between the partition function of a single particle in a general potential V and a necklace of beads connected by springs is called Ring Polymer representation.

It is possible to consider the discretised partition function, as a discretised version of a Feymann path integral in imaginary time of a bead which is influenced not only by the real potential but by the interaction with itself in the past imaginary time instant and the future imaginary time instant.

1.3. Expected values and averages

Now that we have defined an isomorphism between the quantum partition function of a single particle and the classical partition function of a ring of beads connected by springs, we can leverage this analogy to compute the averages of observables.

Let us consider a generic observable $\hat{A(q)}$ function solely of the position of the real particle. Now we wish to compute the average of this quantity by exploiting the isomorphism with the ring polymer. As we know from the theory, we can compute the quantum average value of an observable by $\langle A \rangle = \mathrm{Tr}\left|\hat{A}e^{-\beta\hat{H}}\right| / \mathrm{Tr}\, e^{-\beta\hat{H}}$.

We can now leverage again the Trotter splitting to expand the numerator:

$$\mathrm{Tr}\left|\hat{A}e^{-\beta\hat{H}}\right| = \int dq_1 \ \langle q_1|\, \hat{A}\, e^{-\beta\hat{H}}\, |q_1\rangle = \int dq_1 \ \langle q_1|\, \hat{A}\, e^{-\beta(\hat{T}+\hat{V})}\, |q_1\rangle \tag{1.10}$$

$$= \int dq_1 \ \langle q_1|\, \hat{A}\Big(e^{-\beta_P\hat{V}/2}\, e^{-\beta_P\hat{T}}\, e^{-\beta_P\hat{V}/2}\Big)^P\, |q_1\rangle \ . \tag{1.11}$$

Now, if we define

$$\Delta = e^{-\beta_P\hat{V}/2}\, e^{-\beta_P\hat{T}}\, e^{-\beta_P\hat{V}/2}\,,$$

then, the previous expression can be written as

$$\langle\hat{A}\rangle = \int dq_1 \ \langle q_1|\, \hat{A}\, \Delta\, \Delta \cdots \Delta\, |q_1\rangle \ .$$

Next, by inserting $P-1$ closure relations within the product of the Δ operators, one obtains:

$$\langle \hat{A} \rangle = \int dq_1 \ \langle q_1 | \, \hat{A} \, \Delta \left(\int dq_2 \ |q_2\rangle \, \langle q_2| \right) \Delta \left(\int dq_3 \ |q_3\rangle \, \langle q_3| \right) \cdots \Delta \left(\int dq_P \ |q_P\rangle \, \langle q_P| \right) |q_1\rangle \ .$$

This can be written in compact terms as

$$\langle \hat{A} \rangle = \int dq_1 \, dq_2 \, \cdots \, dq_P \ \langle q_1 | \, \hat{A} \, \Delta \, |q_2\rangle \ \langle q_2 | \, \Delta \, |q_3\rangle \cdots \langle q_P | \, \Delta \, |q_1\rangle \ .$$

Supposing that the operator $\hat{A}$ acts diagonally in the coordinate basis, i.e.

$$\hat{A}(q) \, |q\rangle = A(q) \, |q\rangle \ ,$$

by using the Hermitian property (which gives the "free" bra action), one finds the matrix element

$$\langle q_1 | \, \hat{A} \, \Delta \, |q_2\rangle = A(q_1) \, e^{-\beta_P V(q_1)/2} \ \langle q_1 | \, e^{-\beta_P \hat{T}} \, |q_2\rangle \ e^{-\beta_P V(q_2)/2} \, .$$

Thus, the full expression for the average becomes

$$\begin{aligned} \langle \hat{A} \rangle = \int dq_1 \, dq_2 \, \cdots \, dq_P \ A(q_1) \, e^{-\beta_P V(q_1)} \, e^{-\beta_P V(q_2)} \ldots e^{-\beta_P V(q_P)} \\ \times \langle q_1 | \, e^{-\beta_P \hat{T}} \, |q_2\rangle \ \langle q_2 | \, e^{-\beta_P \hat{T}} \, |q_3\rangle \cdots \langle q_P | \, e^{-\beta_P \hat{T}} \, |q_1\rangle \ . \end{aligned} \tag{1.12}$$

We have already seen how to compute the elements $\langle q_i | \, e^{-\beta_P \hat{T}} \, |q_j\rangle$ in the previous paragraph, hence, by substituting them here we get the final expression for the expected value of $\hat{A}$:

$$\langle A \rangle_P = \frac{\int \mathrm{d}q_1 \ldots \ \mathrm{d}q_P e^{-\beta_P \sum_{i=1}^{P} \left[V(q_i) + \frac{1}{2} m \omega_P^2 (q_i - q_{i+1})^2 \right]} \hat{A(q_1)}}{\int \mathrm{d}q_1 \ldots \ \mathrm{d}q_P e^{-\beta_P \sum_{i=1}^{P} \left[V(q_i) + \frac{1}{2} m \omega_P^2 (q_i - q_{i+1})^2 \right]}} \tag{1.13}$$

In the formula above, we observe that the operator A is evaluated only at q_1. One might argue that there is nothing intrinsically special about the coordinate q_1 compared to the other coordinates q_i introduced in the splitting. One can further recast the expression into a form that is manifestly symmetric in all of the q_i. The full derivation of this symmetric representation is provided in Appendix A.2.

$$\langle A\rangle_P = \frac{\int \mathrm{d}q_1 \ldots \ \mathrm{d}q_P e^{-\beta_P \sum_{i=1}^{P}\left[V(q_i)+\frac{1}{2}m\omega_P^2(q_i-q_{i+1})^2\right]} \frac{1}{P}\sum_{i=1}^{P} A\left(q_i\right)}{\int \mathrm{d}q_1 \ldots \ \mathrm{d}q_P e^{-\beta_P \sum_{i=1}^{P}\left[V(q_i)+\frac{1}{2}m\omega_P^2(q_i-q_{i+1})^2\right]}} \tag{1.14}$$

This average can be computed easily by sampling the ring polymer configurations consistently with the ring polymer energy $\sum_{i=1}^{P}\left[V\left(q_i\right)+\frac{1}{2}m\omega_P^2\left(q_i-q_{i+1}\right)^2\right]$ at the inverse temperature β_P, with Monte Carlo or molecular dynamics [3], and accumulating statistics for each replica.

Next, we address the computation of averages of functions of momentum, rather than position alone. This task is somewhat more involved. As an illustrative example, we consider the total energy of the system and derive an appropriate estimator for it; from this, the kinetic-energy estimator will emerge directly. To begin, we recall the thermodynamic relation that links the total energy to the partition function:

$$\langle E\rangle = -\frac{1}{Z}\partial Z/\partial\beta = -\frac{\partial log(Z)}{\partial\beta} \tag{1.15}$$

By substituting the partition function derived above and carrying out the (lengthy but straightforward) algebraic manipulations, one finally obtains the desired estimator for the total energy. The full derivation is omitted here for brevity.

$$\langle E\rangle = \frac{\int d\mathbf{q}\left[\frac{P}{2\beta} - \frac{1}{P}\sum_{i=1}^{P}\frac{1}{2}\,m\,\omega_P^2\left(q_i-q_{i+1}\right)^2\right]e^{-\beta_P H(\mathbf{q})}}{\mathrm{Tr}\ e^{-\beta\hat{H}}} + \frac{\int d\mathbf{q}\left[\frac{1}{P}\sum_{i=1}^{P}V(q_i)\right]e^{-\beta_P H(\mathbf{q})}}{\mathrm{Tr}\ e^{-\beta\hat{H}}}.$$

where $H = \sum_{i=1}^{P}\left[V\left(q_i\right)+\frac{1}{2}m\omega_P^2\left(q_i-q_{i+1}\right)^2\right]$

One immediately recognizes that the second term is precisely the expectation value of the potential, $\langle V\rangle$, and hence the first term must be the expectation value of the kinetic energy, $\langle T\rangle$. Consequently, the average total energy can be written in the compact form

$$\langle E\rangle = \frac{\int \mathrm{d}q_1 \ldots \ \mathrm{d}q_P e^{-\beta_P \sum_{i=1}^{P}\left[V(q_i)+\frac{1}{2}m\omega_P^2(q_i-q_{i+1})^2\right]} E^{\mathrm{TD}}\left(q_1,\ldots q_P\right)}{\int \mathrm{d}q_1 \ldots \ \mathrm{d}q_P e^{-\beta_P \sum_{i=1}^{P}\left[V(q_i)+\frac{1}{2}m\omega_P^2(q_i-q_{i+1})^2\right]}} \tag{1.16}$$

[3] as we will see later

and

$$\langle \hat{T} \rangle = \frac{\int \mathrm{d}q_1 \ldots \ \mathrm{d}q_P e^{-\beta_P \sum_{i=1}^{P} \left[V(q_i) + \frac{1}{2} m \omega_P^2 (q_i - q_{i+1})^2 \right]} T^{\mathrm{TD}}(q_1, \ldots q_P)}{\int \mathrm{d}q_1 \ldots \ \mathrm{d}q_P e^{-\beta_P \sum_{i=1}^{P} \left[V(q_i) + \frac{1}{2} m \omega_P^2 (q_i - q_{i+1})^2 \right]}} \tag{1.17}$$

where:

$$E^{\mathrm{TD}}(q_1, \ldots q_P) = \frac{P}{2\beta} - \frac{1}{P} \sum_{i=1}^{P} \frac{1}{2} m \omega_P^2 (q_i - q_{i+1})^2 + \frac{1}{P} \sum_{i=1}^{P} V(q_i) \tag{1.18}$$

and

$$T^{\mathrm{TD}}(q_1, \ldots q_P) = \frac{P}{2\beta} - \frac{1}{P} \sum_{i=1}^{P} \frac{1}{2} m \omega_P^2 (q_i - q_{i+1})^2 \tag{1.19}$$

We now highlight an intriguing contrast between the structural forms of the estimators for the potential energy and for the kinetic energy.

By examining the formula for the potential energy estimator, we notice that no coupling between the various q_i and q_j appears, because the estimator involves only a sum of independent contributions of $V(q_i)$. In other words, each bead in the ring contributes individually and independently. This is why we say that the potential energy estimator is "local".

By contrast, in the kinetic energy estimator a cross term involving adjacent beads appears, namely $(q_i - q_{i+1})^2$. Therefore, the kinetic energy expression cannot be simply decomposed into a sum of independent contributions from the individual q_i. Moreover, this coupling affects the efficiency of the estimator, since its variance grows as

$$\frac{P}{\beta^2},$$

whereas for the potential energy estimator the variance grows only as $\sqrt{P}$.

To illustrate the difference, note that the potential-energy estimator comprises a sum of P terms (each being an independent sample of $V(q_i)$ drawn according to the Boltzmann distribution). When P is large, the sum of these independent random variables approaches a Gaussian distribution by virtue of the central limit theorem, and the variance scales as $\sqrt{P}$.

Regarding the kinetic energy estimator, however, the situation is more involved. Intuitively, because the expression involves squared cross terms, a small change in one q_i influences not just one term but two of the terms in the summation (namely, $q_{i-1} - q_i$ and $q_i - q_{i+1}$, both squared). This additional coupling among the beads leads to a higher

variance that scales linearly with P.

However, in order to get an efficient estimator for the kinetic energy, it is usually reasonable to exploit the virial theorem [18], and by integrating by parts the previous expression one obtains:

$$T^{\mathrm{CV}}\left(q_1, \ldots q_P\right) = \frac{1}{2\beta} + \frac{1}{2P}\sum_{i=1}^{P}\left(q_i - \bar{q}\right)\frac{\partial V}{\partial q_i}, \quad \bar{q} = \frac{1}{P}\sum_{i=1}^{P} q_i \tag{1.20}$$

As we can see here, no cross-correlation between the variables q_i occurs.
Morevoer, it is worth to highlight that the estimations of these quantities are completely indipendent of the ring polymer momenta.

1.4. Sampling of the equilibrium distribution

As we have seen in the previous paragraph, the partition functions and the estimators of some observables can be computed by MC simulations. Although this approach efficiently samples phase space, it typically cannot incorporate inter-atomic forces without incurring significant overhead in the evaluation of potential energies, particularly when one wishes to avoid developing custom-tailored Monte Carlo moves for the specific system. [7].

A simple way to overcome this limitation is to integrate Hamilton's equations of motion, thereby generating trajectories that sample the Boltzmann distribution. We will discuss this approach in detail in the following section.

Recalling the partition function as given in Eq.(1.8), we observe a prefactor that can be absorbed by introducing integrals over fictitious momenta p_i. In particular, by inserting for each bead i

$$\int_{-\infty}^{\infty} \frac{\mathrm{d}p_i}{2\pi\hbar} \exp\Big(-\frac{\beta}{2m}p_i^2\Big)\,,$$

the original prefactor is exactly reproduced, and the configurational integral is promoted to a full phase-space integral over $\{q_i, p_i\}$.

The rewritten partition function now looks as:

$$Z_P = \frac{1}{(2\pi\hbar)^P}\int \mathrm{d}p_1 \ldots \mathrm{d}p_P \int \mathrm{d}q_1 \ldots \mathrm{d}q_P e^{-\beta_P \sum_{i=1}^{P}\left[V(q_i) + \frac{p_i^2}{2m} + \frac{1}{2}m\omega_P^2(q_i - q_{i+1})^2\right]} \tag{1.21}$$

It is important to notice that the p_i are not related to the physical real momenta of the real particle. However, they can be seen as the momenta of the beads in the ring polymer

representation. These quantities are just additional sampling tools [25, 26].

Hence, we can define the system's Hamiltonian as follows:

$$H_P = H_0 + V_P = \sum_{i=1}^{P} \left[\frac{p_i^2}{2m} + \frac{1}{2} m\omega_P^2 \left(q_i - q_{i+1} \right)^2 \right] + \sum_{i=1}^{P} V\left(q_i \right) \tag{1.22}$$

and then. we can integrate the Hamilton's equations for the individual beads of the ring:

$$\dot{q}_i = \frac{\partial H_P}{\partial p_i} = \frac{p_i}{m}, \quad \dot{p}_i = -\frac{\partial H_P}{\partial q_i} \tag{1.23}$$

The key idea is to exploit the (assumed) ergodicity of the system to compute equilibrium averages. For an ergodic system, the ensemble average can be replaced by a long-time average taken along a single dynamical trajectory. In practice, instead of sampling many configurations from the Boltzmann distribution via Monte-Carlo, one can

1. choose a suitable initial point in phase space;
2. integrate the equations of motion, recording positions and momenta along the trajectory;
3. compute the time average of the observable of interest.

This procedure works only if the dynamics is ergodic, i.e. if, given infinite time, the trajectory visits every region of phase space and spends in each a fraction of time proportional to its Boltzmann weight. Proving ergodicity, however, is highly non-trivial and depends on the specific Hamiltonian; there is no general theorem that guarantees ergodicity for an arbitrary Hamiltonian system[4].

However, because stationarity is a necessary condition for ergodicity, we can at least demonstrate that our system satisfies stationarity [6]. A system is said to be *stationary* if, at every instant of time, the probability–density function of the phase–space coordinates[5] remains the same; in other words, it does not change with time.

This property can be verified for the present case expliting the Hamilton's equations shown before. Infact, since this system is Hamiltonian, it evolves following trajectories on equi-energy surface.

[4] To the best of my knowledge.

[5] That is, the joint PDF for all positions and momenta (or any other complete set of state variables) describing the microstate of the system.

Therefore we can write that $H_P(\mathbf{p}_t, \mathbf{q}_t) = H_P(\mathbf{p}_0, \mathbf{q}_0)$, hence:

$$e^{-\beta_P H_P(\mathbf{p}_t, \mathbf{q}_t)} = e^{-\beta_P H_P(\mathbf{p}_0, \mathbf{q}_0)} \tag{1.24}$$

Moreover, since Hamiltonian systems preserve the phase space element volume $d^P\mathbf{p}_t d^P\mathbf{q}_t = d^P\mathbf{p}_0 d^P\mathbf{q}_0$, one can easily compute the partition function of the system as follows:

$$Z \simeq \frac{1}{(2\pi\hbar)^P} \int d^P\mathbf{p} \int d^P\mathbf{q} e^{-\beta_P H_P(\mathbf{p},\mathbf{q})} = \frac{1}{(2\pi\hbar)^P} \int d^P\mathbf{p_0} \int d^P\mathbf{q_0} e^{-\beta_P H_P(\mathbf{p_0},\mathbf{q_0})} \tag{1.25}$$

Then we can conclude that the entire probability density function of the system is constant in time and therefore is stationary:

$$\rho(\mathbf{p}_0, \mathbf{q}_0) = \frac{1}{(2\pi\hbar)^P Z} e^{-\beta_P H_P(\mathbf{p}_0,\mathbf{q}_0)} \tag{1.26}$$

This fact, equipped with ergodicity, implies that static equilibrium properties such as the potential and kinetic energies can be obtained by time averaging along ring polymer trajectories whose initial conditions are sampled from the Boltzmann distribution, that we have seen in this paragraph before.

We will discuss later in this thesis the chance of coupling the system to an ergodic thermostat, when system alone fails to explore its full phase space. By doing so we extend the dynamics to include the thermostat degrees of freedom in order to enforce canonical sampling at the target temperature.

1.5. Generalisation to multiple interacting particles

In the previous paragraphs, we have shown how one can implement an isomorphism between a single real particle, subject to a potential, and its representation with the ring polymer. One can imagine to extend this isomorphism for more than one individual particle but for N interacting particles in the following way.

Let us consider a set of N distinguishable particles described by the Hamiltonian:

$$H = \sum_{i=1}^{N} \frac{p_i^2}{2m_i} + V(q_1, \ldots, q_N) \tag{1.27}$$

where $V(q_1, \ldots, q_N)$ is the interacting potential among particles.

We can then manipulate the quantum partition function $Z = \mathrm{tr}\left[e^{-\beta H}\right]$ similarly to how we did in the previous paragraph for the single real particle, to obtain the resulting expression:

$$Z \simeq \frac{1}{(2\pi\hbar)^f} \int d^f\mathbf{p} \int d^f\mathbf{q} e^{-\beta_n H_n(\mathbf{p},\mathbf{q})} \tag{1.28}$$

where $f = Nn$, and n indicates the number of beads that represents the ring polymer representation for each one of the N real particles.

Here we have defined:

$$H_n(\mathbf{p},\mathbf{q}) = H_n^0(\mathbf{p},\mathbf{q}) + V_n(\mathbf{q}) \tag{1.29}$$

where

$$H_n^0(\mathbf{p},\mathbf{q}) = \sum_{i=1}^{N}\sum_{j=1}^{n}\left(\frac{\left[p_i^{(j)}\right]^2}{2m_i} + \frac{1}{2}m_i\omega_n^2\left[q_i^{(j)} - q_i^{(j-1)}\right]^2\right) \tag{1.30}$$

and

$$V_n(\mathbf{q}) = \sum_{j=1}^{n} V\left(q_1^{(j)},\ldots,q_N^{(j)}\right) \tag{1.31}$$

with $\omega_n = 1/\beta_n\hbar$ and $q_i^{(0)} \equiv q_i^{(n)}$.

Be careful to distinguish between the two kinds of indices used here. The parenthesised superscript $(\cdot)^{(j)}$ labels the j-th bead in the ring-polymer representation, whereas the subscript $(\cdot)_i$ labels the i-th real particle. Consequently, beads interact only with the other beads belonging to the same particle; there are no direct bead–bead interactions between different particles.

Following the same procedure used earlier to compute observable averages, we can now write a correspondingly generalised expression for these averages [6]. For the potential energy estimator:

$$\langle V\rangle \simeq \frac{1}{(2\pi\hbar)^f Z} \int d^f\mathbf{p} \int d^f\mathbf{q} e^{-\beta_n H_n(\mathbf{p},\mathbf{q})}\mathcal{V}_n(\mathbf{q}) \tag{1.32}$$

where

$$\mathcal{V}_n(\mathbf{q}) = \frac{1}{n}V_n(\mathbf{q}) = \frac{1}{n}\sum_{j=1}^{n} V\left(q_1^{(j)},\ldots,q_N^{(j)}\right) \tag{1.33}$$

As we can see, the summation over all the beads appears, as it appeared in the expression for an individual particle. The only difference is that, now the exponential depends on the position of the beads of the rings, associated to all the N real particles, and not only of the beads representing the individual real particle.

In the case of the kinetic energy estimation we get:

$$\langle T \rangle \simeq \frac{1}{(2\pi\hbar)^f Z} \int d^f\mathbf{p} \int d^f\mathbf{q} e^{-\beta_n H_n(\mathbf{p},\mathbf{q})} \mathcal{T}_n(\mathbf{q}) \tag{1.34}$$

where

$$\mathcal{T}_n(\mathbf{q}) = \frac{N}{2\beta} + \frac{1}{2n} \sum_{i=1}^{N} \sum_{j=1}^{n} \left(q_i^{(j)} - \bar{q}_i\right) \frac{\partial V\left(q_1^{(j)}, \ldots, q_N^{(j)}\right)}{\partial q_i^{(j)}} \text{ and } \bar{q}_i = \frac{1}{n} \sum_{j=1}^{n} q_i^{(j)} \tag{1.35}$$

As we can see, if $N = 1$ we completely recover the case of the individual real particle.

1.6. Ring polymer evolution integration scheme

Having outlined how to compute theoretical averages of observables via the ring-polymer representation in the path-integral formalism, and having introduced time averaging to sample the Boltzmann distribution, we are now led to the following question: how can the real-time evolution of the ring-polymer system be computed? Which numerical integration scheme is best suited to solve the ring-polymer Hamilton's equations of motion?

Again, we will first examine the case of a single particle in detail, and then extend our treatment to cover multiple interacting particles.

Before going into the details we are going to recall some results form the theory of Hamiltonian systems. Consider a Hamiltonian system with phase–space coordinates $\mathbf{q} = (q_1, \ldots, q_f)$ and $\mathbf{p} = (p_1, \ldots, p_f)$. For an arbitrary phase–space function $A(\mathbf{q}, \mathbf{p})$ the Hamilton's equations imply

$$\frac{dA}{dt} = \{A, H\} = \sum_{i=1}^{f} \left(\frac{\partial A}{\partial q_i} \frac{\partial H}{\partial p_i} - \frac{\partial A}{\partial p_i} \frac{\partial H}{\partial q_i} \right), \tag{1.36}$$

where $\{\cdot, \cdot\}$ is the Poisson bracket and $H(\mathbf{q}, \mathbf{p})$ is the Hamiltonian.

We can now introduce the Liouville operator L so that[6]

$$\frac{dA}{dt} = -LA, \qquad L = \sum_{i=1}^{f} \left(\frac{\partial H}{\partial p_i} \frac{\partial}{\partial q_i} - \frac{\partial H}{\partial q_i} \frac{\partial}{\partial p_i} \right). \tag{1.37}$$

[6]Many authors define $L \equiv \{\cdot, H\}$, in which case $\dot{A} = LA$. Here we adopt the convention $\dot{A} = -LA$ to match the standard sign in Trotter splittings used in molecular dynamics.

Equation (1.37) is a linear first–order ODE with the exact solution as shown here:

$$A(t) \;=\; e^{-Lt}\,A(0), \tag{1.38}$$

where e^{-Lt} is the phase–space evolution operator.

A numerical integration can be performed by applying the propagator over many small time steps Δt,

$$A(t + n\Delta t) \;=\; \left(e^{-L\Delta t}\right)^n A(0).$$

As we will see in the rest of the dissertation, the Liouvillian can be decomposed into two parts,

$$L = L_0 + L_V,$$

where L_0, arising from the part of the Hamiltonian regarding the kinetic energy and spring potentials of the beads $H_0(\mathbf{q}, \mathbf{p})$, and L_V from the real physical potential $V(\mathbf{q})$ acting on the beads. Because L_0 and L_V generally do not commute, the exact single–step propagator cannot be written as a single exponential of a sum of commuting operators. Instead, we approximate it with the second–order Strang (or symmetric Trotter) splitting[7] [30]:

$$e^{-L\Delta t} \;=\; e^{-(L_0+L_V)\Delta t} \;\approx\; e^{-\frac{1}{2}\Delta t\, L_V}\, e^{-\Delta t\, L_0}\, e^{-\frac{1}{2}\Delta t\, L_V} \;+\; \mathcal{O}(\Delta t^3). \tag{1.39}$$

Given this brief review of the properties of the Liouvillian operator we can now move on, and apply this theory to our purposes. The key idea is to use the notions of the Liouvillian to find the evolution in time of the trajectories of the ring polymer beads. The approximation that we have introduced in order to compute the numerical solution is a powerful integrating scheme known as "Velocity Varlet Method". We can now use this integration scheme to integrate the Hamilton's equations.

[7] Properties of the Strang splitting:

- Second–order accuracy: the local error per step is $\mathcal{O}(\Delta t^3)$, giving global $\mathcal{O}(\Delta t^2)$ accuracy.
- Time reversibility: the sequence of sub-steps is symmetric; reversing the order and changing $\Delta t \to -\Delta t$ exactly inverts a single step.
- Symplecticity: each sub-propagator $e^{-\alpha L_0}$ or $e^{-\alpha L_V}$ is itself an exact solution of a Hamiltonian flow and therefore preserves phase-space volume and the symplectic structure. Their composition remains symplectic, making the scheme well suited for long-time molecular dynamics.

Let's first make some remarks to arrange the setting of our probelm to match the expression on the theory.

As a matter of fact, q_i and p_i are functions themselves defined on the phase space, and therefore the theory introduced for generic a function $A(q_i, p_i)$ applies.

We can indeed write that: $\dot{q}_i = \frac{\partial H}{\partial p_i} = -Lq_i$ and $\dot{p}_i = -\frac{\partial H}{\partial p_i} = -Lp_i$

In the case of the ring polymer representation we have written the Hamitonian as:

$$H_P = H_0 + V_P = \sum_{i=1}^{P} \left[\frac{p_i^2}{2m} + \frac{1}{2} m\omega_P^2 \left(q_i - q_{i+1}\right)^2 \right] + \sum_{i=1}^{P} V\left(q_i\right) \tag{1.40}$$

therefore, if we recall the definition of the Liouvillian, we have:

$$L = \sum_{i=1}^{P} \left(\frac{\partial (H_0 + V_P)}{\partial p_i} \frac{\partial}{\partial q_i} - \frac{\partial (H_0 + V_P)}{\partial q_i} \frac{\partial}{\partial p_i} \right) \tag{1.41}$$

$$= \underbrace{\sum_{i=1}^{P} \left(\frac{\partial H_0}{\partial p_i} \frac{\partial}{\partial q_i} - \frac{\partial H_0}{\partial q_i} \frac{\partial}{\partial p_i} \right)}_{L_0} + \underbrace{\sum_{i=1}^{P} \left(\frac{\partial V_P}{\partial p_i} \frac{\partial}{\partial q_i} - \frac{\partial V_P}{\partial q_i} \frac{\partial}{\partial p_i} \right)}_{L_V}. \tag{1.42}$$

Then, one would be tempted to write the integration scheme applied to the variables q_i and p_i as follows:

$$q_i(t + dt) = e^{-\frac{1}{2}\Delta t\, L_V}\, e^{-\Delta t\, L_0}\, e^{-\frac{1}{2}\Delta t\, L_V} q_i(t)$$

$$p_i(t + dt) = e^{-\frac{1}{2}\Delta t\, L_V}\, e^{-\Delta t\, L_0}\, e^{-\frac{1}{2}\Delta t\, L_V} p_i(t)$$

Let's take a look at how the single parts of this integration scheme act on $q_i(t)$ and $p_i(t)$. It is easy to show that:

$$L_V q_i = 0 \quad \Longrightarrow \quad L_V^k q_i = 0 \quad (k \geq 2),$$

$$L_V p_i = F_i \quad \Longrightarrow \quad L_V^2 p_i = 0 \quad \text{and hence} \quad L_V^k p_i = 0 \quad (k \geq 3).$$

Using the series definition of the exponential operator,

$$e^{-\frac{\Delta t}{2}L_V} q_i = \sum_{k=0}^{\infty} \frac{\left(-\frac{\Delta t}{2}\right)^k}{k!} L_V^k q_i = q_i,$$

$$e^{-\frac{\Delta t}{2}L_V} p_i = \sum_{k=0}^{\infty} \frac{\left(-\frac{\Delta t}{2}\right)^k}{k!} L_V^k p_i = p_i - \frac{\Delta t}{2} F_i.$$

So the application of the potential term leaves unchanged the positions and acts only on the momenta.

Unfortunately, the "free" Liouvillian L_0 is not as tame as the potential term L_V. Because H_0 contains the spring interaction $\frac{1}{2} m\omega_P^2 (q_i - q_{i+1})^2$, the action of L_0 on a single bead mixes that bead with its neighbours:

$$L_0 q_i = \frac{p_i}{m}, \qquad L_0^2 q_i = -\omega_P^2 \big(2q_i - q_{i-1} - q_{i+1}\big), \qquad L_0^3 q_i = \cdots$$

Higher powers of L_0 never vanish, so the exponential

$$e^{-\Delta t\, L_0} = \sum_{k=0}^{\infty} \frac{(-\Delta t)^k}{k!} L_0^k$$

cannot be truncated after a few terms as we did for $e^{-\frac{1}{2}\Delta t L_V}$. More important, each update produced by $e^{-\Delta t L_0}$ depends not just on bead i but also on beads $i-1$ and $i+1$; an error made on one bead therefore migrates to its neighbours and can grow rapidly around the ring.

However, there is a trick we can play here: one can integrate the L_0 step analytically in normal–mode space[8].

Because L_V merely applies the physical-potential "kick," the non-trivial part of the Trotter step is the action of L_0. Hence, we focus on the *free* ring–polymer Hamiltonian

$$H_0(p, q) = \sum_{j=1}^{n} \Big[\frac{p_j^2}{2m} + \frac{m\omega_n^2}{2} \big(q_j - q_{j+1}\big)^2 \Big].$$

which is a multi–dimensional harmonic oscillator.

[8] the discrete Fourier transform diagonalises the spring matrix, each mode is propagated as an independent harmonic oscillator, and the result is transformed back to bead coordinates. This avoids both the infinite Taylor series and the uncontrolled error propagation that would arise from a naive, bead-by-bead update.

Transforming the bead coordinates to normal modes (as performed in the Appendix A.3),

$$\tilde{q}_k = \sum_{j=1}^{n} C_{jk}\, q_j, \qquad \tilde{p}_k = \sum_{j=1}^{n} C_{jk}\, p_j,$$

diagonalises the Hamiltonian and yields

$$H_0(p,q) = \sum_{k=0}^{n-1} \Big[\tfrac{\tilde{p}_k^2}{2m} + \tfrac{m\omega_k^2}{2}\, \tilde{q}_k^2 \Big],$$

so each normal mode k behaves as an independent one–dimensional harmonic oscillator.

Now we can integrate the Hamilton's equations for the normal mode variables, and update their value after an interval of time Δt:

By writing the Hamiltons equations:

$$\dot{\tilde{q}}_i \;=\; \frac{\partial H_0}{\partial \tilde{p}_i} \;=\; \frac{\tilde{p}_i}{m}, \qquad \dot{\tilde{p}}_i \;=\; -\,\frac{\partial H_0}{\partial \tilde{q}_i} \;=\; -\,m\omega_i^2\, \tilde{q}_i. \tag{1.43}$$

These equations can be rewritten in the matricial form as:

$$\frac{d}{dt}\begin{pmatrix} \tilde{p}_i \\ \tilde{q}_i \end{pmatrix} = \begin{pmatrix} 0 & -\,m\,\omega_i^2 \\ \dfrac{1}{m} & 0 \end{pmatrix} \begin{pmatrix} \tilde{p}_i \\ \tilde{q}_i \end{pmatrix}. \tag{1.44}$$

This system is in the form $\dot{\boldsymbol{X}} = A\boldsymbol{X}$:

$$\frac{d}{dt}\begin{pmatrix} \tilde{p}_i \\ \tilde{q}_i \end{pmatrix} = A\begin{pmatrix} \tilde{p}_i \\ \tilde{q}_i \end{pmatrix}, \quad A = \begin{pmatrix} 0 & -m\omega_i^2 \\ \frac{1}{m} & 0 \end{pmatrix} \tag{1.45}$$

and the formal solution can be written as:

$$\mathbf{x}(t+\Delta t) = e^{A\Delta t}\mathbf{x}(t), \quad e^{A\Delta t} = \sum_{k=0}^{\infty} \frac{(A\Delta t)^k}{k!} \tag{1.46}$$

Since

$$A^2 = \begin{pmatrix} 0 & -m\omega_i^2 \\ \frac{1}{m} & 0 \end{pmatrix}^2 = \begin{pmatrix} -\omega_i^2 & 0 \\ 0 & -\omega_i^2 \end{pmatrix} = -\omega_i^2 I_2 \tag{1.47}$$

and

$$A^3 = AA^2 = \left(-\omega_i^2\right) A, \quad A^4 = A^2A^2 = \omega_i^4 I_2, \quad \text{etc.} \tag{1.48}$$

we can determine the shape of the exponential[9]:

$$e^{A\Delta t} = \sum_{n=0}^{\infty} \frac{(A\Delta t)^{2n}}{(2n)!} + \sum_{n=0}^{\infty} \frac{(A\Delta t)^{2n+1}}{(2n+1)!} \tag{1.49}$$

$$= \left[\sum_{n=0}^{\infty} \frac{\left(-\omega_i^2 \Delta t^2\right)^n}{(2n)!}\right] I \; + \; \left[A\Delta t \sum_{n=0}^{\infty} \frac{\left(-\omega_i^2 \Delta t^2\right)^n}{(2n+1)!}\right] \tag{1.50}$$

$$= I \cos\!\left(\omega_i \Delta t\right) \; + \; A \, \frac{\sin\!\left(\omega_i \Delta t\right)}{\omega_i} \; . \tag{1.51}$$

then we can write:

$$e^{A\Delta t} = \begin{pmatrix} \cos(\omega_i \Delta t) & -m\omega_i \sin(\omega_i \Delta t) \\ \frac{\sin(\omega_i \Delta t)}{m\omega_i} & \cos(\omega_i \Delta t) \end{pmatrix} \tag{1.52}$$

therefore, the update of a Δt is:

$$\begin{pmatrix} \tilde{p}_i(t+\Delta t) \\ \tilde{q}_i(t+\Delta t) \end{pmatrix} = \begin{pmatrix} \cos(\omega_i \Delta t) & -m\omega_i \sin(\omega_i \Delta t) \\ \frac{\sin(\omega_i \Delta t)}{m\omega_i} & \cos(\omega_i \Delta t) \end{pmatrix} \begin{pmatrix} \tilde{p}_i(t) \\ \tilde{q}_i(t) \end{pmatrix} \tag{1.53}$$

Once the normal-mode variables have been updated, one transforms them back to bead coordinates and then applies the final step of the Trotter–Strang integration scheme.

Therefore, the full algorithm would look like the following:

$$\begin{aligned}
p_i &\leftarrow p_i - \frac{\Delta t}{2} \frac{\partial V\left(q_i\right)}{\partial q_i} \\
\tilde{p}_j &\leftarrow \sum_i p_i C_{ij} \quad \tilde{q}_j \leftarrow \sum_i q_i C_{ij} \\
\begin{pmatrix} \tilde{p}_j \\ \tilde{q}_j \end{pmatrix} &\leftarrow \begin{pmatrix} \cos \omega_j \Delta t & -m\omega_j \sin \omega_j \Delta t \\ [1/m\omega_j] \sin \omega_j \Delta t & \cos \omega_j \Delta t \end{pmatrix} \begin{pmatrix} \tilde{p}_j \\ \tilde{q}_j \end{pmatrix} \\
p_i &\leftarrow \sum_j C_{ij} \tilde{p}_j \quad q_i \leftarrow \sum_j C_{ij} \tilde{q}_j \\
p_i &\leftarrow p_i - \frac{\Delta t}{2} \frac{\partial V\left(q_i\right)}{\partial q_i}.
\end{aligned} \tag{1.54}$$

1.7. Generalisation of the integration scheme

For the general case of N real interacting particles, for which each particle is associated to a ring of beads, we can generalise the integration scheme as we will present now. The

[9] the even powers reduce to scalars times I; the odd powers reduce to scalars times A

splitting of the integrator is the same as introduced before:

$$e^{-\Delta t L} \simeq e^{-(\Delta t/2)L_V} e^{-\Delta t L_0} e^{-(\Delta t/2)L_V} \tag{1.55}$$

where $L = L_0 + L_V$ is the Liouvillian associated with $H_n(\mathbf{p}, \mathbf{q})$ and L_0 and L_V are those associated with $H_n^0(\mathbf{p}, \mathbf{q})$ and $V_n(\mathbf{q})$.

As far as the first and last integrating steps are concerned, we can work in the bead coordinates representation, for the application of the intermediate step which involves H_n^0 we still convert to normal mode representation in the following generalised way:

$$\tilde{p}_i^{(k)} = \sum_{j=1}^{n} p_i^{(j)} C_{jk} \quad \text{and} \quad \tilde{q}_i^{(k)} = \sum_{j=1}^{n} q_i^{(j)} C_{jk} \tag{1.56}$$

where the matrix for the change of basis is the same as seen before. Proceeding with the same approach as before, we derive the normal mode Hamitlonian:

$$H_n^0(\mathbf{p}, \mathbf{q}) = \sum_{i=1}^{N} \sum_{k=0}^{n-1} \left(\frac{\left[\tilde{p}_i^{(k)}\right]^2}{2m_i} + \frac{1}{2} m_i \omega_k^2 \left[\tilde{q}_i^{(k)}\right]^2 \right) \tag{1.57}$$

where $\omega_k = 2\omega_n \sin(k\pi/n)$. The whole algorithm then becomes [6]:

$$\begin{aligned}
p_i^{(j)} &\leftarrow p_i^{(j)} - \frac{\Delta t}{2} \frac{\partial V\left(q_1^{(j)}, \ldots, q_N^{(j)}\right)}{\partial q_i^{(j)}}, \\
\tilde{p}_i^{(k)} &\leftarrow \sum_{j=1}^{n} p_i^{(j)} C_{jk}, \quad \tilde{q}_i^{(k)} \leftarrow \sum_{j=1}^{n} q_i^{(j)} C_{jk}, \\
\begin{pmatrix} \tilde{p}_i^{(k)} \\ \tilde{q}_i^{(k)} \end{pmatrix} &\leftarrow \begin{pmatrix} \cos\omega_k \Delta t & -m_i \omega_k \sin\omega_k \Delta t \\ [1/m_i\omega_k] \sin\omega_k \Delta t & \cos\omega_k \Delta t \end{pmatrix} \begin{pmatrix} \tilde{p}_i^{(k)} \\ \tilde{q}_i^{(k)} \end{pmatrix} \\
p_i^{(j)} &\leftarrow \sum_{k=0}^{n-1} C_{jk} \tilde{p}_i^{(k)}, \quad q_i^{(j)} \leftarrow \sum_{k=0}^{n-1} C_{jk} \tilde{q}_i^{(k)}, \\
p_i^{(j)} &\leftarrow p_i^{(j)} - \frac{\Delta t}{2} \frac{\partial V\left(q_1^{(j)}, \ldots, q_N^{(j)}\right)}{\partial q_i^{(j)}}.
\end{aligned} \tag{1.58}$$

2 | Simulative Thermostats

In the previous chapter we showed that, provided the dynamics is ergodic, propagating a ring–polymer with its native (microcanonical) Hamiltonian yields time-averaged estimators that converge to the quantum Boltzmann distribution of the underlying physical system. In practical applications, however, ergodicity is not guaranteed: low temperatures, rugged potential-energy landscapes, and strongly coupled internal modes can trap the dynamics and lead to slow or biased sampling [16].

Most molecular-dynamics studies aim to compute expectation values at a fixed temperature, i.e. in the canonical (NVT) ensemble. Achieving this with ring-polymer molecular dynamics (RPMD) requires augmenting the bare Hamiltonian evolution, so that the extended system can exchange energy with an ideal heat bath of prescribed temperature. This is accomplished by introducing the so called "thermostats": auxiliary variables or stochastic forces that modify the equations of motion while leaving the canonical distribution invariant.

Besides restoring thermodynamic consistency, an appropriate thermostat accelerates the exploration of phase space, reduces long-time correlations, and thus improves the statistical efficiency of computed averages. Thermostats are commonly grouped into two broad classes:

- **Deterministic** schemes, such as the Nosé–Hoover chain family, which employ time-reversible auxiliary degrees of freedom to mediate energy exchange [19, 24].
- **Stochastic** schemes, such as Langevin and Andersen thermostats, which introduce random forces and friction terms that mimic instantaneous collisions with a heat bath.

In the subsequent chapters, we will undertake an in-depth examination of three popular thermostatting schemes: the standard Langevin thermostat, its extension via the Generalized Langevin Equation (GLE), and the deterministic Nosé–Hoover thermostat.

3 | Langevin Thermostat

The Langevin thermostat is a stochastic thermostat that modifies Hamilton's equations by introducing both a dissipative force and a random noise term in order to mimic the effect of a thermal bath, typically composed of many lighter particles [3]. To integrate the resulting modified equations of motion, in such a way that the correct canonical distribution is sampled, one generally applies an extended version of the Trotter splitting scheme, as we shall see in the next paragraphs.

3.1. Introduction to Langevin Equation

As usual, we consider the simplified case of a single particle. Let us consider a particle of mass m subject to a potential $U(q)$. The canonical distribution at temperature T is described by the probability density

$$\bar{P}(p,q)\,dp\,dq \propto e^{-\beta\frac{p^2}{2m}} e^{-\beta U(q)}\,dp\,dq,$$

The Langevin dynamics modify Hamilton's equations as follows:

$$\begin{aligned} dp(t) &= f(q(t))\,dt - \gamma p(t)\,dt + \sqrt{\frac{2m\gamma}{\beta}}\,dW(t), \\ dq(t) &= \frac{p(t)}{m}\,dt, \end{aligned}$$

where $f(q) = -\frac{\partial U}{\partial q}$ is the deterministic force arising from the potential, γ is a friction coefficient representing the strength of the coupling with the heat bath, and $dW(t)$ denotes an infinitesimal increment of a Wiener process, that is, a Gaussian random variable with zero mean and variance dt.

The second equation, which describes the evolution of the position, remains unchanged from the classical Hamiltonian case, while the first equation, governing the momentum, includes three contributions: the deterministic force due to the potential, a dissipative term proportional to $-\gamma p(t)$ which models friction, and a stochastic term involving the

Wiener noise $dW(t)$ with amplitude $\sqrt{\frac{2m\gamma}{\beta}}$, which represents the thermal fluctuations induced by the environment.

The noise is characterized by the correlation relation

$$\langle dW(t)\, dW(t')\rangle = \delta(t-t')\, dt,$$

which encodes the Fluctuation–Dissipation Theorem (FDT). This fundamental principle guarantees that, when the random and dissipative contributions are properly balanced, the system evolves towards thermal equilibrium and correctly samples the canonical distribution.

The Fluctuation–Dissipation Theorem expresses the deep physical insight that microscopic fluctuations (arising from thermal noise) are inherently linked to macroscopic dissipative behavior (such as friction), and in this context, the specific form of the stochastic term ensures that this balance is maintained. In what follows, we will make use of results from stochastic theory to demonstrate explicitly that the Langevin dynamics indeed sample the canonical distribution.

It is a classical result in stochastic theory that the coupled stochastic differential equations governing a particle's motion can be transformed into a single partial-differential equation for the phase-space probability density $P(q,p,t)$. Equivalently, one may derive the Fokker–Planck equation for $P(q,p,t)$, which gives the probability of finding the particle with position in $[q, q+dq]$ and momentum in $[p, p+dp]$.

We will invoke the general theorem that establishes the equivalence between a system of stochastic differential equations and its Fokker–Planck representation.[1]

[1] This theorem allows us to recast an arbitrary set of SDEs into the corresponding Fokker–Planck equation. For clarity, a detailed proof in the special case of a single SDE is provided in Appendix B.1.

Theorem

Let us consider a system of stochastic differential equations (SDEs) of the form

$$d\mathbf{X}_t = \boldsymbol{\mu}(\mathbf{X}_t, t)\, dt + \boldsymbol{\sigma}(\mathbf{X}_t, t)\, d\mathbf{W}_t,$$

where $\mathbf{X}_t \in \mathbb{R}^N$ is the vector of stochastic variables of interest (for example, the position and momentum of a particle), $\boldsymbol{\mu}(\mathbf{X}_t, t) \in \mathbb{R}^N$ is the drift vector describing the deterministic part of the dynamics, $\boldsymbol{\sigma}(\mathbf{X}_t, t) \in \mathbb{R}^{N\times M}$ is the diffusion matrix which couples the system to noise, and $\mathbf{W}_t \in \mathbb{R}^M$ is a standard M-dimensional Wiener process.

Then, the probability density $p(\mathbf{x}, t)$ associated with the random variable $\mathbf{X}_t$ satisfies the Fokker–Planck equation

$$\frac{\partial p(\mathbf{x}, t)}{\partial t} = -\sum_{i=1}^{N} \frac{\partial}{\partial x_i} \left[\mu_i(\mathbf{x}, t)\, p(\mathbf{x}, t)\right] + \sum_{i=1}^{N}\sum_{j=1}^{N} \frac{\partial^2}{\partial x_i\, \partial x_j} \left[D_{ij}(\mathbf{x}, t)\, p(\mathbf{x}, t)\right],$$

where $\boldsymbol{\mu} = (\mu_1, \ldots, \mu_N)$ is the drift vector and $\mathbf{D}(\mathbf{x}, t)$ is the diffusion tensor defined by

$$D_{ij}(\mathbf{x}, t) = \frac{1}{2}\sum_{k=1}^{M} \sigma_{ik}(\mathbf{x}, t)\, \sigma_{jk}(\mathbf{x}, t),$$

that is, $\mathbf{D} = \frac{1}{2}\boldsymbol{\sigma}\boldsymbol{\sigma}^\top$.

One can easily recognize that the form of the system of our interest is matching the shape of the one shown in the theorem. Therefore one can build the Fokker-Plank equation for the case of our study.

It is just a matter of algebra to show that the system of our interest is equivalent to the following Fokker-Plank formulation:

$$\begin{aligned} &\frac{\partial P(p, q; t)}{\partial t} = -\hat{L} P(p, q; t) \\ &\text{where} \\ &\hat{L} = f(q)\frac{\partial}{\partial p} + \frac{p}{m}\frac{\partial}{\partial q} - \gamma\left(\frac{\partial}{\partial p}p + \frac{m}{\beta}\frac{\partial^2}{\partial p^2}\right) \end{aligned} \tag{3.1}$$

Since the Langevin equation of motions are equivalent to this Fokker-Plank picture, we can easily show that the dynamics samples the canonical distribution by showing that the stationary solution to the Fokker-Plank equation is indeed the Boltzmann distribution. We look for the stationary solutions since once the equilibrium condition is reached, it is

no more left. Moreover, if the stationary solution is unique, then every time dependent solution of the Fokker-Plank eqation tends to the stationary one in the limit $t- > \infty$, which is compatible with the idea of thermalization.

To demonstrate that the Fokker–Planck equation admits the canonical Boltzmann distribution as its stationary solution, we employ a direct method: we insert the equilibrium density into the Fokker–Planck operator and verify that the resulting time derivative vanishes identically.

As shown before, the Canonical distribution has the form:

$$\bar{P}(p,q)dpdp = \frac{1}{Z} e^{-\beta \frac{p^2}{2m}} e^{-\beta U(q)} dpdp \tag{3.2}$$

Let us write the Liouvillian operator as a summation of individual Liouvillian operators, as follows:

$$\hat{L} = \hat{L_p} + \hat{L_q} + \hat{L_\gamma}$$

where $\hat{L_p} = f(q)\frac{\partial}{\partial p}$, $\hat{L_q} = \frac{p}{m}\frac{\partial}{\partial q}$ and $\hat{L_\gamma} = -\gamma\left(\frac{\partial}{\partial p}p + \frac{m}{\beta}\frac{\partial^2}{\partial p^2}\right)$.

Now by simple algebra we can compute the action of each of these operators on the Canonical distribution:

$$\hat{L_p}\bar{P} = -f(q)\frac{\beta p}{m}\bar{P}$$

$$\hat{L_q}\bar{P} = -\frac{\beta p}{m}\frac{\partial U}{\partial q}\bar{P} = f(q)\frac{\beta p}{m}\bar{P}$$

$$\hat{L_\gamma}\bar{P} = 0$$

Therefore, since the contributions given by the actions of $\hat{L_p}$ and $\hat{L_q}$ are equal and opposite, they cancel out and yield to:

$$\hat{L}\bar{P} = 0$$

This proves that the canonical distribution is exactly the stationary solution for the Fokker-Plank equation[2].

[2]one can easily see this by plugging this result into the Fokker-Plank equation

3.2. Langevin integration scheme

Let us now examine the canonical distribution in greater detail. If our simulation begins from a non-equilibrium (non-thermalized) configuration, the phase-space distribution $P(q,p,0)$ will not initially be canonical. Hence, we must investigate how this arbitrary initial density evolves under the Fokker–Planck equation

$$\frac{\partial P}{\partial t} \;=\; \mathcal{L}_{\mathrm{FP}}\, P$$

to approach the equilibrium distribution as $t \to \infty$.

The evolution of the phase–space probability density [3] is given by:

$$P(p,q;t+\Delta t) = \mathrm{e}^{-\Delta t \hat{L}} P(p,q;t), \qquad\qquad \hat{L}\,\bar{P} = 0,$$

so that the canonical density is invariant,

$$\mathrm{e}^{-\Delta t \hat{L}}\bar{P} = \bar{P}, \qquad \bar{P}(p,q;t+\Delta t) = \bar{P}(p,q;t).$$

Writing the Liouvillian as the sum of two contributions,

$$\hat{L} = \hat{L}_{pq} + \hat{L}_{\gamma}, \qquad \hat{L}_{pq} = f(q)\,\partial_p + \frac{p}{m}\,\partial_q, \qquad \hat{L}_{\gamma} = -\gamma\left(p\,\partial_p + \frac{m}{\beta}\,\partial_p^2\right),$$

and applying a symmetric Trotter factorization one obtains:

$$\mathrm{e}^{-\Delta t \hat{L}} \simeq \mathrm{e}^{-\frac{\Delta t}{2}\hat{L}_{\gamma}} \mathrm{e}^{-\Delta t \hat{L}_{pq}} \mathrm{e}^{-\frac{\Delta t}{2}\hat{L}_{\gamma}},$$

which leaves the equilibrium measure unchanged because each factor separately satisfies $\mathrm{e}^{-\frac{\Delta t}{2}\hat{L}_{\gamma}}\bar{P} = \bar{P}$ and $\mathrm{e}^{-\Delta t \hat{L}_{pq}}\bar{P} = \bar{P}$. The resulting trajectory is only approximate, with local error of order $\mathcal{O}(\Delta t^3)$[4], but the long–time sampling of the canonical ensemble is exact [3].

Although the factor $\mathrm{e}^{-\frac{\Delta t}{2}\hat{L}_{\gamma}}$ can be evaluated analytically, the factor $\mathrm{e}^{-\Delta t \hat{L}_{pq}}$ has no closed–form expression for a generic potential $U(q)$ (as shown in the Appendix B.2) and must be

[3] formal solution to the general Fokker-Plank equation

[4] error in the trajectory not on the sampling introduced by the spliting

split further[5]. Splitting $\hat{L}_{pq}$ into

$$\hat{L}_p = f(q)\,\partial_p, \qquad \hat{L}_q = \frac{p}{m}\,\partial_q,$$

and applying the usual velocity-Verlet ordering yields the practical integrator

$$\mathrm{e}^{-\Delta t \hat{L}} \simeq \mathrm{e}^{-\frac{\Delta t}{2}\hat{L}_\gamma}\mathrm{e}^{-\frac{\Delta t}{2}\hat{L}_p}\mathrm{e}^{-\Delta t \hat{L}_q}\mathrm{e}^{-\frac{\Delta t}{2}\hat{L}_p}\mathrm{e}^{-\frac{\Delta t}{2}\hat{L}_\gamma},$$

In this case, however, the splitting of L_{pq} does not yield exact sampling of the canonical distribution, but only an approximation.[6]

With this Trotter–Strang splitting of the propagator in hand, it is natural to examine its effect on the phase-space coordinates. As demonstrated in Appendix B.2, each sub-propagator admits a closed-form update that acts exclusively on either the positions or the momenta.

Therefore, it is now easy to explicit the integrating scheme here.
We recall from the appendix, that the first step[7] of integration is:

$$p^* = p_t\,\mathrm{e}^{-\gamma\frac{\Delta t}{2}} + \sqrt{\frac{m}{\beta}\big(1-\mathrm{e}^{-2\gamma\frac{\Delta t}{2}}\big)}\;\eta, \qquad \eta \sim \mathcal{N}(0,1).$$

which we can rewrite as:

$$p^* = c_1 p(t) + c_2 R_1(t)$$

where $c_1 = \mathrm{e}^{-\gamma\frac{\Delta t}{2}}$ and $c_2 = \sqrt{\frac{m}{\beta}(1-c_2^2)}$

[5]When an operator that defines an evolution equation has no closed–form propagator, one seeks a splitting into a product of sub–operators that do admit closed forms. Each sub–move can then be performed exactly; the approximation error is confined to the non-commutativity of the factors and is therefore smaller than the error incurred by integrating the original operator with a purely numerical scheme. This is because if we integrate numerically a one step scheme with Euler or Runge-Kutta we introduce errors of first or second order. Instead if we proceed with the Trotter splitting as seen here the error is in third order in time

[6]As we have seen, the canonical distribution is invariant under the exact propagators generated by L_γ and L_{pq}, but not under the Trotter–Strang decomposition

$$\exp\!\big(-\tfrac{\Delta t}{2}\hat{L}_p\big)\,\exp\!\big(-\Delta t\,\hat{L}_q\big)\,\exp\!\big(-\tfrac{\Delta t}{2}\hat{L}_p\big),$$

which only approximates $\exp(-\Delta t\,\hat{L}_{pq})$ and therefore fails to preserve the canonical distribution exactly.

[7]Friction-noise kick

Then we apply the second step of the integration [8], acting again on the momentum

$$p^{**} = p^{*} + f(q(t))\frac{\Delta t}{2}$$

Now we apply the third step of integration, which acts on q and advances the position of a time step Δt:

$$q(t+\Delta t) = q(t) + \frac{p^{**}}{m}\Delta t = q(t) + \frac{p^{*}}{m}\Delta t + \frac{f(q(t))\Delta t^2}{2m}$$

where, in the last equality, we have already substituted the expression for p^{**}.

We now apply the forth step [9], which acts on the momenta but with the new calculated positions:

$$p^{***} = p^{**} + f(q(t+\Delta t))\frac{\Delta t}{2} = p^{*} + \frac{f(q(t) + f(q(t+\Delta t)))}{2}\Delta t$$

where, again, we have performed the necessary substitutions.

Now let us apply the last step [10], which is again:

$$p(t+\Delta t) = c_1 p^{***} + c_2 R_2(t+\Delta t)$$

We thus recover the same integration scheme reported by Ceriotti *et al.*,[3], which we reproduce below:

$$\begin{aligned} p\left(t^{+}\right) &= c_1 p(t) + c_2 R_1(t) \\ q(t+\Delta t) &= q(t) + \frac{p\left(t^{+}\right)}{m}\Delta t + \frac{f(q(t))}{m}\frac{\Delta t^2}{2} \\ p\left(t^{-}+\Delta t\right) &= p\left(t^{+}\right) + \frac{f(q(t)) + f(q(t+\Delta t))}{2}\Delta t \\ p(t+\Delta t) &= c_1 p\left(t^{-}+\Delta t\right) + c_2 R_2(t+\Delta t) \end{aligned} \tag{3.3}$$

and where the first and last sub-steps represent the thermostat action, i.e. the exact propagation with $e^{-\frac{\Delta t}{2}L_\gamma}$. We denote by $p(t^{+})$ the momentum immediately *after* this thermostat step, and by $p(t^{-})$ the momentum immediately *before* it.

[8] deterministic kick
[9] second deterministic Kick
[10] Friction-noise kick

There are two important concepts to highlight here: the first one is that c_1 is tightly related to the γ factor: the higher the friction the lower c_1 is, and therefore the more the update in p are influenced by the stochasticity. Instead, the relation that links c_2 and c_1 guarantees the correctness of the sampling [3], since if p is distributed as a guassian (as it should be at equilibrium), then its update through $\hat{L}_\gamma$ is still a gaussian, as proved in the Appendix B.3.

3.3. PIMD Langevin Thermostat

We now turn to the implementation of a Langevin thermostat for the ring–polymer Hamiltonian. The stochastic dynamics can be applied either (i) directly to the beads in Cartesian space or (ii) after transforming the polymer into its normal-mode coordinates. We adopt the latter approach: working in normal modes yields a thermostatting algorithm that is only a slight modification of the Path-Integral Molecular-Dynamics scheme already presented in Eq. (1.58).

In the ring-polymer representation, the Hamiltonian is more elaborate, because it includes both the external potential and the harmonic couplings between neighbouring beads, namely:

$$
\begin{aligned}
H_n(\mathbf{p},\mathbf{q}) &= H_n^0(\mathbf{p},\mathbf{q}) + V_n(\mathbf{q}),\\
H_n^0(\mathbf{p},\mathbf{q}) &= \sum_{i=1}^{N}\sum_{j=1}^{n}\left[\frac{\left[p_i^{(j)}\right]^2}{2m_i} + \frac{1}{2}\,m_i\omega_n^2\big(q_i^{(j)} - q_i^{(j-1)}\big)^2\right],\\
V_n(\mathbf{q}) &= \sum_{j=1}^{n} V\big(q_1^{(j)},\ldots,q_N^{(j)}\big).
\end{aligned}
$$

Now we can proceed to find the Hamilton's equations for each bead

$$
\dot{q}_i^{(j)} = \frac{\partial H_n}{\partial p_i^{(j)}} = \frac{p_i^{(j)}}{m_i},
$$

$$
\dot{p}_i^{(j)} = -\frac{\partial H_n}{\partial q_i^{(j)}} = -m_i\omega_n^2\Big(2q_i^{(j)} - q_i^{(j-1)} - q_i^{(j+1)}\Big) - \frac{\partial V\big(q_1^{(j)},\ldots,q_N^{(j)}\big)}{\partial q_i^{(j)}},
$$

with $q_i^{(n+1)} \equiv q_i^{(1)}$.

To thermostat the ring polymer, we augment the momentum equations of motion by adding a friction term and its corresponding stochastic (Gaussian) force. For every i, j

we choose a friction coefficient $\gamma^{(j)}$[11] and write the Itô stochastic differential system as:

$$\begin{aligned} \mathrm{d}q_i^{(j)} &= \frac{p_i^{(j)}}{m_i}\,\mathrm{d}t, \\ \mathrm{d}p_i^{(j)} &= \big[-m_i\omega_n^2\big(2q_i^{(j)} - q_i^{(j-1)} - q_i^{(j+1)}\big) - \partial_{q_i} V\big(q_1^{(j)},\dots,q_N^{(j)}\big) - \gamma_i\, p_i^{(j)}\big]\mathrm{d}t \\ &\quad + \sqrt{2m_i\gamma_i k_{\mathrm{B}}T}\;\mathrm{d}W_i^{(j)}(t). \end{aligned} \tag{3.4}$$

where $\{\mathrm{d}W_i^{(j)}\}$ are independent Wiener increments satisfying $\langle \mathrm{d}W_i^{(j)}(t)\,\mathrm{d}W_{i'}^{(j')}(t)\rangle = \delta_{ii'}\delta_{jj'}\,\mathrm{d}t$.

Using the standard definition of a Liouvillian, together with the ring-polymer Hamiltonian derived earlier, we can now write explicit expressions for (i) the Liouvillian of the free ring-polymer (kinetic + spring) part and (ii) the Liouvillian that corresponds to the external-potential part.

$$\begin{aligned} \hat{L}_0 &= \{H_n^0,\,\cdot\} = \sum_{i=1}^{N}\sum_{j=1}^{n}\Big[\frac{p_i^{(j)}}{m_i}\,\frac{\partial}{\partial q_i^{(j)}} - m_i\omega_n^2\big(2q_i^{(j)} - q_i^{(j-1)} - q_i^{(j+1)}\big)\,\frac{\partial}{\partial p_i^{(j)}}\Big], \\ \hat{L}_V &= \{V_n,\,\cdot\} = \sum_{i=1}^{N}\sum_{j=1}^{n}\Big[-\frac{\partial}{\partial q_i^{(j)}}V\big(q_1^{(j)},\dots,q_N^{(j)}\big)\,\frac{\partial}{\partial p_i^{(j)}}\Big]. \end{aligned} \tag{3.5}$$

Given the Langevin equations in (3.4), the corresponding Fokker–Planck equation can be constructed. For the full ring-polymer phase-space density $P(\{q,p\},t)$ it reads:

$$\begin{aligned} \frac{\partial P}{\partial t} &= -\sum_{i=1}^{N}\sum_{j=1}^{n}\frac{\partial}{\partial q_i^{(j)}}\Big[\frac{p_i^{(j)}}{m_i}\,P\Big] \\ &\quad -\sum_{i=1}^{N}\sum_{j=1}^{n}\frac{\partial}{\partial p_i^{(j)}}\Big[\big(-m_i\omega_n^2(2q_i^{(j)} - q_i^{(j-1)} - q_i^{(j+1)}) - \partial_{q_i^{(j)}}V - \gamma_i\,p_i^{(j)}\big)\,P\Big] \\ &\quad +\sum_{i=1}^{N}\sum_{j=1}^{n}\frac{m_i\,\gamma_i}{\beta}\frac{\partial^2 P}{\partial\big(p_i^{(j)}\big)^2}\,. \end{aligned}$$

[11] Following Ceriotti *et al.*,[6], we assign a bead–dependent friction coefficient, i.e. each normal mode of the same ring polymer is coupled to its own friction constant rather than using a single value for all beads.

Equivalently, we can write $\partial_t P = -\hat{L}\,P$, where the total Liouvillian is

$$\hat{L} = \sum_{i=1}^{N}\sum_{j=1}^{n}\Big[\frac{p_i^{(j)}}{m_i}\,\frac{\partial}{\partial q_i^{(j)}} - m_i\omega_n^2(2q_i^{(j)} - q_i^{(j-1)} - q_i^{(j+1)})\,\frac{\partial}{\partial p_i^{(j)}} - \frac{\partial V}{\partial q_i^{(j)}}\,\frac{\partial}{\partial p_i^{(j)}} + \gamma_i\Big(p_i^{(j)}\,\frac{\partial}{\partial p_i^{(j)}} + \frac{m_i}{\beta}\,\frac{\partial^2}{\partial (p_i^{(j)})^2}\Big)\Big].$$

Where one can recognize the expression for L_0 and L_V in the first part, and we can define the friction (thermostat) part alone[12] as

$$\hat{L}_\gamma = \sum_{i=1}^{N}\sum_{j=1}^{n}\gamma_i\Big(p_i^{(j)}\,\frac{\partial}{\partial p_i^{(j)}} + \frac{m_i}{\beta}\,\frac{\partial^2}{\partial (p_i^{(j)})^2}\Big). \tag{3.6}$$

We then can write:

$$\hat{L} = \hat{L}_0 + \hat{L}_V + \hat{L}_\gamma$$

where the definitions of $\hat{L}_0$, $\hat{L}_V$ and $\hat{L}_\gamma$ are the same as previously shown in (3.5) and (3.6)[13]

As we did in the previous paragraph we can now use the Trotter splitting and find:

$$e^{-\Delta t L} \simeq e^{-(\Delta t/2)L_\gamma} e^{-(\Delta t/2)L_V} e^{-\Delta t L_0} e^{-(\Delta t/2)L_V} e^{-(\Delta t/2)L_\gamma} \tag{3.7}$$

We have already derived the action of these individual propagators in the Path-Integral Molecular Dynamics chapter, when integrating the ring-polymer equations of motion.[14]. The present integration scheme differs slightly from that of the previous chapter, Eq. (1.55), because of the extra factors $e^{(\Delta t/2)\hat{L}_\gamma}$. We can nevertheless adapt the earlier algorithm shown in (1.58) simply by inserting two additional steps—one at the beginning and one at the end—to apply these thermostat operators.

[12] as one would expect from the dissertation shown in the previous paragraph for the simplified case

[13] In the case of $\hat{L}_\gamma$, the operator has the same functional form, but it is written separately for each bead of every interacting particle.

[14] It is worth emphasising that the operator $\exp(-\Delta t\,\hat{L}_0)$ has a closed-form propagator. The Liouvillian $\hat{L}_0$ stems from the "free" ring-polymer Hamiltonian H_n^0, which contains only the kinetic term and the harmonic spring coupling between adjacent beads. After transforming the polymer to normal-mode coordinates, H_n^0 decomposes into a sum of independent one–dimensional harmonic oscillators. As shown in Appendix B.2 (with the Exponential-Series argument and Quadrature argument), each oscillator can be propagated analytically; therefore the full operator $\exp(-\Delta t\,\hat{L}_0)$ can be applied exactly.

$$\begin{aligned}
\tilde{p}_i^{(k)} &\leftarrow \sum_{j=1}^{n} p_i^{(j)} C_{jk}, \\
\tilde{p}_i^{(k)} &\leftarrow c_1^{(k)} \tilde{p}_i^{(k)} + \sqrt{\frac{m_i}{\beta_n}} c_2^{(k)} \xi_i^{(k)}, \\
p_i^{(j)} &\leftarrow \sum_{k=0}^{n-1} C_{jk} \tilde{p}_i^{(k)}.
\end{aligned} \tag{3.8}$$

Where $\xi_i^{(k)}$ is a normally distributed random variable with 0 mean and unit variance and which assumes different values for every degree of freedom, each normal mode of the ring polymer, and different at each application of the iterative step. And where the coefficients $c_1^{(k)}$ and $c_2^{(k)}$ are:

$$c_1^{(k)} = e^{-(\Delta t/2)\gamma^{(k)}}$$

$$c_2^{(k)} = \sqrt{1 - \left[c_1^{(k)}\right]^2}$$

This extra step is precisely the realisation of the propagator $e^{(\Delta t/2)\hat{L}_\gamma}$ discussed in B.2.

Herein lies the chief advantage of working in the normal-mode representation when coupling the ring polymer to a Langevin thermostat. Because each mode k behaves as an independent harmonic oscillator, we can estimate an optimal friction coefficient $\gamma^{(k)}$ by analysing the *free* ring polymer in normal-mode space. [15].

If we rewrite the previously derived equations of motion in normal-mode coordinates and omit the external potential V, we obtain:

$$\begin{aligned}
\frac{d}{dt}\tilde{q}_i^{(k)} &= \frac{\tilde{p}_i^{(k)}}{m_i} \\
\frac{d}{dt}\tilde{p}_i^{(k)} &= -m_i \omega_k^2 \tilde{q}_i^{(k)} - \gamma^{(k)} \tilde{p}_i^{(k)} + \sqrt{\frac{2 m_i \gamma^{(k)}}{\beta_n}} \xi_i^{(k)}(t)
\end{aligned} \tag{3.9}$$

where $\xi_i^{(k)}(t)$ represents an uncorrelated, normally distributed random force with unit variance and zero mean $\left\langle \xi_i^{(k)} \right\rangle = 0$ and $\left\langle \xi_i^{(k)}(0) \xi_i^{(k)}(t) \right\rangle = \delta(t)$. We will then define the optimum value of the friction coefficient as the one that minimises the autocorrelation

[15] Naturally, in actual simulations one must thermalise the *entire* ring-polymer Hamiltonian—including the physical potential V—rather than the free ring polymer alone. Even so, the analysis of the free polymer offers valuable guidance for choosing the set of friction coefficients $\gamma^{(k)}$.

time of the harmonic oscillator Hamiltonian given by the formula:

$$\tau_H = \frac{1}{\langle H^2 \rangle - \langle H \rangle^2} \int_0^\infty \langle (H(0) - \langle H \rangle)(H(t) - \langle H \rangle) \rangle dt \tag{3.10}$$

The autocorrelation time τ_H quantifies how rapidly the system evolves and forgets its initial state. A small τ_H means that the energy of the free ring polymer departs from its initial value in a very short time, allowing the trajectory to sample different energy shells quickly. Once the energy fluctuations become so fast that their average correlation vanishes, the integrand in the correlation integral is effectively zero thereafter. Hence, a small autocorrelation time is synonymous with rapid exploration of phase space according to the canonical distribution.

We can now answer the earlier question: why focus on the free ring polymer? Because in this simplified setting one can derive an explicit formula for the energy autocorrelation time $\tau_H(\gamma)$ and then perform an analytical optimisation. The result provides a simple guideline for choosing the optimal friction coefficients $\gamma^{(k)}$.

Since the normal mode individual Hamiltonian for each bead is:

$$H = \frac{\left[\tilde{p}_i^{(k)}\right]^2}{2m_i} + \frac{1}{2} m_i \omega_k^2 \left[\tilde{q}_i^{(k)}\right]^2 \tag{3.11}$$

by calculating the quantities involved in the definition of τ_H we get the following form [13]:

$$\tau_H = \frac{1}{\gamma^{(k)}} + \frac{\gamma^{(k)}}{4\,\omega_k^2} \tag{3.12}$$

Then the minimum of this function is in the correspondence of the value:

$$\gamma^{(k)} = 2\omega_k \tag{3.13}$$

Note that this expression is valid only if $k > 0$, and it is not valid for the centroid mode $k = 0$. This is due to the fact that if we recall the expression for the $\omega_k = 2\omega_n \sin(k\pi/n)$. In this case if $k = 0$ then $\omega_k = 0$ and this is probelmatic, since inserting the optimal value for $\gamma^{(k)}$ into the expression for τ_0, we would get a zero in the denominator.

Therefore, it is necessary to redefine the expression for the optimal value of $\gamma^{(0)}$. Then we define $\gamma^{(0)} = \frac{1}{\tau_0}$ where τ_0 is a time constant for the centroid mode. Substituting this into the expression for computing the autocorrelation time of energy, we can again find

the value that ensures the minimisation.

In the following chapters, we will extend the standard Langevin thermostat to a more versatile framework via the Generalized Langevin Equation (GLE). We will examine the properties of its memory kernel that allow a flexible modeling of system–bath interactions. Before introducing the GLE itself, however, we first present the microscopic model of a heat bath, and show how, by eliminating its degrees of freedom, naturally yields the GLE form, highlighting its suitability for thermostat design.

4 | Modeling the action of a Heat Bath on a system

Before delving into the Generalized Langevin Equation (GLE) thermostat, it is instructive to understand why the GLE provides a natural description of system–bath coupling. To this end, we consider the paradigmatic model of a thermal reservoir: an infinite set of harmonic oscillators bilinearly coupled to our system degrees of freedom. By formally integrating out the bath coordinates, one arrives at the GLE for the system variables, complete with a memory kernel and a fluctuating force that together satisfy the fluctuation–dissipation theorem. This construction demonstrates how the GLE emerges directly from a microscopic heat-bath model and why it is particularly well suited for thermostat design.

4.1. A heat bath model

How can one model the heat bath and its action on the system analytically? One possible way, as shown in [31], is the following. Let us consider, for simplicity, a one-dimensional system consisting of a single particle of mass m, whose position is x and whose momentum is p. This particle is subject to an external potential $U(x)$. The total system, comprising the particle and the heat bath, is described by the following Hamiltonian [17]:

$$H = \frac{p^2}{2M} + U(x) + \sum_\alpha \left[\frac{p_\alpha^2}{2m_\alpha} + \frac{m_\alpha \omega_\alpha^2}{2} \left(x_\alpha - \frac{c_\alpha}{m_\alpha \omega_\alpha^2} x \right)^2 \right] \tag{4.1}$$

where we have modeled the heat bath as a collection of harmonic oscillators with masses m_α and frequencies ω_α. The variables x_α and p_α are the fictitious positions and momenta of these oscillators and, from now on we will refer to them as the degrees of freedom of the heat bath.

The c_α are coupling constants that determine how strongly each oscillator (i.e., each frequency) interacts with the system.

Conceptually, one can visualize this fictitious system as the primary particle connected via springs (with elastic constants $m_\alpha\omega_\alpha^2$) to multiple additional fictitious particles.

In what follows, we will show how this Hamiltonian yields the "Generalized Langevin Equation" by integrating out the equations of motion for the bath's degrees of freedom.

By applying Hamilton's equations, we obtain the following equations of motion for the particle of the system:

$$\begin{aligned} \dot{x} &= \frac{p}{M} \\ \dot{p} &= -\frac{\partial U}{\partial x} + \sum_\alpha c_\alpha \left(x_\alpha - \frac{c_\alpha}{m_\alpha \omega_\alpha^2} x \right) \end{aligned} \tag{4.2}$$

and for the degrees of freedom of the bath:

$$\begin{aligned} \dot{x}_\alpha &= \frac{p_\alpha}{m_\alpha} \\ \dot{p}_\alpha &= -m_\alpha \omega_\alpha^2 x_\alpha + c_\alpha x \end{aligned} \tag{4.3}$$

We now assume that the expression of $x(t)$ is known and proceed to formally integrate the equations of motion for the bath's degrees of freedom using Green's functions, as shown in Appendix C.1. The result of integration is the following expression for $x_\alpha(t)$:

$$\begin{aligned} x_\alpha(t) = x_\alpha(t_0)\cos\left(\omega_\alpha(t-t_0)\right) + \tfrac{p_\alpha(t_0)}{m_\alpha\omega_k}\sin\left(\omega_\alpha(t-t_0)\right) \\ + \tfrac{c_\alpha}{m_\alpha\omega_\alpha}\int_{t_0}^{t} \mathrm{d}s \sin\left(\omega_\alpha(t-s)\right) x(s) \end{aligned} \tag{4.4}$$

By substituting the previous expression into (4.2), we obtain:

$$\begin{aligned} \dot{p} = M\ddot{x} = &-\frac{\partial U}{\partial x} - \sum_\alpha \frac{c_\alpha^2}{m_\alpha\omega_\alpha^2} x(t) \\ &+ \sum_\alpha \frac{c_\alpha^2}{m_\alpha\omega_\alpha^2} \int_{t_0}^{t} \mathrm{d}s \omega_\alpha \sin\left(\omega_\alpha(t-s)\right) x(s) \\ &+ \sum_\alpha c_\alpha \left[q_\alpha(t_0)\cos\left(\omega_\alpha(t-t_0)\right) + \frac{p_\alpha(t_0)}{m_\alpha\omega_\alpha}\sin\left(\omega_\alpha(t-t_0)\right) \right] \end{aligned} \tag{4.5}$$

By factoring out the the coeffients in the summations of the second and third term, and by denoting as $F(t)$ the last one, we get the following expression:

$$\dot{p} = -\frac{\partial U}{\partial x} + \sum_{\alpha} \frac{c_\alpha^2}{m_\alpha \omega_\alpha^2} \left[\int_{t_0}^{t} \mathrm{d}s x(s) \frac{\partial}{\partial s} \cos\left(\omega_\alpha (t-s)\right) - x(t) \right] + F(t) \tag{4.6}$$

By partially integrating once the integral present in square brackets [1] we get:

$$\begin{aligned} \dot{p} = F(t) - \tfrac{\partial U}{\partial x} - \textstyle\sum_\alpha \tfrac{c_\alpha^2}{m_\alpha \omega_\alpha^2} \Big[\int_{t_0}^{t} \mathrm{d}s \dot{x}(s) \cos\left(\omega_\alpha (t-s)\right) \\ + x\left(t_0\right) \cos\left(\omega_\alpha \left(t - t_0\right)\right) \Big] \end{aligned} \tag{4.7}$$

If we now distribute the summation of the third term inside the squared parenthesis and denote the friction memory kernel as:

$$\gamma(t-s) = \frac{1}{M} \sum_{\alpha} \frac{c_\alpha^2}{m_\alpha \omega_\alpha^2} \cos\left(\omega_\alpha (t-s)\right) \tag{4.8}$$

we almost obtain the General Langevin equation:

$$M\ddot{x} + M \int_{t_0}^{t} \mathrm{d}s \gamma(t-s) \dot{x}(s) + \frac{\partial U}{\partial x} = -M\gamma\left(t - t_0\right) x\left(t_0\right) + F(t) \tag{4.9}$$

Before discussing the difference with the actual expression of the GLE, let us address a subtle point.
Considering the force $F(t)$, we immediately notice that it depends on the initial positions and momenta $\{x_k(t_0), p_k(t_0)\}$ of the bath oscillators at time t_0. Strictly speaking, if these initial conditions were precisely known, then $F(t)$ would be deterministic. However, this term inherits stochastic behavior, since it is practically impossible to determine all these initial variables with infinite accuracy. Consequently, the deterministic nature of $F(t)$ is effectively lost, and it is more appropriate to treat it as a fluctuating force by considering $\{x_k(t_0), p_k(t_0)\}$ as random variables following the Boltzmann distribution when the heat bath is in equilibrium.

Furthermore, we notice that $F(t)$ is a colored Gaussian fluctuating force that obeys the Fluctuation-Dissipation Theorem of the second kind (see Appendix C.2).

$$\begin{aligned} \langle F(t) \rangle_{\rho_B} &= 0 \\ \langle F(t) F(s) \rangle_{\rho_B} &= MkT\gamma(t-s) \end{aligned} \tag{4.10}$$

[1] Notice that the $x(t)$ present in the square brackets cancels after the integration by parts since a positive $x(t)$ arises from evaluating the first term in the integration by parts

where the averages have been taken with respect to a bath in equilibrium

$$\rho_B = Z^{-1} \exp\left\{-\beta\left[\sum_\alpha \left(\frac{p_\alpha^2}{2m_\alpha} + \frac{m_\alpha \omega_\alpha^2}{2} q_\alpha^2\right)\right]\right\} \tag{4.11}$$

Let us now discuss how to obtain the final form of the GLE. The expression obtained before is slightly different from the actual GLE since the additional term $-M\gamma\left(t-t_0\right)x\left(t_0\right)$ appears.
However, we can absorb it into the definition of the fluctuating force, by defining

$$\eta(t) = -M\gamma\left(t-t_0\right)x\left(t_0\right) + F(t)$$

In this way, one can recover the correct expression of the GLE:

$$M\ddot{x} + M\int_{t_0}^{t} \mathrm{d}s\gamma(t-s)\dot{x}(s) + \frac{\partial U}{\partial x} = \eta(t) \tag{4.12}$$

However, we should now care about the new properties of the stochastic force, since it should still be a stationary gaussian process with zero mean and that satisfies the fluctuation dissipation relation of the second kind, in order to be a properly defined GLE.

At a first glance, this could seem a problem, since $\eta(t)$ has no more a stationary autocorrelation, if we average using the Boltzmann distribution of the unperturbed bath, that we have used before. However, it recovers this property if conditionally averaged with the equilibrium distribution of the complete system bath+system (this is provable in a similar way to the one we have used in the appendix to show that $F(t)$ follows the FDT).

$$\begin{aligned}&\hat{\rho}\left(\{p_\alpha, q_\alpha\} \mid x\left(t_0\right) = x\right)\\ &\quad = Z^{-1} \exp\left\{-\beta\left[\sum_\alpha \frac{p_\alpha^2}{2m_\alpha} + \frac{m_\alpha\omega_\alpha^2}{2}\left(q_\alpha - \frac{c_\alpha}{m_\alpha\omega_\alpha^2}x\right)^2\right]\right\}\end{aligned} \tag{4.13}$$

However, one might argue that the expression for the friction memory kernel is not truly general since it is expressed as a summation of cosine terms. How can this be a generic form of a memory friction kernel? The key is to recognize that the frequencies ω_k can be distributed according to an arbitrary distribution. This allows the complete memory

kernel to assume any desired form.

To explore this in more detail, let us consider that the friction memory kernel is initially given as a sum over the degrees of freedom of the bath—each oscillator characterized by its own mass, frequency, and coupling constant.
Now, by taking the limit as the number of bath degrees of freedom tends to infinity, and by allowing the coupling constant to depend on the frequency, the summation transforms into an integral. In this limit, the general form of the friction memory kernel can be written as

$$\gamma(t) = \int_0^\infty g(\omega) \cos(\omega t)\, d\omega,$$

where

$$g(\omega) = \frac{c(\omega)}{\omega^2 m}.$$

Notice that this expression is precisely the Fourier cosine transform. Therefore, if we desire a specific functional form for $\gamma(t)$, we can obtain the corresponding function $g(\omega)$ by taking the inverse cosine transform of the desired $\gamma(t)$.

4.2. Markovian and Non Markovian dynamics

Before turning to the use of the Generalized Langevin Equation as a thermostat, we pause to examine its intrinsic properties, which will be crucial for our later developments. We begin with the simplest setting, a single particle evolving under the GLE, and then indicate how to extend to many-body systems. Note that, in this illustrative section, the particle has no direct relation to the real physical particle or the ring-polymer beads introduced previously. Our focus here is purely theoretical: to derive and understand the GLE formalism. In subsequent sections, we will show how to leverage these results for thermostatting in path-integral molecular dynamics.

Let us recall the Generalized Langevin Equation (4.12) from the previous paragraph. By relabeling the coordinate $x \to q$ and the stochastic term $\eta \to \zeta$ and $\gamma \to K$ [2], the single second-order stochastic differential equation can be written as the following system of two first-order equations:

$$\begin{aligned} \dot{q} &= p/m \\ \dot{p} &= -\frac{\partial V}{\partial q} - \int_{-\infty}^{t} K(t-s)p(s)\mathrm{d}s + \zeta(t) \end{aligned} \tag{4.14}$$

We immediately notice that the generalized Langevin dynamics is non-Markovian: the momentum update at time t depends not only on its current value but also on its entire past history, weighted by the friction memory kernel $K(t-s)$.

Moreover, as discussed in the previous section, if we wish to enforce the sampling of the Boltzmann distribution at thermal equilibrium, a fluctuation-dissipation relation must hold. Consequently, the Gaussian noise is no longer uncorrelated in time but instead reflects the specific form of the friction memory kernel.

Integrating such an equation of motion is impractical because it requires [7]:

- Generating Gaussian random numbers with prescribed temporal correlations,
- Storing the complete past trajectory of $p(t)$
- Evaluating an integral over the entire history of the system to compute the friction term.

To overcome these difficulties, we demonstrate that the non-Markovian dynamics can be transformed into a Markovian one by extending the dynamics through the addition

[2] These new symbols will be more convenient for the rest of the discussion.

of extra fictitious momenta. These additional degrees of freedom restore a Markovian structure to the system.

In order to substantiate this approach, we will work backward by showing that a system of Markovian differential equations can be recast into a single non-Markovian differential equation. We first illustrate this process with a simple example and then formalize the approach in a more general context.

As an example, we will show how non-Markovian behavior can arise is by elimination of the momentum in the Brownian motion of a harmonic oscillator. The equation of motions are:

$$\begin{aligned} \frac{dx}{dt} &= \frac{p}{m} \\ \frac{dp}{dt} &= -m\omega^2 x - \zeta \frac{p}{m} + F(t) \end{aligned} \tag{4.15}$$

By formally integrating the second equation we get the expression:

$$p(t) = \int_{-\infty}^{t} ds e^{-\xi(t-s)} \left[-m\omega_0^2 x(s) + F(s) \right] \tag{4.16}$$

Substituting in the first equation of the system we get:

$$\frac{dx}{dt} = -\int_{-\infty}^{t} ds K(t-s)x(s) + F_{\text{eff}}(t) \tag{4.17}$$

were we have set

$$K(t-s) = \omega_0^2 e^{-\xi(t-s)}, \quad F_{\text{eff}}(t) = \frac{1}{m} \int_{-\infty}^{t} ds e^{-\xi(t-s)} F(s) \tag{4.18}$$

The full calculations are available in the Appendix D.1.

A more detailed and generic dissertation has been developed by Zwanzig in [31].

From a strictly Markovian system of two coupled stochastic equations, we can eliminate the auxiliary variable to obtain a single non-Markovian equation for the primary coordinate. This reduced equation features a convolution with a friction memory kernel and a fluctuating force whose statistics are time-correlated, reflecting their dependence on the system's entire history.
Crucially, the kernel that emerges is not arbitrary but takes the specific exponential form inherited from the original coupling. The reverse construction, embedding a non-

Markovian process into a higher-dimensional Markovian system by introducing auxiliary variables, is likewise possible, but only when the memory kernel is exactly exponential. This raises an important question: if we are given an arbitrary memory kernel, how can we still cast the dynamics into a Markovian form? The main idea will be developed in the following dissertation.

Let us now show that if the kernel is expressed as a combination of exponentials, then one can introduce a corresponding number of fictitious variables to convert the system into a Markovian dynamics. Once this is demonstrated, one can further argue that, for any general kernel, an approximation can be made by representing it as a sum of exponentials. This exponential expansion then allows us to embed the non-Markovian dynamics into an extended Markovian framework.

Suppose we have a memory kernel given by a linear combination of exponentials,

$$K(t) = \sum_{k=1}^{N} c_k \, e^{-\lambda_k \, t}, \tag{4.19}$$

The non-Markovian evolution equation for a generic variable $x(t)$ is:

$$\dot{x} = -\int_0^t K(t-s)\, x(s)\, ds + F(t) \tag{4.20}$$

$$= -\int_0^t \left[\sum_{k=1}^{N} c_k \, e^{-\lambda_k \, (t-s)}\right] x(s)\, ds + F(t) \tag{4.21}$$

$$= -\sum_{k=1}^{N} c_k \int_0^t e^{-\lambda_k \, (t-s)}\, x(s)\, ds + F(t) = -\sum_{k=1}^{N} c_k y_k + F(t). \tag{4.22}$$

Where we have defined the auxiliary variables

$$y_k(t) \;:=\; \int_0^t e^{-\lambda_k \, (t-s)}\, x(s)\, ds, \quad k = 1, \ldots, N. \tag{2}$$

Let's now differentiate $y_k(t)$ with respect to t:

$$\dot{y}_k(t) = \frac{d}{dt}\int_0^t e^{-\lambda_k\,(t-s)}\,x(s)\,ds \tag{4.23}$$

$$= x(t) - \lambda_k \int_0^t e^{-\lambda_k\,(t-s)}\,x(s)\,ds \tag{4.24}$$

$$= x(t) - \lambda_k\, y_k(t). \tag{4.25}$$

where we have used Liebeniz Integral Rule.

Then we can rewrite the initial equation as the following Markovian system:

$$\begin{cases} \dot{x}(t) = -\sum_{k=1}^{N} c_k\, y_k(t) + F(t), \\ \dot{y}_k(t) = -\lambda_k\, y_k(t) + x(t), \quad k = 1, \ldots, N, \end{cases} \tag{6}$$

[3]

However, in the previous case, we are not considering that the fluctuating force $F(t)$ could be some colored noise, since we could require that it obeys the fluctuation dissipation theorem. In this case, when we start from the non Markovian dynamics, $F(t)$ has a prescribed correlation function of the form:

$$\langle F(t)F\,(t')\rangle = k_B T K\,(|t-t'|) \tag{4.26}$$

When we construct the Markovian dynamics, we would like to rewrite it using only uncorrelated noise. To fulfill this purpose, we should introduce some more support variables to the system.

First of all, let's start by rewriting the FD relation using the expression of the kernel:

$$\langle F(t)F\,(t')\rangle = k_B T K\,(|t-t'|) = k_B T \sum_{k=1}^{N} c_k e^{-\lambda_k|t-t'|} \tag{4.27}$$

[3]For completeness, in Appendix D.2 we examine a memory kernel given by a continuous superposition of exponentials (Laplace transform). Such a kernel cannot be represented by a finite system of Markovian differential equations, but only by an infinite hierarchy. Therefore, in the main text we restrict ourselves to kernels admitting a discrete Laplace representation, which can be embedded in a finite-dimensional Markovian form. One might note that a discrete Laplace expansion only covers functions defined on the positive real axis; however, this is sufficient here because the memory kernel enters only through the integral over $s \in [0, t]$, so that only non-negative arguments $t - s$ ever appear.

For each k let's introduce the variables z_k such that they obey the Ornstein–Uhlenbeck Process defined as:

$$\dot{z}_k(t) = -\lambda_k z_k(t) + \sqrt{2\lambda_k}\xi_k(t) \tag{4.28}$$

where

$$\langle \xi_k(t)\xi_j\left(t'\right)\rangle = \delta_{kj}\delta\left(t-t'\right) \tag{4.29}$$

It is a well-known property of the Ornstein–Uhlenbeck process that the autocorrelation function of z_k satisfies [12]:

$$\langle z_k(t)z_k\left(t'\right)\rangle = e^{-\lambda_k|t-t'|} \tag{4.30}$$

Now, if one writes $F(t)$ as[4]:

$$F(t) = \sum_{k=1}^{N} \sigma_k z_k(t) \tag{4.31}$$

Since the processes z_k are independent we can show that:

$$\langle F(t)F\left(t'\right)\rangle = \sum_{k=1}^{N} \sigma_k^2 \left\langle z_k(t)z_k\left(t'\right)\right\rangle = \sum_{k=1}^{N} \sigma_k^2 e^{-\lambda_k|t-t'|} \tag{4.32}$$

where we have to choose $\sigma_k^2 = k_B T c_k$ in order for this expression to match Eq. (4.27).

Therefore, the complete extended equations of motions become:

$$\begin{aligned}
\dot{x}(t) &= -\sum_{k=1}^{N} c_k y_k(t) + \sum_{k=1}^{N} \sqrt{k_B T c_k} z_k(t) \\
\dot{y}_k(t) &= -\lambda_k y_k(t) + x(t), \quad k = 1, \ldots, N \\
\dot{z}_k(t) &= -\lambda_k z_k(t) + \sqrt{2\lambda_k}\xi_k(t), \quad k = 1, \ldots, N
\end{aligned} \tag{4.33}$$

which can be recast to a matricial form. The general form used to implement thermostatting and molecular dynamics will be displayed in the next chapter.

[4] we are now guessing the shape of $F(t)$

5 | GLE Thermostat

We now leverage the theory developed above to demonstrate the principal advantages and practical implementation of the GLE as a simulation thermostat.

The key benefit of the GLE is its flexibility: by tailoring the form of the memory kernel, one can precisely control the sampling characteristics of a molecular-dynamics trajectory. In the following discussion, we will show how different kernel choices affect sampling efficiency and dynamical properties.

As before, we first illustrate the method on the simplest system, a single particle, and then indicate how to generalise to many-body systems. Our presentation follows the treatment of Ceriotti *et al.* [8], and for clarity we adopt their notation throughout.

The equations of motion are:

$$\begin{aligned} \dot{q} &= p/m \\ \dot{p} &= -\frac{\partial V}{\partial q} - \int_{-\infty}^{t} K(t-s)p(s)\mathrm{d}s + \zeta(t) \end{aligned} \tag{5.1}$$

As explained in the previous chapter, in order to bypass the complexity of dealing with a non-Markovian formulation directly, we supplement the system with n additional degrees of freedom, $\{s_i\}$, which are linearly coupled to the physical momentum and among themselves. The resulting SDE can be cast into the compact form[1]:

$$\begin{aligned} \dot{q} &= p \\ \begin{pmatrix} \dot{p} \\ \dot{\mathbf{s}} \end{pmatrix} &= \begin{pmatrix} -V'(q) \\ \mathbf{0} \end{pmatrix} - \begin{pmatrix} a_{pp} & \mathbf{a}_p^T \\ \overline{\mathbf{a}}_p & \mathbf{A} \end{pmatrix} \begin{pmatrix} p \\ \mathbf{s} \end{pmatrix} + \begin{pmatrix} b_{pp} & \mathbf{b}_p^T \\ \mathbf{b}_p & \mathbf{B} \end{pmatrix} (\boldsymbol{\xi}) \end{aligned} \tag{5.2}$$

Here, $\boldsymbol{\xi}$ is a vector of $n+1$ uncorrelated Gaussian random numbers, with

$$\xi_i(t)\,\xi_j(0) = \delta_{ij}\,\delta(t).$$

[1] we choose a unitary mass.

We can notice that if n=0 we recover the standard Ornstein–Uhlenbeck process for the momentum equation only, present in the simple Langevin Equation dissertation.

We will adopt the following notation to distinguish between matrices acting on the full state vector $x = (q, p, s)^T$ or on parts of it:

$$\begin{array}{c|ccc} & q & p & \mathbf{s} \\ q & m_{qq} & m_{qp} & \mathbf{m}_q^T \\ p & \bar{m}_{qp} & m_{pp} & \mathbf{m}_p^T \\ \mathbf{s} & \bar{\mathbf{m}}_q & \bar{\mathbf{m}}_p & \mathbf{M} \end{array} \quad \left.\begin{array}{l} \\ \\ \\ \end{array}\right\} \mathbf{M}_p \Bigg\} \mathbf{M}_{qp}$$

5.1. Free-Particle Limit

To build intuition, we first consider the simplest case in which no external forces act on the particle (i.e. $\partial V/\partial q = 0$). In this limit, the coordinate q decouples and we focus on the coupled dynamics of momentum p and auxiliary variables $\mathbf{s}$.

Starting from the GLE in Eq. (5.1), the momentum equation reduces to

$$\dot{p}(t) = -\int_{-\infty}^{t} K(t-s)\, p(s)\, \mathrm{d}s + \zeta(t)\,. \tag{5.3}$$

Ceriotti *et al.* [8] show that, for this free-particle OU embedding, the memory kernel $K(t)$ is related to the drift matrix $\mathbf{A}_p$ and coupling vector $\mathbf{a}_p$ by

$$K(t) = 2\, a_{pp}\, \delta(t) \;-\; \mathbf{a}_p^T\, e^{-|t|\mathbf{A}}\, \bar{\mathbf{a}}_p\,. \tag{5.4}$$

Moreover, since $(p, \mathbf{s})$ evolves as a multivariate Ornstein–Uhlenbeck process, its stationary covariance $\mathbf{C}_p = \langle (p, \mathbf{s})^T (p, \mathbf{s}) \rangle$ must satisfy the the following relation

$$\mathbf{A}_p\, \mathbf{C}_p + \mathbf{C}_p\, \mathbf{A}_p^T = \mathbf{B}_p\, \mathbf{B}_p^T\,. \tag{5.5}$$

To enforce canonical sampling at temperature T, hence enforce the FDT, it is simply possible to set $\mathbf{C}_p = k_\mathrm{B}T\, \mathbf{I}$, which implies the standard noise–kernel relation $H(t) = \langle \zeta(t)\, \zeta(0) \rangle = k_\mathrm{B}T\, K(t)$. [2] Enforcing FDT, Eq. (5.5) becomes:

$$\mathbf{A}_p + \mathbf{A}_p^T = \beta \mathbf{B}_p\, \mathbf{B}_p^T\,. \tag{5.6}$$

[2] Here, $H(t)$ is just the notation to indicate the correlation of the fluctuating force

Since $\mathbf{A}_p$ may be chosen as any real matrix with eigenvalues of positive real part[3], the resulting form of $K(t)$ is a superposition of exponentially damped oscillations. This shows that our finite-dimensional Markovian embedding can realize a broad class of non-Markovian kernels.

Finally, because the q–$\mathbf{s}$ coupling vanishes in this free limit, the conclusions above extend unchanged once an arbitrary physical potential $V(q)$ is reintroduced. The full GLE then reads

$$\begin{aligned}\dot{q} &= p,\\ \dot{p} &= -\frac{\partial V}{\partial q} - \int_{-\infty}^{t} K(t-s)\, p(s)\, \mathrm{d}s + \zeta(t)\,,\end{aligned}$$

which is the non-Markovian dynamics we set out to thermostat.

5.2. Harmonic Oscillator toy model

Let us delve deeper into the thermostating properties of the GLE by examining a simple, but still highly instructive, toy model. Most MD thermostats rely on only a handful of tunable parameters, often chosen by trial and error [8]. By contrast, a GLE–based thermostat introduces many more degrees of freedom, and hence many more parameters, to optimize, as one does when using colored-noise methods to sample nuclear quantum effects in solids [5]. Finding the optimal parameter set for efficient thermostatting is therefore substantially more complex.

Before delving into the full parameter-fitting procedure, we consider the paradigmatic example of a one-dimensional harmonic oscillator,

$$V(q) = \tfrac{1}{2}\,\omega^2 q^2.$$

Despite its simplicity, this model allows us to derive many key properties of GLE thermostatting in closed form—and it also represents the small-oscillation limit of any nonlinear system around equilibrium.

In this setting,the force term becomes linear and the dynamics of $\boldsymbol{x} = (q, p, \boldsymbol{s})T$ is the OU process defined by the equation:

$$\dot{\mathbf{x}} = -\mathbf{A}_{qp}\mathbf{x} + \mathbf{B}_{qp}\boldsymbol{\xi} \tag{5.7}$$

Since the degrees of freedom $\boldsymbol{s}$ are uncoupled from the variable q the most of the entries

[3]Positive real parts ensure that the homogeneous dynamics decays as $e^{-\Re(\lambda)\,t}$.

of $\boldsymbol{A}_{qp}$ and $\boldsymbol{B}_{qp}$ are null.

In matricial form, Eq.(5.2) becomes:

$$\begin{pmatrix} \dot{q} \\ \dot{p} \\ \dot{\mathbf{s}} \end{pmatrix} = - \begin{pmatrix} 0 & -1 & \mathbf{0} \\ \omega^2 & a_{pp} & \mathbf{a}_p^T \\ \mathbf{0} & \bar{\mathbf{a}}_p & \mathbf{A} \end{pmatrix} \begin{pmatrix} q \\ p \\ \mathbf{s} \end{pmatrix} + \begin{pmatrix} 0 & 0 & \mathbf{0} \\ 0 & \mathbf{B}_p & \\ \mathbf{0} & & \end{pmatrix} \begin{pmatrix} 0 \\ \boldsymbol{\xi} \end{pmatrix} \tag{5.8}$$

As noted by Ceriotti *et al.* [8], in the harmonic-oscillator case the propagator can be obtained in closed form.
With the analytical propagator in hand, any ensemble average or time-correlation function can be computed exactly. Of particular interest are quantities such as $\langle q^2 \rangle$ and $\langle p^2 \rangle$, and their time correlations $\langle q^2(t)\, q^2(0) \rangle$. The latter reveals how rapidly the system loses memory of its initial state and approaches equilibrium, thereby quantifying the strength of coupling to the heat bath, and the efficiency with which the thermostat samples the target frequency spectrum.

As we saw for the standard Langevin equation, one selects the friction coefficient γ to minimise the energy autocorrelation time τ_H, thereby maximising sampling efficiency at a specific frequency ω [4]. In the GLE framework, however, we no longer have a single γ, but rather an entire set of parameters encoded in the matrix $\mathbf{A}_p$.[5] Therefore, the GLE allows efficient sampling across a whole band of frequencies. Our task is therefore to devise a prescription for selecting the entries of $\mathbf{A}_p$ (or, more generally, $\mathbf{A}_{qp}$) so as to optimise sampling over a desired spectral range.

As we have seen before, we again initially focus on the dependency of the correlation times, whose definitions are:

$$\begin{aligned} \tau_V &= \frac{1}{\langle V^2 \rangle} \int_0^\infty \langle (V(t) - \langle V \rangle)(V(0) - \langle V \rangle) \rangle \mathrm{d}t \\ \tau_H &= \frac{1}{\langle H^2 \rangle} \int_0^\infty \langle (H(t) - \langle H \rangle)(H(0) - \langle H \rangle) \rangle \mathrm{d}t. \end{aligned} \tag{5.9}$$

In the harmonic-oscillator case, the availability of an analytical propagator $G(t; \mathbf{A}_p, \omega)$ allows us to derive closed-form expressions the energy autocorrelation time τ_H and the potential autocorrelation time τ_V. Since the propagator depends explicitly on both the

[4] at the expense of less efficient sampling of others

[5] When the fluctuation, dissipation theorem is enforced—so that $\mathbf{A}_p$ and $\mathbf{B}_p$ satisfy Eq. (5.6), specifying $\mathbf{A}_p$ automatically fixes $\mathbf{B}_p$ and thus the noise properties for all modes at temperature T.

oscillator frequency ω and the GLE drift matrix $\mathbf{A}_p$, these correlation times

$$\tau_H = \tau_H(\mathbf{A}_p, \omega), \quad \tau_V = \tau_V(\mathbf{A}_p, \omega)$$

are themselves functions of $\mathbf{A}_p$ and ω.

In the absence of any auxiliary variables, one recovers the familiar Langevin-thermostat expressions for the autocorrelation times:

$$\tau_H(\omega) = \frac{1}{a_{pp}} + \frac{a_{pp}}{4\,\omega^2}, \quad \tau_V(\omega) = \frac{1}{2\,a_{pp}} + \frac{a_{pp}}{2\,\omega^2}. \tag{5.10}$$

Let us now introduce an efficiency cost function motivated by the following reasoning: since sampling a normal mode of frequency ω requires at least a time on the order of its vibrational period [8], we define the sampling efficiency as

$$\kappa(\omega) \;=\; \big[\tau(\omega)\,\omega\big]^{-1}. \tag{5.11}$$

This quantity measures how effectively the thermostat couples to a mode of frequency ω. By construction, $\kappa(\omega) \in [0, 1]$, and larger values indicate more efficient coupling. In a log–log plot, the efficiency curve for the simple Langevin thermostat attains its maximum value $\kappa = 1$ exactly at $\omega = \gamma/2$ and then decreases linearly away from that peak, as shown in Figure 5.1

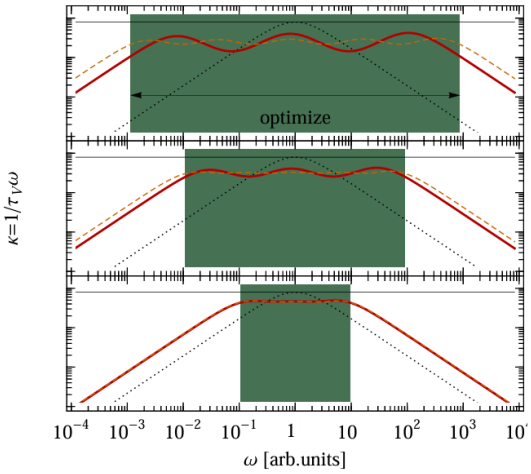

Figure 5.1: Sampling efficiency $\kappa(\omega)$ for a GLE-based thermostat (solid line) versus a standard Langevin thermostat (dashed line), reproduced from Ceriotti *et al.* [8].

To optimise the GLE parameters, one selects a discrete set of target frequencies $\{\omega_i\}$

spanning the range $(\omega_{\min}, \omega_{\max})$. Starting from an initial guess for the drift matrix $\mathbf{A}_p$, one computes $\kappa(\omega_i)$ for each ω_i. One then adjust $\mathbf{A}_p$ so as to maximise the worst-case efficiency

$$\min_i \kappa(\omega_i),$$

aiming for a flat, near-unity $\kappa(\omega)$ profile over the desired frequency band.

This approach is particularly valuable when the system's normal modes are unknown or impractical to analyse: by tuning the free parameters in $\mathbf{A}_p$, one can ensure efficient and frequency-independent thermostatting across the range $(\omega_{\min}, \omega_{\max})$, which is chosen based on prior physical insight into the system's characteristic frequencies.

To conclude this paragraph, in the general case of a non-harmonic potential, where the forces are no longer linear, no closed-form propagator exists as it does for the harmonic example. However, by employing a Trotter–Strang splitting of the full propagator into analytically tractable sub-steps, one can still construct an integration scheme that delivers efficient sampling across the desired frequency range [8]. This splitting closely mirrors the Trotter–Strang scheme used to integrate the standard Langevin dynamics.

5.3. GLE for ring polymer representation

The thermostats based on the equivalence between a non-Markovian GLE and a Markovian dynamics in an extended phase space admit a simple matrix representation, as shown earlier. We can leverage this insight to construct a GLE thermostat for the PIMD formalism.

As previously noted, the integration scheme will closely resemble that of the simple Langevin dynamics. Importantly, because the GLE is invariant under orthonormal transformations [8], there is no need to transform to normal-mode coordinates: we may apply the thermostat directly in the bead representation.

Consequently, the final integrator is obtained by replacing the steps shown in Eq. (3.8) with the GLE-extended updates:

$$\mathbf{p}_i^{(j)} \leftarrow \mathbf{C}_1 \mathbf{p}_i^{(j)} + \sqrt{\frac{m_i}{\beta_n}} \mathbf{C}_2 \boldsymbol{\xi}_i^{(j)}. \tag{5.12}$$

Here $\boldsymbol{\xi}_i^{(j)}$ is a vector of $n_s + 1$ independent Gaussian numbers,

$$\mathbf{p}_i^{(j)} = \begin{pmatrix} p_i^{(j)} \\ \mathbf{s}_i^{(j)} \end{pmatrix}$$

is a vector containing the momentum of bead j and n_s auxilliary momenta $\mathbf{s}_i^{(j)}$, and

$$\mathbf{C}_1 = e^{-(\Delta t/2)\boldsymbol{\gamma}^T} \tag{5.13}$$

and

$$\mathbf{C}_2^T\mathbf{C}_2 = \mathbf{I} - \mathbf{C}_1^T\mathbf{C}_1 \tag{5.14}$$

are the appropriate generalisations of the correspoding scalar relations that we have seen in the LE application.

Note that γ is the friction matrix optimised as described in the previous paragraph, on top of which we construct $\mathbf{C}_1$ and $\mathbf{C}_2$.

6 | Nose Hoover Thermostat

Let us now introduce, in a more general way, an alternative thermostatting scheme. We focus first on the method originally proposed by Nosè and later reformulated by Hoover. We will then briefly discuss its ergodicity limitations, introduce the Nosè–Hoover chain extension, and conclude with its application to the PIMD formalism.

6.1. Nosè Thermostat

The core idea of Nosè was to augment the N-body Lagrangian of the system with an additional degree of freedom s representing the heat bath. Specifically, one defines the extended Lagrangian as:

$$\mathcal{L}_{\text{Nose}} = \sum_{i=1}^{N} \frac{m_i}{2} s^2 \dot{\mathbf{r}}_i^2 - \mathcal{U}\left(\mathbf{r}^N\right) + \frac{Q}{2}\dot{s}^2 - \frac{L}{\beta}\ln s \tag{6.1}$$

Here, s and its conjugate momentum p_s are introduced as the fictitious coordinate and momentum of a single "bath" particle of mass Q, representing the additional degrees of freedom of the heat reservoir. Moreover, L is a tunable parameter that controls the coupling to the heat bath, and is chosen to ensure correct sampling of the Boltzmann distribution; we will clarify its role in the following discussion.

As one may notice, the key distinction between this deterministic Nosè–Hoover thermostat and the stochastic methods, that we have discussed earlier, is that Nosè–Hoover relies exclusively on deterministic equations of motion rather than leveraging random forces.

From the extended Lagrangian defined above, the conjugate momenta follow immediately as:

$$\begin{aligned} \boldsymbol{p}_{\mathrm{i}} &\equiv \frac{\partial \mathcal{L}}{\partial \dot{\mathbf{r}}_{\mathrm{i}}} = \mathrm{m_i}\ \mathrm{s}^2 \dot{\mathbf{r}}_{\mathrm{i}} \\ \boldsymbol{p}_{\mathrm{s}} &\equiv \frac{\partial \mathcal{L}}{\partial \dot{s}} = \mathrm{Q}\dot{s}. \end{aligned} \tag{6.2}$$

And then we can construct the following Hamiltonian:

$$\mathcal{H}_{\text{Nose}} = \sum_{i=1}^{N} \frac{\mathbf{p}_i^2}{2m_i s^2} + \mathcal{U}\left(\mathbf{r}^N\right) + \frac{p_s^2}{2Q} + \mathrm{L}\frac{\ln s}{\beta} \tag{6.3}$$

As shown in [11], for an N-particle system the extended Hamiltonian samples the microcanonical ensemble of $6N+2$ degrees of freedom, so that the number of accessible states at fixed energy is given by:

$$Q_{\text{Nose}} = \frac{1}{N!}\int \mathrm{dp_s}\ \mathrm{d}s\ \mathrm{d}\mathbf{p}^{\mathrm{N}}\ \mathrm{d}\mathbf{r}^{\mathrm{N}}\delta\left(\mathrm{E} - \mathcal{H}_{\text{Nose}}\right) \tag{6.4}$$

If we now introduce the variable $p_i' = p_i/s$, we can rewrite the $\mathcal{H}_{\text{Nose}}$ as:

$$\mathcal{H}_{\text{Nose}} = H(\mathbf{p}', \mathbf{r}) + \frac{p_s^2}{2Q} + \mathrm{L}\frac{\ln s}{\beta} \tag{6.5}$$

where we have defined:

$$\mathcal{H}\left(\mathbf{p}', \mathbf{r}\right) = \sum_{i=1}^{N} \frac{\mathbf{p}_{\mathrm{i}}'^2}{2m_{\mathrm{i}}} + \mathcal{U}\left(\mathbf{r}^{\mathrm{N}}\right) \tag{6.6}$$

by applying the substitution from $\mathbf{p}$ to $\mathbf{p}'$ in Eq. (6.4), and by expanding the expression of the $\mathcal{H}_{\text{Nose}}$ in the argument of the δ, we get:

$$\begin{aligned} Q_{\text{Nose}} &= \frac{1}{\mathrm{N!}}\int \mathrm{d}p_s\ \mathrm{d}s\ \mathrm{d}\mathbf{p}'^N \mathrm{d}\mathbf{r}^{\mathrm{N}}\ \mathrm{s}^{3\ \mathrm{N}} \\ &\times \delta\left[\sum_{i=1}^{N} \frac{\mathbf{p}_i'^2}{2m_i} + \mathcal{U}\left(\mathbf{r}^{\mathrm{N}}\right) + \frac{\mathrm{p_s^2}}{2Q} + \frac{\mathrm{L}}{\beta}\ln s - \mathrm{E}\right] \end{aligned} \tag{6.7}$$

For a δ function, whose argument is itself a function $h(s)$, we can write

$$\delta[h(s)] = \delta\left(s - s_0\right) / \left|h'\left(s_0\right)\right|,$$

where $h(s)$ is a function that has a single root at s_0. Therefore, by applying this rule to the Dirac delta in the integral, and making some manipulations[1], we get the following formula:

$$Q_{\text{Nose}} = C\frac{1}{\mathrm{N!}}\int \mathrm{d}\mathbf{p}'^N\ \mathrm{d}\mathbf{r}^{\mathrm{N}} \exp\left[-\beta\frac{3\ \mathrm{N}+1}{\mathrm{L}}\mathcal{H}\left(\mathbf{p}', \mathbf{r}\right)\right] \tag{6.8}$$

By inspecting this result, one sees that setting $L = 3N+1$ makes $Q_{\text{Nosé}}$ precisely the Boltzmann weight for an ensemble of particles with coordinates $\mathbf{r}$ and momenta $\mathbf{p}'$. Con-

[1] we omit for brevity the calculations

sequently, for any phase-space observable $A(\mathbf{r}, \mathbf{p}')$, its ensemble average becomes:

$$\langle \mathcal{A}(\mathbf{p}/\mathrm{s}, \mathbf{r}) \rangle_{\mathrm{Nose}} \equiv \frac{\int \mathrm{d}\mathbf{p}'^N \ \mathrm{d}\mathbf{r}^N \mathcal{A}\left(\mathbf{p}', \mathbf{r}\right) \exp\left[-\beta \mathcal{H}\left(\mathbf{p}', \mathbf{r}\right)(3\ \mathrm{N}+1)/\mathrm{L}\right]}{\int \mathrm{d}\mathbf{p}'^N \ \mathrm{d}\mathbf{r}^N \exp\left[-\beta \mathcal{H}\left(\mathbf{p}', \mathbf{r}\right)(3\ \mathrm{N}+1)/\mathrm{L}\right]} \tag{6.9}$$

Now, multiplying both numerator and denominator by $1/N!$[2] and setting $L = 3N+1$, the denominator becomes the canonical partition function. Hence, the ratio reduces exactly to the canonical thermal average of $A(\mathbf{r}, \mathbf{p}')$.

$$\langle \mathcal{A}(\mathbf{p}/\mathrm{s}, \mathbf{r}) \rangle_{\mathrm{Nose}} = \frac{(1/\mathrm{N}!) \int \mathrm{d}\mathbf{p}'^N \ \mathrm{d}\mathbf{r}^{\mathrm{N}} A\left(\mathbf{p}', \mathbf{r}\right) \exp\left[-\beta \mathcal{H}\left(\mathbf{p}', \mathbf{r}\right)\right]}{\mathrm{Q(NVT)}} = \langle A\left(\mathbf{p}', \mathbf{r}\right) \rangle_{\mathrm{NVT}} \tag{6.10}$$

Assuming the system is ergodic, the previous average in the ensamble must be equal to the time average:

$$\bar{A} = \lim_{\tau \to \infty} \frac{1}{\tau} \int_0^{\tau} \mathrm{dt} A(\mathbf{p}(\mathrm{t})/\mathrm{s}(\mathrm{t}), \mathbf{r}(\mathrm{t})) \equiv \langle A(\mathbf{p}/\mathrm{s}, \mathbf{r}) \rangle_{\mathrm{Nose}} \tag{6.11}$$

It is now instructive to consider the role of the variable s in some detail. In the ensamble average presented before, the phase space is spanned by the coordinates $\mathbf{r}$ and the scaled momenta $\mathbf{p}'$. As the scaled momentum is most directly related to observable properties[3], we refer to p' as the real momentum, while p is interpreted as a virtual momentum. We make the same real–virtual distinction for the other variables, always indicating real variables with a prime to distinguish them from their virtual counterparts.

The real and virtual variables are related by[4]:

$$\begin{aligned} \mathrm{r}' &= \mathrm{r} \\ \mathrm{p}' &= \mathrm{p}/\mathrm{s} \\ \mathrm{s}' &= \mathrm{s} \\ \Delta\mathrm{t}' &= \Delta\mathrm{t}/\mathrm{s} \end{aligned} \tag{6.12}$$

From the last relation, it follows that s acts as a time-scaling factor. This means that

[2]Depending on the definition of $Q_{\mathrm{Nosé}}$, a normalization constant C may also appear.

[3]Because, as shown above, ensemble averages of an observable A can be computed using the primed momentum variables.

[4]One might ask why the time variable is scaled in the same way of the momentum. This is easily showable by considering the extended Lagrangian of Nosè. The kinetic term of the system of N bodies is contaminated by the presence of the s^2. In a normal Lagrangian one would expect only the positions and mass to appear in the form $m(\frac{dr_i}{dt})^2$. One can account for the appearance of s by considering the term $s^2\dot{r}^2$ as the derivative with respect to a time primed t' such that $\frac{dr_i}{dt'} = \frac{dr_i}{dt}\frac{dt}{dt'} = s\dot{r}_i$ so that $\frac{dt}{dt'} = s$.

during a simulation in which we consider the step of integration δt constant, the real $\delta t'$ fluctuates. This is the case of the sampling of the equation that we have written before, and that calculates the average of A in time t. Since we have introduced the real time, we could also ask ourself if it is possible to sample with equally defined steps in real time $\delta t'$. The answer is positive, and we are going to show why. If we rewrite Eq. (6.11) using primed varibales we get:

$$\lim_{\tau' \to \infty} \frac{1}{\tau'} \int_0^{\tau'} dt' A\left[\mathbf{p}\left(t'\right)/s\left(t'\right), \mathbf{r}\left(t'\right)\right] \tag{6.13}$$

Now we have that this relation samples (in time) the canonical distribution. Since Eq. (6.12) is valid, the relation $dt' = dt/s$ holds, and therefore the relation between the integration extremes of the time averages in the case of sampling with constant intervals in t or t' is:

$$\tau' = \int_0^{\tau} \mathrm{dt1/s(t)} \tag{6.14}$$

We are going to use this relation soon. We can manipulate the expression (6.13) as:

$$\begin{aligned} &\lim_{\tau' \to \infty} \frac{1}{\tau'} \int_0^{\tau'} d\mathrm{t}' A\left[\mathbf{p}\left(\mathrm{t}'\right)/\mathrm{s}\left(\mathrm{t}'\right), \mathbf{r}\left(\mathrm{t}'\right)\right] \\ &\quad = \lim_{\tau' \to \infty} \frac{\tau}{\tau'} \frac{1}{\tau} \int_0^{\tau} \mathrm{dt} A[\mathbf{p}(\mathrm{t})/\mathrm{s}(\mathrm{t}), \mathbf{r}(\mathrm{t})]/\mathrm{s}(\mathrm{t}) \end{aligned} \tag{6.15}$$

by using (6.14) we get:

$$\begin{aligned} &= \frac{\lim_{\tau \to \infty} \frac{1}{\tau} \int^{\tau} \mathrm{dt} A[\mathbf{p}(\mathrm{t})/\mathrm{s}(\mathrm{t}), \mathbf{r}(\mathrm{t})]/\mathrm{s}(\mathrm{t})}{\lim_{\tau \to \infty} \frac{1}{\tau} \int_0^{\tau} \mathrm{dt1/s(t)}} \\ &= \langle \mathrm{A}(\mathbf{p}/\mathrm{s}, \mathbf{r})/\mathrm{s} \rangle / \langle 1/\mathrm{s} \rangle \end{aligned} \tag{6.16}$$

where the last equality holds due to ergodicity. To conclude our point, we have to prove that the last term is equal to the canonical average of A.

In order to do so, let us revisit the partition function of Eq. (6.4). We perform the same manipulations as before, but now include a factor of $1/s$ under the integral[5]. Reapplying the Dirac delta constraint then yields the transformed partition function:

$$Q_{Nose} = C \frac{1}{\mathrm{N!}} \int \mathrm{d}\mathbf{p}'^{N} \; \mathrm{d}\mathbf{r}^{\mathrm{N}} \exp\left[-\beta \frac{3\ \mathrm{N}}{\mathrm{L}} \mathcal{H}\left(\mathbf{p}', \mathbf{r}\right)\right] \tag{6.17}$$

[5]This factor ensures that we obtain the distribution of the scaled variables divided by s, as when computing averages of the form $\langle A/s \rangle$.

In other words, the ensemble average of $\dfrac{A(\mathbf{p}/s,\mathbf{r})}{s}$ under the original Nosé distribution (with $L = 3N+1$) can be equivalently written as the average of $A(\mathbf{p}/s,\mathbf{r})$ under the new distribution

$$\exp\Big[-\beta\,\frac{3N}{L}\,\mathcal{H}(\mathbf{p}',\mathbf{r})\Big].$$

6

$$\begin{aligned}\frac{\langle A(\mathbf{p}/\mathrm{s},\mathbf{r})/\mathrm{s}\rangle}{\langle 1/\mathbf{s}\rangle} &\equiv \frac{\left\{\frac{\int \mathrm{dp}'^N \mathrm{dr}^N\ \mathrm{A}(\mathbf{p}',\mathbf{r})\exp[-\beta\mathcal{H}(\mathbf{p}',\mathbf{r})3\ \mathrm{N/L}]}{\int \mathrm{dp}'^N \mathrm{dr}^N \exp[-\beta\mathcal{H}(\mathbf{p}',\mathbf{r})3(\ \mathrm{N+1})/\mathrm{L}]}\right\}}{\left\{\frac{\int \mathbf{dp}'^N \mathrm{dr}^N \exp[-\beta[\mathcal{H}(\mathbf{p}',\mathbf{r})3\ \mathrm{N/L}]}{\int \mathrm{dp}^N \mathrm{dr}^N \exp[-\beta[\mathcal{H}(\mathbf{p}',\mathbf{r})|3(\ \mathrm{N+1})/\mathrm{L}]}\right\}} \\ &= \frac{\int \mathrm{d}\mathbf{p}'^N\ \mathrm{d}\mathbf{r}^{\mathrm{N}}\ \mathrm{A}(\mathbf{p}/\mathrm{s},\mathbf{r})\exp\left[-\beta\mathcal{H}\left(\mathbf{p}',\mathbf{r}\right)3\ \mathrm{N/L}\right]}{\int \mathrm{d}\mathbf{p}'^N\ \mathrm{d}\mathbf{r}^N \exp\left[-\beta\left[\mathcal{H}\left(\mathbf{p}',\mathbf{r}\right)\right]3\ \mathrm{N/L}\right]} \\ &= \langle A(\mathbf{p}/\mathbf{s},\mathbf{r})\rangle_{\mathrm{NVT}}.\end{aligned} \tag{6.18}$$

where the last equality is true only if we take $L = 3N$.

This shows that, if we evolve the extended system using the primed variables, and record their trajectories $(\mathbf{r}'(t),\mathbf{p}'(t))$, then the canonical thermal average of any observable $A(\mathbf{r},\mathbf{p})$ for the original system is recovered as the long-time average of $A(\mathbf{r}'(t),\mathbf{p}'(t))$ via Eq. (6.13).

Indeed, we could instead evolve the dynamics in the unprimed variables and compute thermal averages via Eq. (6.11). However, as we will demonstrate, the approach using the primed variables is more convenient.

Now we have the following question to answer: how do we find the equations of motion for the primed variables?

This is a very simple task, since we can start from the equations of motion for the unprimed variables, which we obtain from the extended Hamiltonian $\mathcal{H}_{\mathrm{Nose}}$. These equations take the form:

[6] To clarify the previous point: by introducing the factor $1/s$ into the integrand and recomputing the partition function, we obtain exactly the distribution followed by the scaled variables $(\mathbf{p}/s,\mathbf{r})$. Thus, instead of averaging A/s with the original Nosé weight, we can average A with this new distribution. The denominator of the corresponding expression involves $\langle 1/s\rangle$ under the new measure, which by construction matches the distribution of $1/s$, and similarly for all variables scaled by s.

$$\begin{aligned}
\frac{\mathrm{d}\mathbf{r}_i}{\mathrm{dt}} &= \frac{\partial \mathcal{H}_{\mathrm{Nose}}}{\partial \mathbf{p}_i} = \mathbf{p}_i / \left(\boldsymbol{m}_i \ \mathrm{s}^2\right) \\
\frac{\mathrm{d}\mathbf{p}_i}{\mathrm{dt}} &= -\frac{\partial \mathcal{H}_{\mathrm{Nose}}}{\partial \mathbf{r}_i} = -\frac{\partial \mathcal{U}\left(\mathbf{r}^{\mathrm{N}}\right)}{\partial \mathbf{r}_i} \\
\frac{\mathrm{ds}}{\mathrm{dt}} &= \frac{\partial \mathcal{H}_{\mathrm{Nose}}}{\partial p_s} = p_s / \mathrm{Q} \\
\frac{\mathrm{d}p_s}{\mathrm{dt}} &= -\frac{\partial \mathcal{H}_{\mathrm{Nose}}}{\partial \mathrm{s}} = \left(\sum_i p_i^2 / \left(m_i s^2\right) - \frac{\mathrm{L}}{\beta}\right) / \mathrm{s}
\end{aligned} \tag{6.19}$$

Now since Eq. (6.12) hold, one knows how to connect the unprimed time derivative to the primed time derivative and obtain:

$$\begin{aligned}
\frac{d\mathbf{r}_i'}{dt'} &= s\frac{d\mathbf{r}_i}{dt} = \mathbf{p}_i / \left(m_i s\right) = \mathbf{p}_i' / m_i \\
\frac{d\mathbf{p}_i'}{dt'} &= s\frac{d\mathbf{p}_i / s}{dt} = \frac{d\mathbf{p}_i}{dt} - \frac{1}{s}\mathbf{p}_i\frac{ds}{dt} \\
&= -\frac{\partial \mathcal{U}\left(\mathbf{r}'^N\right)}{\partial \mathbf{r}_i'} - \left(s' p_s' / Q\right) \mathbf{p}_i' \\
\frac{1}{s}\frac{ds'}{dt'} &= \frac{s}{s}\frac{ds}{dt} = s' p_s' / Q \\
\frac{d\left(s' p_s' / Q\right)}{dt'} &= \frac{s}{Q}\frac{dp_s}{dt} \\
&= \left(\sum_i p_i'^2 / m_i - \frac{L}{\beta}\right) / Q
\end{aligned} \tag{6.20}$$

Where we set $L = 3N$. One can show that these equations allow for a conserved quantity which is[7]:

$$H'_{\mathrm{Nose}} = \sum_{i=1}^{N} \frac{\mathbf{p}_i'^2}{2m_i} + \mathcal{U}\left(\mathbf{r}'^N\right) + \frac{s'^2 p_s'^2}{2Q} + \mathrm{L}\frac{\ln\ \mathrm{s}'}{\beta} \tag{6.21}$$

However, this is *not* the Hamiltonian for the primed variables, because if we were to derive Hamilton's equations from this expression we would not recover the correct equations of motion for the primed variables, as obtained above.[8] Nevertheless, the fact that this quantity remains conserved throughout the integration provides a valuable check on the accuracy of the numerical scheme.

[7] It is very easy to show this, since we can simply take the time derivative of the allegedly conserved quantity, and insert the expressions for the time derivtives of the primed variables that we have shown before. All the terms cross out, hence proving the quote.

[8] The difference arises because the original $H_{\mathrm{Nosé}}$ comes from a Lagrangian formulation, whereas the expression obtained here does not.

6.2. Hoover Implementation

As seen, the Nosé equations of motion can be written either in terms of the virtual variables or in terms of the real (physical) variables. In practical simulations it is inconvenient to integrate using fluctuating time intervals, so the real-variable formulation is recommended.[9] Hoover has shown that the equations derived by Nosé can be further simplified. In the equations of motions for the primed varibales, the variables s', p'_s, and Q occur only as $s'p'_s/Q$. To simplify these equations, we can introduce the thermodynamic friction coefficient $\xi = s'p'_s/Q$. The equations of motion then become (dropping the primes and using dots to denote time derivatives)

$$\begin{aligned}
\dot{\mathbf{r}}_i &= \mathbf{p}_\mathrm{i}/\mathrm{m_i} \\
\dot{\mathbf{p}}_\mathrm{i} &= -\frac{\partial \mathcal{U}\left(\mathbf{r}^\mathrm{N}\right)}{\partial \mathbf{r}_\mathrm{i}} - \xi \mathbf{p}_\mathrm{i} \\
\dot{\xi} &= \left(\sum_i \mathrm{p_i^2}/m_i - \frac{\mathrm{L}}{\beta}\right)/\mathrm{Q} \\
\dot{\mathbf{s}}/\mathrm{s} &= \frac{\mathrm{d}\ln\ \mathrm{s}}{\mathrm{dt}} = \xi.
\end{aligned}$$

However, the last equation is not necessary, since the first three are enough to determine how the entire system of variables evolves. However, if we solve the fourth as well, we get the evolution of s, and as said before, one can use the fact that H'_{Nose} is conserved in time to show the quality of the integration. If one rewrites the H'_{Nose} with the introduction of the new variable ξ one gets:

$$H_\mathrm{Nose} = \sum_{i=1}^{N} \frac{p_i^2}{2m_i} + \mathcal{U}\left(r^N\right) + \frac{\xi^2 Q}{2} + \mathrm{L}\frac{\ln s}{\beta} \tag{6.22}$$

where $L = 3N$ if we want to sample the thermal canonical disitrbution with the primed variables.[10]

[9] However, one could argue that there is no a priori reason to insist on constant steps in the scaled time rather than in the physical time; the choice of which time coordinate to discretize uniformly is not uniquely determined.

[10] See pages 152–153 of [11] for additional properties of the Hoover formulation, including the requirement that no conserved quantities other than the total energy be admitted, and the discussion of external forces.

6.3. Nosè-Hoover chains

The previous implementation of the Nosè-Hoover thermostat is efficient in several cases but it is not still perfect. As a matter of fact, it fails to sample a canonical distribution if the system is modeled as a one dimentional harmonic oscillator [20]. In this case, the method we have shown does not yield to a canonical distribution in phase space, and the evolution of the trajectory, given an initial condition, remains bounded in a ring region around the classical Hamiltonian trajectory[11] [11]. One can show that the reason why the Nosè-Hoover algorithm can't sample the canonical distribution is linked to the fact that energy is not the only quantity conserved in this system[12].
In the case of multiple conserved quantities, one can show that by constructing a series of chained thermostats one can still sample the correct canonical distribution[13]. [23].

The equations of motion for a system of N particles coupled with M Nosé-Hoover chains are given (in real variables, hence $L = 3N$) by

$$\begin{aligned}
\dot{\mathbf{r}}_i &= \frac{\mathbf{p}_i}{m_i} \\
\dot{p}_i &= \mathbf{F}_i - \frac{p_{\varepsilon_1}}{Q_1} p_i \\
\dot{\xi}_k &= \frac{p_{\varepsilon_k}}{Q_k} \quad k = 1, \ldots, M \\
\dot{p}_{\xi_1} &= \left(\sum_i \frac{p_i^2}{m_i} - L k_B T \right) - \frac{p_{\xi_2}}{Q_2} p_{\xi_1} \\
\dot{p}_{\xi_k} &= \left[\frac{p_{\xi_k}^2}{Q_{k-1}} - k_B T \right] - \frac{p_{\xi_{k+1}}}{Q_{k+1}} p_{\xi_k} \\
\dot{p}_{\xi_M} &= \left[\frac{p_{\xi_M}^2}{Q_{M-1}} - k_B T \right].
\end{aligned}$$

For these equations of motion the conserved energy is

$$H_{NHC} = \mathcal{H}(\mathbf{r}, \mathbf{p}) + \sum_{k=1}^{M} \frac{p_{\varepsilon_k}^2}{2Q_k} + L k_B T \xi_1 + \sum_{k=2}^{M} k_B T \xi_k.$$

the latter can be used to check the quality of the integration.

[11] which is a circle
[12] The proof of this statement is in the Appendix of ref. [11]
[13] The proof of this statement is in the Appendix of ref. [11]

6.4. Application to Ring Polymer Representation

Let us now implement the Nosè–Hoover chains in our bead-representation problem. We can apply a different thermostatting chain to each polymer bead. If we rewrite the Hamiltonian of the ring-polymer representation to include the additional bath degrees of freedom, as prescribed by the Nosè–Hoover approach, and again derive the Liouvillian (in a manner similar to before), we obtain its decomposition in the following form:

$$L = L_0 + L_V + L_{NHC} \tag{6.23}$$

where L_0 and L_V are defined as in the previous chapters, and L_{NHC} is defined as the remaining part of the Liouvillian, and which includes the contributions from the bath degrees of freedom.

We can then write the following splitting for the propagator [6]:

$$e^{-\Delta t L} \simeq e^{-(\Delta t/2)L_{NHC}} e^{-(\Delta t/2)L_V} e^{-\Delta t L_0} e^{-(\Delta t/2)L_V} e^{-(\Delta t/2)L_{NHC}} \tag{6.24}$$

We can choose to work in the normal mode representation, as we did in the case of Langevin equation thermostat. Therefore, we can modify the algorithm of integration of the Langevin thermostat including the thermostatting Nosè-Hoover chain and get rid of the stochastic update of the momenta in eq.(63).

$$\frac{d}{dt}\tilde{p}_i^{(k)} = -\tilde{p}_i^{(k)} \frac{\pi_{i,1}^{(k)}}{Q^{(k)}} \tag{6.25}$$

$$\begin{aligned}
\frac{d}{dt}\pi_{i,1}^{(k)} &= \left(\frac{\left[\tilde{p}_i^{(k)}\right]^2}{m_i} - \frac{1}{\beta_n} \right) - \pi_{i,1}^{(k)} \frac{\pi_{i,2}^{(k)}}{Q^{(k)}}, \\
\frac{d}{dt}\pi_{i,l}^{(k)} &= \left(\frac{\left[\pi_{i,l-1}^{(k)}\right]^2}{Q^{(k)}} - \frac{1}{\beta_n} \right) - \pi_{i,l}^{(k)} \frac{\pi_{i,l+1}^{(k)}}{Q^{(k)}}, \\
\frac{d}{dt}\pi_{i,L}^{(k)} &= \left(\frac{\left[\pi_{i,L-1}^{(k)}\right]^2}{Q^{(k)}} - \frac{1}{\beta_n} \right) \\
\frac{d}{dt}\eta_{i,l}^{(k)} &= \frac{\pi_{i,l}^{(k)}}{Q^{(k)}}.
\end{aligned} \tag{6.26}$$

Here $\pi_{i,l}^{(k)}$ and $\eta_{i,l}^{(k)}$ are the momentum and position variables of the Nosé-Hoover chain attached to the k-th normal mode of the ring polymer for the i-th real particle, for $l = 1, \ldots, L$[14].

We can check the quality of the integration over all the steps by verifying that the following local quantity is conserved (this is given by the Thermostat properties)

$$H'^{(k)}_i = \frac{\left[\tilde{p}_i^{(k)}\right]^2}{2m_i} + \sum_{l=1}^{L} \left(\frac{\left[\pi_{i,l}^{(k)}\right]^2}{2Q^{(k)}} + \frac{\eta_{i,l}^{(k)}}{\beta_n} \right) \tag{6.27}$$

and the global conserved quantity (this is given by the Trotter splitting)

$$H'_n = H_n(\mathbf{p}, \mathbf{q}) + \sum_{i=1}^{N} \sum_{k=0}^{n-1} \sum_{l=1}^{L} \left(\frac{\left[\pi_{i,l}^{(k)}\right]^2}{2Q^{(k)}} + \frac{\eta_{i,l}^{(k)}}{\beta_n} \right) \tag{6.28}$$

We have to specify the values of the thermostat masses $Q^{(k)}$. Again, as in the previous cases, one can look for the optimal definition of these coefficients in the simplified case of the free ring polymer, by minimising the autocorrelation time of the energy.

By doing so we obtain [22]:

$$Q^{(k)} = 1/\beta_n \omega_k^2 \tag{6.29}$$

However, regarding the centroid mode, we get the very same issue that was presented in the Langevin optimisation for the friction coefficient $\gamma^{(0)}$. In fact, as before, we get $\omega_0 = 0$, and therefore a non defined $Q^{(0)}$. To solve the problem, we act as we did in the case of $\gamma^{(0)}$, by defining a separate thermostat time constant τ_0 for the centroid mode and replacing ω_0 with $1/2\tau_0$. By doing so we then get the following general definition of the fictitious masses [6]:

$$Q^{(k)} = \begin{cases} 4\tau_0^2/\beta_n, & k = 0 \\ 1/\beta_n \omega_k^2, & k > 0 \end{cases} \tag{6.30}$$

[14] l index which refers to the l-th heat bath of the chain. L is the total number of heat baths. In the previous paragraph, it was noted as M.

7 | Global vs Local Thermostats

In previous chapters, we introduced the main techniques to implement a thermostat enabling the sampling of the canonical (NVT) ensemble. Despite the variety of approaches, ranging from stochastic to deterministic thermostats, we have focused on the so-called *local thermostatting* procedures. By this term, we mean that each degree of freedom (or polymer bead) is separately and individually coupled to its own thermostat. This allows rapid and efficient thermalization of the system, leading to optimal sampling of local observables such as the potential energy or total energy.

However, certain physical properties arising from collective motions are not well sampled using local thermostats such as dynamical properties or quantities computed using time correlations. This limitation arises because the modifications introduced to the physical Hamiltonian, necessary to model the heat bath and thermostat coupling, are sufficiently intrusive to disrupt the intrinsic dynamics governing the system's internal interactions[1]. In technical terms, local thermostats can suppress the natural diffusion of phase-space trajectories along slow collective modes.

We very biefly mention how can implement the so called "Global" version of the thermostatting algorithms which couple with the system in a more gentle way, avoiding the disruption of the Hamiltonian diffusion.

7.1. Global Langevin

It has been shown by Bussi and Parrinello et al [4], that one can construct a globalized version of the Langevin thermostat by acting on the total kinetic energy of N degrees of freedom, rather than coupling each degree of freedom independently.

In the context of ring-polymer molecular dynamics, this globalized thermostat could in principle be applied to every bead labeled by the index k. However, it is has been shown that it is far more convenient to apply it only to the centroid mode ($k = 0$), while retaining the stronger, local thermostatting on the higher internal modes, which are less ergodic.

[1] Given by the physical Hamiltonian and not by the extended one

In practice, this modification, affecting only the centroid mode, requires a single change to the update of the centroid momenta in the Langevin integration step of Eq (3.8). One replaces the usual update by the following velocity-rescaling algorithm [6][2]:

$$\tilde{p}_i^{(0)} \;\leftarrow\; \alpha\, \tilde{p}_i^{(0)}, \tag{7.1}$$

where

$$\alpha^2 \;=\; c \;+\; \frac{(1-c)\Big([\xi_1^{(0)}]^2 + \sum_{i=2}^{N}[\xi_i^{(0)}]^2\Big)}{2\,\beta_n\,K} \;+\; 2\,\xi_1^{(0)}\sqrt{\frac{c\,(1-c)}{2\,\beta_n\,K}}, \tag{7.2}$$

and the sign of α is chosen according to

$$\mathrm{sign}[\alpha] = \mathrm{sign}\Big[\xi_1^{(0)} + \sqrt{\tfrac{2\,\beta_n\,K\,c}{1-c}}\Big]. \tag{7.3}$$

Here,

$$K = \sum_{i=1}^{N} \frac{\big[\tilde{p}_i^{(0)}\big]^2}{2\,m_i}, \qquad c = e^{-\Delta t\,\gamma^{(0)}}. \tag{7.4}$$

7.2. Global NH

Similarly to the Langevin case, one can construct a globalized version of the Nosé–Hoover thermostat that acts only on the ring-polymer centroid ($k = 0$). The resulting equations of motion for the centroid mode become [6]:

$$\begin{aligned}
\frac{d}{dt}\tilde{p}_i^{(0)} &= -\,\tilde{p}_i^{(0)}\,\frac{\pi_1^{(0)}}{Q^{(0)}},\\
\frac{d}{dt}\pi_1^{(0)} &= \Big(\sum_{i=1}^{N}\frac{\big[\tilde{p}_i^{(0)}\big]^2}{m_i} - \frac{N}{\beta_n}\Big) - \pi_1^{(0)}\,\frac{\pi_2^{(0)}}{Q^{(0)}},\\
\frac{d}{dt}\pi_l^{(0)} &= \Big(\frac{\big[\pi_{l-1}^{(0)}\big]^2}{Q^{(0)}} - \frac{1}{\beta_n}\Big) - \pi_l^{(0)}\,\frac{\pi_{l+1}^{(0)}}{Q^{(0)}},\\
\frac{d}{dt}\pi_L^{(0)} &= \Big(\frac{\big[\pi_{L-1}^{(0)}\big]^2}{Q^{(0)}} - \frac{1}{\beta_n}\Big),\\
\frac{d}{dt}\eta_l^{(0)} &= \frac{\pi_l^{(0)}}{Q^{(0)}}.
\end{aligned} \tag{7.5}$$

[2] just for the centroid mode

The modified conserved quantity for this single-chain thermostat is

$$H'^{(0)} = \sum_{i=1}^{N} \frac{\left[\tilde{p}_i^{(0)}\right]^2}{2\,m_i} + \sum_{l=1}^{L} \frac{\left[\pi_l^{(0)}\right]^2}{2\,Q^{(0)}} + \frac{N\,\eta_1^{(0)}}{\beta_n} + \sum_{l=2}^{L} \frac{\eta_l^{(0)}}{\beta_n}. \tag{7.6}$$

Notice that the N separate Nosé–Hoover chains of the local thermostat are replaced by a single chain that couples to the total kinetic energy of the centroid via the second equation of the block (7.5)[3]. Concretely, in that equation one sets $K = 0$ and then averages over all physical particles ($\sum_{i=1}^{N}$), whereas in the local NH algorithm (see block (6.26)), fixing $k = 0$ still updates each centroid momentum $\tilde{p}_i^{(0)}$ individually. Here, by contrast, the centroid modes of all N physical particles are thermostatted collectively.

[3]Instead of having a different chain for each centroid mode of each real particle, we use the same chain for each of the centroid mode of each real particle, as the elimination of the lower index i in the degrees of freedom of the bath suggests. Moreover, we notice that the second step is computed exploiting the total kinetic energy of the centroids of each real particle, whereas before, the very same step was dependent solely on the kinetic energy of each specific centroid (see Eq. (6.26))

8 | i-PI: Client–Server Design and Usage

i-PI is a Python 3–based path-integral engine designed for performing PIMD simulations. It was developed to be highly scalable, readily accessible, and easy to interface with external codes. Internally, i-PI employs a client–server architecture: the i-PI process functions as the server, managing the propagation of the nuclear degrees of freedom, while one or more external programs act as clients, responsible for calculating the potential energy, forces, and the virial contribution to the pressure.

i-PI maintains a list of active client processes and, at each integration step, transmits only the essential information, such as the simulation box dimensions h and the nuclear coordinates x. Each client is assumed to know the atomic species and any electronic-structure parameters from its own input. Once a client completes its calculation, it immediately returns the ionic forces f and the electronic energy U to the i-PI server. i-PI supports client programs that compute empirical, semi-empirical, or machine-learned potentials.

Lightweight Communication

To maximize compatibility, `i-PI` uses TCP/IP or UNIX sockets.
Only the minimal data required for integration is exchanged:

Server → Client: bead coordinates and, if running constant-pressure, cell parameters.

Client → Server: forces on each bead, potential energy, and optionally the virial.

Workflow

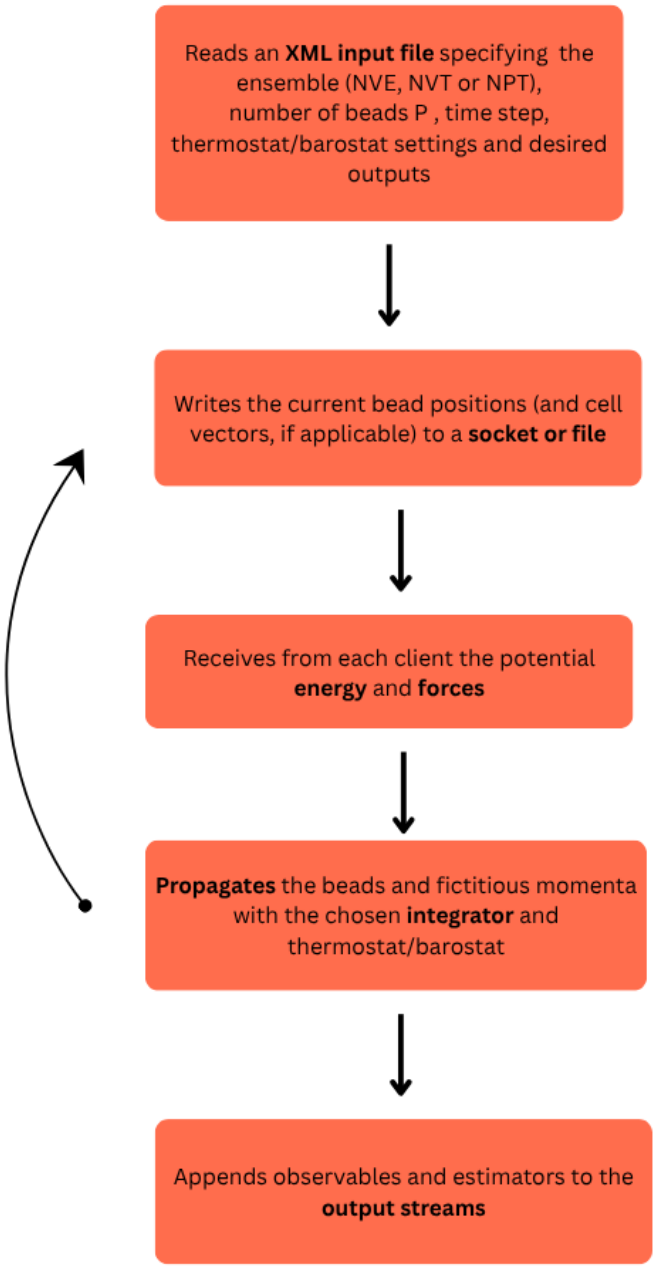
Reads an **XML input file** specifying the ensemble (NVE, NVT or NPT), number of beads P , time step, thermostat/barostat settings and desired outputs
Writes the current bead positions (and cell vectors, if applicable) to a **socket or file**
Receives from each client the potential **energy** and **forces**
Propagates the beads and fictitious momenta with the chosen **integrator** and thermostat/barostat
Appends observables and estimators to the **output streams**

XML Input Format

Simulation settings are organized in a hierarchical XML file. Each tag name corresponds to a class or variable; nested tags define object contents; attributes provide metadata such as units or algorithmic modes.
For example:

```
<simulation>
  <initialize nbeads='16'>
      <file mode='ase' units='angstrom'> mg_h_supercell_rescaled.pimd </file>
      <velocities mode='thermal' units='kelvin'>300</velocities>
  </initialize>
  ...
  <ensemble>
      <temperature units='kelvin'>300</temperature>
  </ensemble>
  ...
  <dynamics mode='nvt'>
        <thermostat mode='pile_l'>
          <tau units='femtosecond'> 25 </tau>
        </thermostat>
        <timestep units='femtosecond'> 0.5 </timestep>
  </dynamics>
      ...
</simulation>
```

Flexible Output Control

Under the '<output>' section of the XML, the user can declare multiple output streams, each managed independently:

Properties file: Records system-level quantities (total energy, temperature, pressure) in columns with headers and units. An example is shown in Fig. 9.1

Trajectory files: Dumps bead or atomic coordinates in formats readable by visualization software.

Checkpoint files: Save the full integrator state (positions, momenta, thermostat variables) at user-chosen intervals, enabling restarts from any saved point.

```
# column   1     --> step : The current simulation time step.
# column   2     --> conserved{kelvin} : The value of the conserved energy quantity per bead.
# column   3     --> temperature{kelvin} : The current temperature, as obtained from the MD kinetic energy.
# column   4     --> potential{kelvin} : The physical system potential energy.
# column   5     --> kinetic_cv{kelvin} : The centroid-virial quantum kinetic energy of the physical system.
# column   6     --> volume{angstrom3} : The volume of the cell box.
   0.00000000e+00    -6.94242176e+05     3.01553827e+02    -2.59611010e+06     6.45144800e+04     4.84136956e+03
   5.00000000e+00    -6.94230923e+05     2.96813099e+02    -2.59585937e+06     6.50712934e+04     4.84136956e+03
   1.00000000e+01    -6.94229486e+05     2.95012587e+02    -2.59593786e+06     6.48459854e+04     4.84136956e+03
   1.50000000e+01    -6.94233593e+05     2.97274334e+02    -2.59625309e+06     6.40922668e+04     4.84136956e+03
   2.00000000e+01    -6.94242730e+05     3.02705566e+02    -2.59647302e+06     6.37873510e+04     4.84136956e+03
   2.50000000e+01    -6.94229131e+05     3.03381463e+02    -2.59612039e+06     6.42827327e+04     4.84136956e+03
   3.00000000e+01    -6.94233110e+05     3.08593564e+02    -2.59646210e+06     6.40812648e+04     4.84136956e+03
```

Figure 8.1: Example of a property file illustrating its overall layout and structure.

9 | Simulation of a Para-Hydrogen system

The hydrogen molecule can exist in two distinct nuclear-spin isomers: *ortho*-hydrogen and *para*-hydrogen. Para-hydrogen consists of the two protons in a singlet state, whereas ortho-hydrogen has them in a triplet state. The abundance of para and ortho isomers in an H_2 gas mixture is temperature-dependent according to Boltzmann statistics:

$$\begin{aligned} Z_{\text{para}} &= \sum_{J=0,2,4,\ldots} (2J+1)\, \exp\!\left[-\tfrac{J(J+1)\,\hbar^2}{2\,I\,k_{\text{B}}\,T}\right], \\ Z_{\text{ortho}} &= 3 \sum_{J=1,3,5,\ldots} (2J+1)\, \exp\!\left[-\tfrac{J(J+1)\,\hbar^2}{2\,I\,k_{\text{B}}\,T}\right]. \end{aligned} \tag{9.1}$$

At standard temperature the equilibrium ratio is 3:1 (ortho:para), but below 20 K the para fraction rises to about 99.8 % [9].

Para-hydrogen has a low mass ($m \approx 2\,\text{u}$), making nuclear quantum effects significant at cryogenic temperatures ($< 30\,\text{K}$).

9.1. Set-up

We simulate a supercell containing 172 pH_2 molecules at a density $\rho = 0.019\ A^{-3}$ with periodic boundary conditions.

The aim of this study is to compute the radial distribution function of H_2 molecules at low temperature, compare the results obtained with different thermostats, and different choice of number of beads (16, 32, 64) and examine the arrangements of H atoms as the temperature decreases.

The simulations were carried out at temperatures of 1 K, 5 K, 25 K, 50 K, and 300 K using the following thermostats: PILE-L, PILE-G, and GLE, where "PILE" denotes Path–Integral Langevin Equation thermostats and the flags "L" and "G" indicate local or global coupling, respectively. Unfortunately, i-PI does not include Nosé–Hoover chains

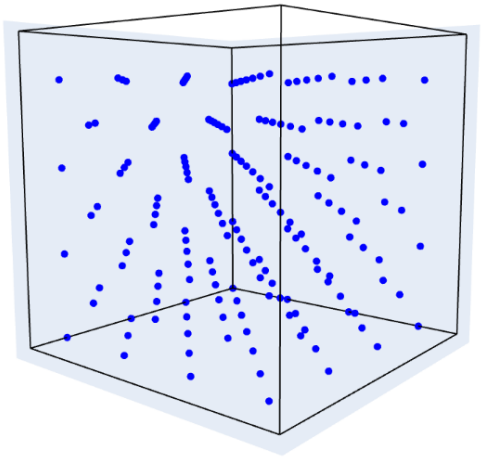

Figure 9.1: Snapshot of the initial configuration of the para-hydrogen molecules

out of the box; implementing them externally is beyond the scope of this tutorial.

The coefficient matrix **A** used in this work to implement GLE was taken from the optimal-sampling GLE parameters tabulated in `library/optimal/kh_4-4.a`, and shifted to span a frequency range from $\omega_{\min} = 0.4$ cm^{-1} to $\omega_{\max} = 4000$ cm^{-1}.

We performed NVT ensemble dynamics with a time step of 1 fs and a thermostat characteristic time of 25, over a total of 10 000 steps.

9.2. The Silvera–Goldman intermolecular potential

For our simulations of para-hydrogen we use the Silvera–Goldman intermolecular potential. A concise overview of this potential is given below.

The Silvera–Goldman intermolecular potential is built in two steps. First, an isolated H_2—H_2 pair is described by

$$\varphi_p(r) = \underbrace{Q\, e^{-(\alpha r - \beta r^2)}}_{\text{short–rangerepulsion}} - \underbrace{\left(\frac{C_6}{r^6} + \frac{C_8}{r^8} + \frac{C_{10}}{r^{10}}\right) f_c(r)}_{\text{long-range, Van-der Waals damped}} ,$$

where the switching function

$$f_c(r) = \begin{cases} \exp\left[-(1.28\, r_m/r - 1)^2\right], & r < 1.28\, r_m, \\ 1, & r \geq 1.28\, r_m, \end{cases}$$

damps the dispersion terms at very short range so that the total potential remains finite; r_m is the position of the potential minimum. The parameters are obtained from gaseous hydrogen data as shown in ref [28].

Because $\varphi_p(r)$ contains only two-body physics, it is the appropriate form for low–density gas or dilute liquid simulations, where many-body effects are negligible.

In a dense liquid or crystal, however, triple-dipole (Axilrod–Teller–Muto) interactions become appreciable. Silvera and Goldman include the isotropic average of this three-body term in an effective way, adding a single pair contribution proportional to C_9/r^9:

$$\varphi_s(r) = \varphi_p(r) + \frac{C_9}{r^9} f_c(r).$$

It is important to highlight that this correction is unimportant in the gas phase but provides the leading many-body contribution needed to reproduce lattice energies and the equation of state of the molecular solid.

9.3. Radial Distribution Function

In an ideal monoatomic gas of uniform density ρ, the probability $p(r)\,dr$ of finding another particle in a spherical shell of radius r and thickness dr around a reference particle is

$$p(r)\,dr = 4\pi r^2\,\rho\,dr,$$

since $4\pi r^2\,dr$ is the shell's volume and ρ is constant (particles do not interact). Here the r^2–dependence is purely geometric.

When interactions are present, the local density around each particle is no longer uniform. To isolate the effects of interparticle forces from this trivial geometric factor, we define the radial distribution function

$$g(r) = \frac{1}{4\pi r^2\,\rho\,N}\Big\langle \sum_{i\neq j} \delta\big(r - |\mathbf{r}_i - \mathbf{r}_j|\big)\Big\rangle,$$

where N is the total number of particles and $\langle\cdots\rangle$ denotes an ensemble (time) average. In this formulation:

- For an ideal gas, $g(r) \equiv 1$ for all r.
- Interactions produce $g(r) \approx 0$ at short distances (hard-core repulsion).
- Shell-like ordering appears as peaks in $g(r)$ at characteristic interparticle spacings.

- At long distances, $g(r) \to 1$ as spatial correlations vanish.

Practical Computation of $g(r)$

We extracted $g(r)$ from time snapshots , discarding an initial equilibration period. For each saved bead configuration:

1. Build a histogram of all pairwise distances up to a chosen $r_{\max}$, using n_{bins} equally spaced bins.
2. Normalize each bin by its spherical shell volume $4\pi r^2\, dr$ and by the factor $\rho\, N$, so that an ideal gas yields $g(r) = 1$.
3. Average the normalized histogram over all time frames to obtain $g(r)$ for each bead.
4. Finally, average these bead-wise $g(r)$ curves over all P replicas to produce the bead-averaged radial distribution function.

9.4. Results

Panels 9.2a, 9.2b, and 9.2c in Fig. 9.2 confirm the following trend: at lower temperatures the RDF peaks become higher and narrower, reflecting the fact that the H_2 molecules arrange themselves in a locked, solidified lattice and only vibrate about their equilibrium positions with smaller and smaller vibrations[1].

As the temperature increases above the freezing point (approximately 16 K) , the peaks rapidly broaden and decrease in height, and $g(r)$ converges toward 1 beyond about 4 Å, indicating that correlations at larger separations become negligible. The position of the first peak remains essentially bounded in the range [3.375, 3.675] Å over the entire temperature range, as summarized in Table 9.1.

This result is in agreement with Lindenau *et al.* [21], who studied the system at $T = 16$ K and a density of $\rho = 0.021 A^{-3}$, reporting the first RDF peak at $r \approx 3.7$ Å.

As shown in panel 9.2d, at 300 K the radial distribution function rapidly converges to unity and exhibits only a single, broad peak in the same region as at lower temperatures, as expected for gaseous H_2. Furthermore, there are no significant differences between the results obtained with 16, 32, or 64 beads.

One final clarification: at very low temperatures, our results would, in principle, require corrections to account for the symmetry-exchange properties of indistinguishable parti-

[1] by inspection of the first peak's width

cles; effects that arise from their true quantum behavior. However, incorporating such quantum-exchange corrections lies beyond the scope of the present study.

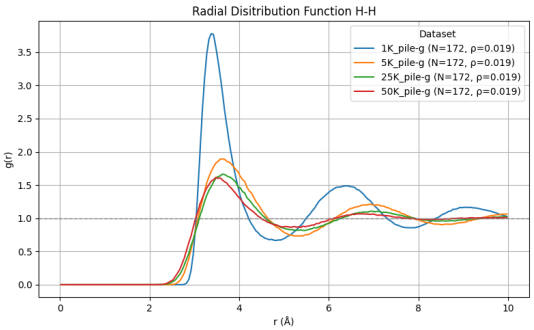

(a) Bead–averaged $g(r)$ at the chosen temperatures using the PILE-G thermostat.

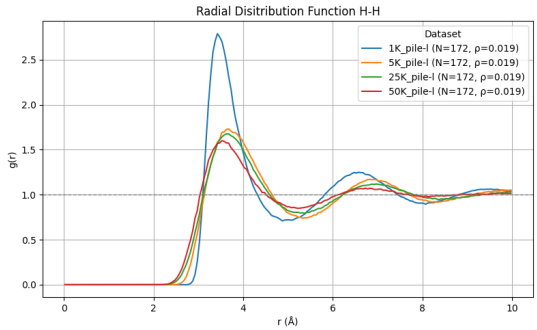

(b) Bead–averaged $g(r)$ at the chosen temperatures using the PILE-L thermostat.

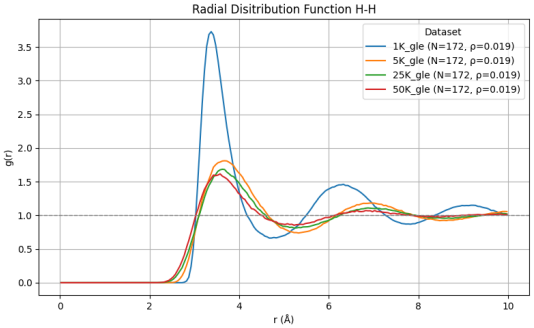

(c) Bead–averaged $g(r)$ at the chosen temperatures using the GLE thermostat.

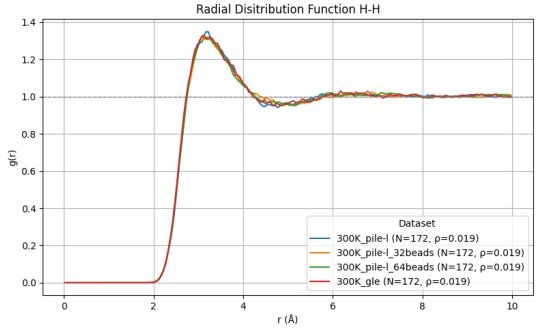

(d) Comparison of bead–averaged $g(r)$ at 300 K for PILE-L, and GLE and number of beads.

Figure 9.2: Radial distribution functions of liquid para-hydrogen obtained under different thermostat schemes and temperatures. Panels (a)–(c) show the RDFs at 1 K, 5 K, 25 K and 50 K using PILE-G, PILE-L, and GLE respectively, while panel (d) compares the bead-averaged RDFs at 300 K for PILE-L obtained with number of beads 16, 32, 64.

Table 9.1: Abscissa (Å) and ordinate of the **first** RDF as extracted from 9.2

Thermostat	1 K	5 K	25 K	50 K
PILE–L	3.425 - 2.788	3.675 - 1.731	3.675 - 1.676	3.525 - 1.601
PILE–G	3.375 - 3.779	3.625 - 1.893	3.625 - 1.665	3.475 - 1.613
GLE	3.375 - 3.727	3.675 - 1.810	3.625 - 1.684	3.575 - 1.616

Table 9.2: Abscissa (Å) and ordinate of the **second** RDF as extracted from 9.2

Thermostat	1 K	5 K	25 K	50 K
PILE–L	6.575 - 1.249	6.825 - 1.170	6.975 - 1.119	6.725 - 1.072
PILE–G	6.425 - 1.489	7.075 - 1.203	6.975 - 1.107	6.725 - 1.067
GLE	6.325 - 1.460	6.925 - 1.183	6.875 - 1.110	6.625 - 1.072

Table 9.3: Abscissa (Å) and ordinate of the **third** RDF as extracted from 9.2

Thermostat	1 K	5 K	25 K	50 K
PILE–L	9.525 - 1.062	9.875 - 1.051	9.825 - 1.030	9.725 - 1.016
PILE–G	9.075 - 1.166	9.725 - 1.053	9.925 - 1.028	9.592 - 1.010
GLE	9.175 - 1.150	9.925 - 1.058	9.925 - 1.027	9.825 - 1.018

10 | Hydrogen diffusion in Magnesium

The diffusion of hydrogen in magnesium is of great interest for practical hydrogen-storage devices aimed at green-energy applications. Magnesium offers a high gravimetric capacity (7%), but its use is hindered by sluggish hydrogen-sorption kinetics [1, 15].

Now, we aim to calculate the relevant RDFs $g_{\text{Mg–Mg}}(r)$, $g_{\text{Mg–H}}(r)$, $g_{\text{H–H}}(r)$ to reveal the structural properties of the system, and then extract an order of magnitude estimate of hydrogen's self-diffusion coefficient for a system at $T = 300$ K, and at a hydrogen-to-magnesium ratio of 8 : 128 ($MgH_{0.0625}$).

10.1. Setup and procedure

In this work a $4 \times 4 \times 4$ supercell was utilized, comprising 128 Mg atoms in the hcp crystal symmetry, with 8 H atoms randomly distributed in the lattice, as shown in Fig. 10.1.

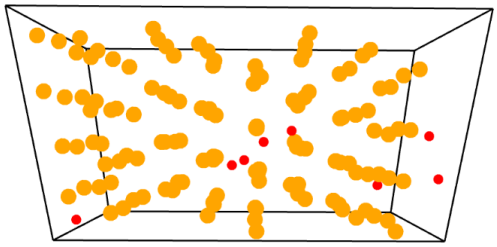

Figure 10.1: Initial configuration showing the hcp magnesium lattice (orange) with eight hydrogen atoms (red) randomly distributed.

During the thermalization phase, an NpT ensemble with fixed cell shape was employed, using a Langevin thermostat and an isobaric barostat with characteristic time $\tau = 250$ fs. The average lattice volume was determined over a 10 ps period at fixed temperatures of 300K.

This average volume was then used in subsequent NVT simulation. After 15ps of NVT dynamics, three configurations whose instantaneous energies were close to the mean NVT were extracted. To minimize correlations, each snapshot was chosen at least 3ps apart.

From each of these, a separate 10ps NVE trajectory was run.

Due to limitations in time and computational resources, the NPT, NVT, and NVE simulations were performed using 4, 10, and 2 beads, respectively.

For the force calculations, a pre-trained, fine-tuned machine-learning potential specifically parameterized for Mg–H interactions was employed: MACE_FT [2].

10.2. Diffusion calculation

For each NVE trajectory, the centroid was considered. The mean square displacement (MSD) of each centroid of Hydrogen was calculated as a time average:

$$\mathrm{MSD}(t) = \frac{1}{T-t}\int_0^{T-t} [\mathbf{r}(t+\Delta) - \mathbf{r}(\Delta)]^2 d\Delta \tag{10.1}$$

where $\mathbf{r}$ is the position of the centroid.

We discarded the initial snapshots, those farthest from equilibrium, before computing each ≈ 10 ps MSD curve.

The MSD was first averaged over all eight hydrogen atoms, and the diffusion coefficient D was then obtained by fitting the linear regime of the MSD to the Einstein relation:

$$MSD(t) = 6Dt$$

Prior to fitting, the initial sub-diffusive regime, characterized by $\mathrm{MSD}(t) \propto \sqrt{t}$, was discarded.

The NVE trajectory spanned approximately 10 ps, but the MSD is statistically reliable only at short times, where independent displacements are more numerous. Consequently, we limited our analysis to $t \leq 1.0$ ps. After discarding the initial sub-diffusive regime, the linear fit to extract D was performed over the interval

$$t \in [0.5,\ 1.0] \text{ ps}.$$

The final value of D at 300K is obtained by computing the average over the three independent NVE runs, and its uncertainty was estimated as the standard error of the

mean.

$$\mathrm{SEM} = \frac{\mathrm{SD}}{\sqrt{3}},$$

where SD is the sample standard deviation of the three D values.

10.3. Results

10.3.1. RDF

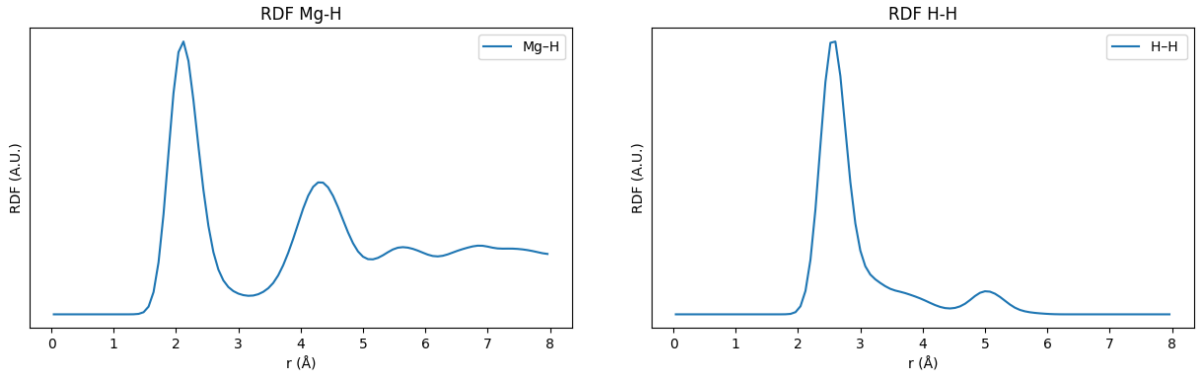

(a) Magnesium–Hydrogen RDF (b) Hydrogen–Hydrogen RDF

Figure 10.2: Radial distribution functions involving hydrogen: (a) Mg–H and (b) H–H.

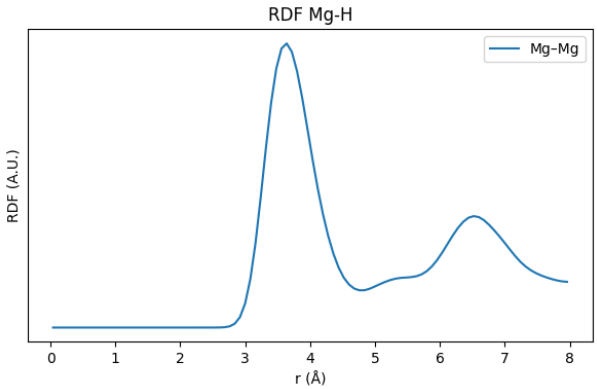

Figure 10.3: Magnesium-Magnesium RDF

The Mg–H and H–H RDFs shown in Fig. 10.2 are in good agreement with the data reported in [2]. In particular, Fig. 10.2a displays a pronounced first peak at $r \approx 2\,\text{Å}$, followed by a deep minimum near 3 Å. The zero-intensity region for $r < 2\,\text{Å}$ is correctly reproduced. Secondary features, most notably around 4–4.5 Å, also appear, although they are somewhat broader and shifted to larger r compared to the reference data.

For the H–H RDF (Fig. 10.2b), a sharp peak between 2 and 3 Å is again observed, with zero probability for $r < 2$ Å, in perfect agreement with [2]. The decay after the main peak and the shoulder extending to about 4.5 Å are present, as is a smaller tertiary peak near 5 Å.

The Mg–Mg RDF (Fig. 10.3) exhibits the expected first-neighbor peak between 3 and 4 Å, close to the known nearest-neighbor distance of 3.20 Å in hcp magnesium. However, this first peak is noticeably broader than in Ref. [2]. Two further minor peaks are visible, but their positions are slightly shifted relative to the literature data.

These discrepancies likely arise from the relatively short equilibration period and overall simulation time compared to the referenced study. Nonetheless, our simulations capture the principal structural features of hydrogen in magnesium.

10.3.2. Diffusion coefficient

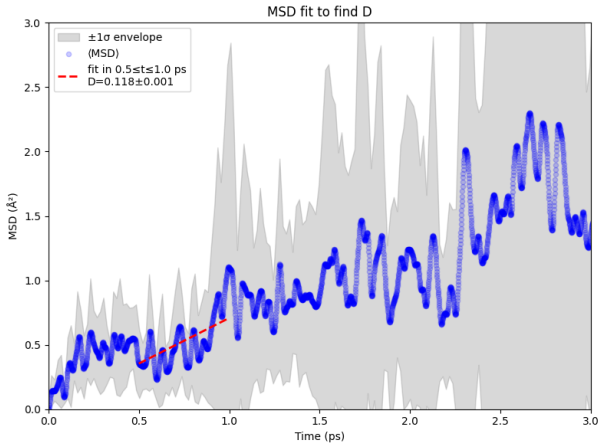

Figure 10.4: Mean-square displacement of hydrogen atoms as a function of time, with the linear fit over the chosen time window used to extract the diffusion coefficient D.

In Fig. 10.4 we show one of the three NVE MSD curves, highlighting both the sub-diffusive regime at $t < 0.5$ ps and the linear fitting window used to extract D. The diffusion coefficients obtained from the three independent NVE runs are

$$D_1 = \left(1.269 \pm 0.022\right) \times 10^{-9}\ \mathrm{m}^2/\mathrm{s},$$
$$D_2 = \left(1.180 \pm 0.014\right) \times 10^{-9}\ \mathrm{m}^2/\mathrm{s},$$
$$D_3 = \left(1.297 \pm 0.014\right) \times 10^{-9}\ \mathrm{m}^2/\mathrm{s}.$$

Averaging these results yields

$$\bar{D} = \left(1.25 \pm 0.04\right) \times 10^{-9}\ \mathrm{m}^2/\mathrm{s}.$$

This result confirms that D lies on the order of $10^{-9}\,\mathrm{m}^2/\mathrm{s}$, in agreement with the values reported in [2] using the non–fine-tuned MACE_MP potential. Although we employed the fine-tuned MACE_FT model, our estimate remains at $10^{-9}\,\mathrm{m}^2/\mathrm{s}$, rather than the $10^{-11}\,\mathrm{m}^2/\mathrm{s}$ reported for MACE_FT in the same work. We attribute this discrepancy to our very short equilibration runs and limited statistics; nonetheless, our values closely match the generic MACE_MP benchmark.

11 | Conclusions and future developments

Conclusion

This thesis has established the theoretical foundations of PIMD, providing a detailed comparison of stochastic and deterministic thermostat schemes and of local versus global coupling algorithms.

We validated these methods on para-hydrogen at cryogenic temperatures by computing bead-averaged radial distribution functions that closely reproduced literature results, and demonstrated that structural correlations remain robust down to 25K with negligible dependence on the number of beads at 300K.

We then applied our PIMD+MACE_FT workflow to hydrogen dissolved in an hcp magnesium crystal at 300K. Using the fine-tuned MACE_FT potential for all interatomic interactions, we computed the H–H, Mg–H, and Mg–Mg RDFs, each reproducing the key peaks and minima reported in experimental and first-principles studies.
Finally, from short NVE trajectories we extracted a diffusion coefficient $D \approx 10^{-9}\,\mathrm{m}^2/\mathrm{s},$, in agreement with the generic MACE_MP benchmark but two orders of magnitude larger than the MACE_FT value reported in [2].
This discrepancy highlights the critical importance of sufficiently long equilibration and extensive sampling for reliable dynamical properties.

Future work should pursue the following directions:

1. Para-hydrogen at cryogenic temperatures: incorporate nuclear-exchange effects into PIMD formalism to capture true quantum statistics below 25 K.
2. H in Mg at 300 K: extend equilibration and production runs, increase the number of beads, and improve sampling statistics to fully converge both the RDFs and the diffusion coefficient.

Bibliography

[1] M. D. Allendorf, V. Stavila, A. A. Talin, P. Grad, N. Campagnol, X. Yu, and D. A. Shultz. Challenges to developing materials for the transport and storage of hydrogen. *Nature Chemistry*, 14:1214–1223, 2022.

[2] A. Angeletti, L. Leoni, D. Massa, et al. Hydrogen diffusion in magnesium using machine learning potentials: a comparative study. *npj Computational Materials*, 11:85, 2025. doi: 10.1038/s41524-025-01555-z. URL `https://doi.org/10.1038/s41524-025-01555-z`. Received 20 July 2024; Accepted 13 February 2025; Published 31 March 2025.

[3] G. Bussi and M. Parrinello. Accurate sampling using langevin dynamics. *Physical Review E*, 75:056707, 2007. doi: 10.1103/PhysRevE.75.056707.

[4] G. Bussi and M. Parrinello. Accurate sampling using langevin dynamics. *Computer Physics Communications*, 179:26–29, 2008. doi: 10.1016/j.cpc.2008.01.001.

[5] M. Ceriotti, G. Bussi, and M. Parrinello. Nuclear quantum effects in solids using a colored-noise thermostat. *Physical Review Letters*, 103(030603):1–4, 2009. doi: 10.1103/PhysRevLett.103.030603. Also available as arXiv:0903.4551 [cond-mat.stat-mech].

[6] M. Ceriotti, M. Parrinello, T. E. Markland, and D. E. Manolopoulos. Efficient stochastic thermostatting of path integral molecular dynamics. *arXiv e-prints*, Sept. 2010. version 1, 6 Sep 2010.

[7] M. Ceriotti, G. Sutmann, J. Grotendorst, D. Gompper, and D. Marx. Modeling the quantum nature of atomic nuclei by imaginary time path integrals and colored noise. In *Computational Trends in Solvation and Transport in Liquids*, volume IAS Series; 28 of *Schriften des Forschungszentrums Jülich*, pages 1–24. Forschungszentrum Jülich, Jülich, Germany, 2015. ISBN 978-3-95806-030-2. EPFL COSMO unit; available at `https://infoscience.epfl.ch/handle/20.500.14299/112837`.

[8] M. Ceriotti, M. Parrinello, and G. Bussi. Colored-noise thermostats “à la carte”. *Axive*, Oct. 2018. Dated: October 31, 2018.

[9] J. H. Eggert, E. Karmon, R. J. Hemley, H.-k. Mao, and A. F. Goncharov. Pressure-enhanced ortho-para conversion in solid hydrogen up to 58 gpa. *Proceedings of the National Academy of Sciences*, 96, 1999. Contributed by Ho-kwang Mao, August 18, 1999.

[10] R. P. Feynman and A. R. Hibbs. *Quantum Mechanics and Path Integrals*. McGraw-Hill, New York, 1964.

[11] D. Frenkel and B. Smit. *Understanding Molecular Simulation: From Algorithms to Applications*. Academic Press, a division of Harcourt, Inc., 2002. ISBN 0-12-267351-4.

[12] C. W. Gardiner. *Handbook of Stochastic Methods for Physics, Chemistry and the Natural Sciences*. Springer, Berlin, 2 edition, 1985.

[13] C. W. Gardiner. *Handbook of Stochastic Methods*. Springer, Berlin, 3 edition, 2003.

[14] G. Gerhartz. Langevin and fokker–planck equation. Seminar, Theoretical Statistical Physics, Heidelberg University, Year unknown. Unpublished seminar notes.

[15] A. Gupta and M. Faisal. Magnesium based multi-metallic hybrids with soot for hydrogen storage. *International Journal of Hydrogen Energy*, 53:93–104, 2024.

[16] R. W. Hall and B. J. Berne. Nonergodicity in path integral molecular dynamics. *The Journal of Chemical Physics*, 81(8):3641–3643, Oct. 1984. doi: 10.1063/1.448112.

[17] P. Hänggi. Generalized langevin equations: A useful tool for the perplexed modeller of nonequilibrium fluctuations? Lecture Notes in Physics.

[18] M. F. Herman, E. J. Bruskin, and B. J. Berne. On path integral monte carlo simulations. *J. Chem. Phys.*, 76:5150–5155, 1982. doi: 10.1063/1.442815.

[19] W. G. Hoover. Canonical dynamics: Equilibrium phase-space distributions. *Physical Review A*, 31:1695–1697, 1985. doi: 10.1103/PhysRevA.31.1695.

[20] F. Legoll, M. Luskin, and R. Moeckel. Non-ergodicity of nosé–hoover dynamics. *Nonlinearity*, 22(7):1793–1815, 2009. doi: 10.1088/0951-7715/22/7/011. Also available as arXiv:0812.3320 [math.DS].

[21] T. Lindenau, M. L. Ristig, K. A. Gernoth, and J. Dawidowski. The physics of liquid para-hydrogen. *International Journal of Modern Physics B*, 20(30):5035–5046, Dec. 2006. doi: 10.1142/9789812772787_0007.

[22] G. J. Martyna, M. L. Klein, and M. E. Tuckerman. Nosé–hoover chains: The canonical ensemble via continuous dynamics. *The Journal of Chemical Physics*, 97, 1992. doi: 10.1063/1.463940.

[23] G. J. Martyna, M. E. Tuckerman, D. J. Tobias, and M. L. Klein. Explicit reversible integrators for extended system dynamics. *Molecular Physics*, 87(5):1117–1157, Apr. 1996. doi: 10.1080/00268979600100761.

[24] S. Nosé. A unified formulation of the constant temperature molecular dynamics methods. *The Journal of Chemical Physics*, 81(1):511–519, 1984. doi: 10.1063/1.447334.

[25] M. Parrinello and A. Rahman. Molecular dynamics of atomistic systems in the isothermal–isobaric ensemble. In M. H. Kalos, editor, *Monte Carlo Methods in Quantum Problems*, pages 105–120. Reidel, Dordrecht.

[26] M. Parrinello and A. Rahman. Study of an f center in molten kcl. *J. Chem. Phys.*, 80:860–867, 1984. doi: 10.1063/1.447334.

[27] L. S. Schulman. *Techniques and Applications of Path Integration*. Dover Publications, New York, 2005.

[28] I. F. Silvera and V. V. Goldman. The isotropic intermolecular potential for H_2 and D_2 in the solid and gas phases. *The Journal of Chemical Physics*, 69:4209–4213, 1978. doi: 10.1063/1.436889.

[29] H. F. Trotter. On the product of semi-groups of operators. *Proceedings of the American Mathematical Society*, 10:545–551, 1959.

[30] M. E. Tuckerman, B. J. Berne, and G. J. Martyna. Reversible multiple time scale molecular dynamics. *J. Chem. Phys.*, 97(3):1990–2001, 1992. doi: 10.1063/1.463137.

[31] R. Zwanzig. *Nonequilibrium Statistical Mechanics*. Oxford University Press, 1 edition, 2001.

[32] B. Øksendal. *Stochastic Differential Equations: An Introduction with Applications*. Springer, 6 edition, 2003. ISBN 978-3540047582.

A | Path integral molecular dynamics Appendix

A.1. Approximating the partition function with Trotter Splitting

We start with the definition of the partition function:

$$Z = \mathrm{Tr}\left[e^{-\beta\hat{H}}\right] = \int dq_1 \, \langle q_1 | e^{-\beta\hat{H}} | q_1 \rangle. \tag{A.1}$$

Next, we introduce the Trotter splitting. In this approach we write:

$$Z \approx \int dq_1 \, \langle q_1 | \left(e^{-\beta_P \hat{V}/2} \, e^{-\beta_P \hat{T}} \, e^{-\beta_P \hat{V}/2}\right)^P | q_1 \rangle, \tag{A.2}$$

where the factor β_P is defined as β/P.

By explicitly writing some of the factors and inserting the resolution of the identity, we obtain:

$$\begin{aligned} Z = & \int dq_1 \, \langle q_1 | \left(e^{-\beta_P \hat{V}/2} \, e^{-\beta_P \hat{T}} \, e^{-\beta_P \hat{V}/2}\right) \left(\int dq_2 \, |q_2\rangle\langle q_2|\right) \\ & \times \left(e^{-\beta_P \hat{V}/2} \, e^{-\beta_P \hat{T}} \, e^{-\beta_P \hat{V}/2}\right) \cdots \left(\int dq_P \, |q_P\rangle\langle q_P|\right) \left(e^{-\beta_P \hat{V}/2} \, e^{-\beta_P \hat{T}} \, e^{-\beta_P \hat{V}/2}\right) |q_1\rangle \\ = & \int dq_1 \, dq_2 \, \cdots \, dq_P \; \langle q_1 | \left(e^{-\beta_P \hat{V}/2} \, e^{-\beta_P \hat{T}} \, e^{-\beta_P \hat{V}/2}\right) |q_2\rangle \\ & \times \cdots \times \langle q_P | \left(e^{-\beta_P \hat{V}/2} \, e^{-\beta_P \hat{T}} \, e^{-\beta_P \hat{V}/2}\right) |q_1\rangle. \end{aligned} \tag{A.3}$$

Now, let us compute the action of the operator $e^{-\beta_P \hat{V}/2}$ on the eigenstate position $|q\rangle$:

$$e^{-\beta_P \hat{V}/2}|q\rangle = \sum_{n=0}^{\infty} \frac{\left(-\frac{\beta_P}{2}\right)^n}{n!} \hat{V}^n |q\rangle. \tag{A.4}$$

Since we have that

$$\hat{V}(q)|q\rangle = V(q)|q\rangle,$$

follows that

$$\hat{V}^n|q\rangle = V(q)^n|q\rangle.$$

Thus, we can write:

$$e^{-\beta_P \hat{V}/2}|q\rangle = e^{-\beta_P V(q)/2}|q\rangle, \tag{A.5}$$

which shows that the operator acts as a scalar multiplication. Moreover, since $\hat{V}$ is Hermitian, the same result holds for the bra:

$$\langle q|e^{-\beta_P \hat{V}/2} = e^{-\beta_P V(q)/2}\langle q|. \tag{A.6}$$

Therefore, the matrix element becomes:

$$\langle q_i|e^{-\beta_P \hat{V}/2}\, e^{-\beta_P \hat{T}}\, e^{-\beta_P \hat{V}/2}|q_j\rangle = e^{-\beta_P V(q_i)/2}\, \langle q_i|e^{-\beta_P \hat{T}}|q_j\rangle\, e^{-\beta_P V(q_j)/2}. \tag{A.7}$$

Thus, the overall integral in the partition function expression becomes

$$\int dq_1\, dq_2\, \cdots\, dq_P\; e^{-\beta_P V(q_1)/2}\langle q_1|e^{-\beta_P \hat{T}}|q_2\rangle\, e^{-\beta_P V(q_2)/2} \cdots e^{-\beta_P V(q_P)/2}\langle q_P|e^{-\beta_P \hat{T}}|q_1\rangle\, e^{-\beta_P V(q_1)/2}.$$

Since we have shown that

$$\langle q_i|e^{-\beta_P \hat{V}/2} = e^{-\beta_P V(q_i)/2}\langle q_i| \quad \text{and} \quad e^{-\beta_P \hat{V}/2}|q_j\rangle = e^{-\beta_P V(q_j)/2}|q_j\rangle,$$

each of the matrix elements can be written as

$$\langle q_i|e^{-\beta_P \hat{V}/2}\, e^{-\beta_P \hat{T}}\, e^{-\beta_P \hat{V}/2}|q_j\rangle = e^{-\beta_P V(q_i)/2}\, \langle q_i|e^{-\beta_P \hat{T}}|q_j\rangle\, e^{-\beta_P V(q_j)/2}.$$

Thus, by factoring out all these potential factors from each term, the partition function

becomes:

$$Z = \int dq_1\, dq_2 \cdots dq_P \; \exp\left[-\beta_P \sum_{i=1}^{P} V(q_i)\right] \prod_{i=1}^{P} \langle q_i | e^{-\beta_P \hat{T}} | q_{i+1} \rangle, \tag{A.8}$$

where the periodic boundary condition $q_{P+1} \equiv q_1$ is understood.

Following the theoretical procedure, one then analyzes the kinetic energy matrix elements and, in the continuum limit $P \to \infty$, obtains the path-integral formulation of the partition function.

A.2. Symmetrization of expectation value

Let's start the demonstration of the symmetrization by recalling the expression for the expected value of a generic operator $\hat{A}$:

$$\langle A \rangle = \mathrm{Tr} \left| \hat{A} e^{-\beta \hat{H}} \right| / \mathrm{Tr}\, e^{-\beta \hat{H}} \tag{A.9}$$

Let us now consider the following important property of the Trace of an operator. Given two whichever operators $\hat{X}$ and $\hat{Y}$ the following relation holds:

$$\mathrm{Tr}(\hat{X}\hat{Y}) = \mathrm{Tr}(\hat{Y}\hat{X}) \tag{A.10}$$

Then for a set of N generic operators $\hat{X}_1, \hat{X}_2, ..., \hat{X}_n$ we get:

$$\mathrm{Tr}\left(\hat{X}_1 \hat{X}_2 \ldots \hat{X}_n\right) = \mathrm{Tr}\left(\hat{X}_2 \ldots \hat{X}_n \hat{X}_1\right) = \cdots = \mathrm{Tr}\left(\hat{X}_n \hat{X}_1 \ldots \hat{X}_{n-1}\right) \tag{A.11}$$

Therefore when we consider the averaging of $\hat{A}$ using the Trotter splitting

$$\mathrm{Tr}\left[\hat{A}\left(e^{-\beta_P \hat{H}}\right)^P\right] \tag{A.12}$$

we can swap the order of $\hat{A}$ with whichever of the P terms $e^{-\beta_P \hat{H}}$ and still get the same value for the average.

Therefore we can write in total generality that:

$$\langle A \rangle = \mathrm{Tr}\left[\left(e^{-\epsilon \hat{H}}\right)^k A \left(e^{-\epsilon \hat{H}}\right)^{P-k}\right]$$

for k ranging from 0 to P.

Let's now consider the summation of the P identical terms:

$$\sum_{k=1}^{P} \mathrm{Tr}\left[\left(e^{-\hat{H}}\right)^{k-1} \hat{A}\left(e^{-\hat{H}}\right)^{P-(k-1)}\right] = P\,\mathrm{Tr}\left[\hat{A}\left(e^{-\beta_P \hat{H}}\right)^{P}\right]$$

If we now divide by P both sides, and divide as well by $\mathrm{Tr}\, e^{-\beta\hat{H}}$, we get:

$$\langle A\rangle = \frac{\mathrm{Tr}\left[\hat{A}\left(e^{-\beta_P \hat{H}}\right)^{P}\right]}{\mathrm{Tr}\left[e^{-\beta\hat{H}}\right]} = \frac{1}{P}\sum_{k=1}^{P} \frac{\mathrm{Tr}\left[\left(e^{-\beta_P \hat{H}}\right)^{k-1} \hat{A}\left(e^{-\beta_P \hat{H}}\right)^{P-(k-1)}\right]}{\mathrm{Tr}\left[e^{-\beta\hat{H}}\right]}$$

the numerator of the last term can be expanded by inserting the P-1 closure relations, as we did in the chapter, yielding to the form:

$$\begin{aligned} Num = \int dq_1 dq_2 \cdots dq_P A\left(q_k\right) e^{-\beta_P V(q_1)} e^{-\beta_P V(q_2)} \cdots e^{-\beta_P V(q_P)} \\ \times \left\langle q_1\right| e^{-\beta_P \hat{T}} \left|q_2\right\rangle \left\langle q_2\right| e^{-\beta_P \hat{T}} \left|q_3\right\rangle \cdots \left\langle q_P\right| e^{-\beta_P \hat{T}} \left|q_1\right\rangle . \end{aligned} \tag{A.13}$$

then we can bring the summation over k inside the integral with the coefficient and obtain the final form[1].

A.3. Diagonalising free ring polymer Hamiltonian

Let us consider one physical degree of freedom sampled with P beads, so that $Q = (q_1, \ldots, q_P)^\top$ and P-periodic boundary conditions imply $q_{P+1} \equiv q_1$. The free (spring) part of the ring–polymer Hamiltonian reads

$$\frac{m\omega_P^2}{2}\sum_{j=1}^{P}\left(q_j - q_{j+1}\right)^2 \;=\; \frac{m\omega_P^2}{2}\, Q^\top A Q,$$

[1] after having expressed the matricial elements as we have discussed in the relative chapter

with the circulant matrix

$$A \;=\; \begin{pmatrix} 2 & -1 & 0 & \cdots & 0 & -1 \\ -1 & 2 & -1 & \ddots & & 0 \\ 0 & -1 & 2 & \ddots & \ddots & \vdots \\ \vdots & \ddots & \ddots & \ddots & -1 & 0 \\ 0 & & \ddots & -1 & 2 & -1 \\ -1 & 0 & \cdots & 0 & -1 & 2 \end{pmatrix}_{P\times P} .$$

Because A is circulant and symmetric, it is diagonalised by the real discrete Fourier / cosine–sine matrix C:

$$C^{\top} A C \;=\; D = \operatorname{diag}\big(\lambda_0, \ldots, \lambda_{P-1}\big),$$

where the eigenvalues are

$$\lambda_k = 2\big[1 - \cos(2\pi k/P)\big] \;=\; 4\sin^2\!\big(\pi k/P\big), \qquad k = 0, \ldots, P-1$$

A convenient real orthogonal choice for C is (rows indexed by $i = 0, \ldots, P-1$; columns by k):

$$C_{ik} = \sqrt{\frac{2}{P}} \begin{cases} \frac{1}{\sqrt{2}}, & k = 0, \\ \cos\!\big(2\pi i k/P\big), & 1 \le k < P/2, \\ \frac{(-1)^i}{\sqrt{2}}, & k = P/2 \ (P \text{ even}), \\ \sin\!\big(2\pi i k/P\big), & P/2 < k < P. \end{cases}$$

Define the normal–mode (diagonal) variables

$$\tilde{Q} = (\tilde{q}_0, \ldots, \tilde{q}_{P-1})^{\top}, \qquad Q = C^{\top}\tilde{Q} \iff \tilde{Q} = CQ.$$

Substituting in the spring energy gives

$$\frac{m\omega_P^2}{2}\, Q^{\top} A Q = \frac{m\omega_P^2}{2}\, \tilde{Q}^{\top} D \tilde{Q} = \frac{m}{2} \sum_{k=0}^{P-1} \underbrace{\big[\omega_P^2 \lambda_k\big]}_{\omega_k^2} \tilde{q}_k^2 .$$

With $\lambda_k = 4\sin^2(\pi k/P)$ we define

$$\omega_k = 2\omega_P \sin\!\Big(\frac{\pi k}{P}\Big), \qquad k = 0, \ldots, P-1.$$

Hence, the spring (potential) energy is a sum of independent one–dimensional harmonic oscillators:

$$\frac{m\omega_P^2}{2}\sum_j (q_j - q_{j+1})^2 = \frac{m}{2}\sum_{k=0}^{P-1} \omega_k^2\, \tilde{q}_k^2.$$

Together with the kinetic term $\sum_j p_j^2/(2m) = \sum_k \tilde{p}_k^2/(2m)$, the full free ring–polymer Hamiltonian becomes

$$H_0 = \sum_{k=0}^{P-1}\left[\frac{\tilde{p}_k^2}{2m} + \frac{m\omega_k^2}{2}\,\tilde{q}_k^2\right],$$

demonstrating that each normal mode k is an uncoupled harmonic oscillator with frequency ω_k.

B | Langevin Thermostat Appendix

B.1. Ito's lemma and Fokker-Plank picture

First of all, let us cite the statement of Ito's lemma. Let f be a twice differentiable function of the process x and the time t. Where the process x is given by:

$$\mathrm{d}x = A(x,t)\mathrm{d}t + B(x,t)\mathrm{d}W_t \tag{B.1}$$

Then the differential of the function f is given by:

$$\mathrm{d}f = \left[\frac{\partial f}{\partial t} + A(x,t)\frac{\partial f}{\partial x} + \frac{B^2(x,t)}{2}\frac{\partial^2 f}{\partial x^2}\right]\mathrm{d}t + B(x,t)\frac{\partial f}{\partial x}\,\mathrm{d}W_t \tag{B.2}$$

We are not going to give a proof of this since it is widely documented on textbooks as [32], but for the sake of the record, it can be derived heuristically (as outlined in [14]) by applying Taylor expansion to the function f.

We are now going to show how the stochastic equation that defines the process x will lead to the corresponding Fokker-Plank equation.

Given the equation

$$\mathrm{d}x = A(x,t)\mathrm{d}t + B(x,t)\mathrm{d}W_t \tag{B.3}$$

and the function $f(x,t)$, by applying Ito's Lemma we get:

$$\mathrm{d}f = \left[\frac{\partial f}{\partial t} + A(x,t)\frac{\partial f}{\partial x} + \frac{B^2(x,t)}{2}\frac{\partial^2 f}{\partial x^2}\right]\mathrm{d}t + B(x,t)\frac{\partial f}{\partial x}\,\mathrm{d}W_t \tag{B.4}$$

Although improperly, this can be written in the form of differential equation to get a

better visualisation:

$$\frac{\mathrm{d}f}{\mathrm{d}t} = \left[\frac{\partial f}{\partial t} + A(x,t)\frac{\partial f}{\partial x} + \frac{B^2(x,t)}{2}\frac{\partial^2 f}{\partial x^2}\right] + B(x,t)\frac{\partial f}{\partial x}\frac{\mathrm{d}W_t}{\mathrm{d}t} \tag{B.5}$$

Let's now take the expectation value of the differential equation to get:

$$\frac{\mathrm{d}}{\mathrm{d}t}\langle f\rangle = \left\langle \frac{\mathrm{d}f}{\mathrm{d}t}\right\rangle = \underbrace{\left\langle \frac{\partial f}{\partial t}\right\rangle}_{=0} + \left\langle A(x,t)\frac{\partial f}{\partial x}\right\rangle + \left\langle \frac{B^2(x,t)}{2}\frac{\partial^2 f}{\partial x^2}\right\rangle \tag{B.6}$$

where we have set $\langle dW_t\rangle = 0$. If we write the expectation values explicitly using the pdf we get:

$$\int_{\mathbb{R}} \mathrm{d}x f(x)\partial_t p(x,t) = \int_{\mathbb{R}} \mathrm{d}x A(x,t)\frac{\partial f}{\partial x}p(x,t) + \int_{\mathbb{R}} \mathrm{d}x \frac{B^2(x,t)}{2}\frac{\partial^2 f}{\partial x^2}p(x,t) \tag{B.7}$$

By partially integrating this equation and using $p(x,t), \partial_x p(x,t), \partial_x^2 p(x,t) \to 0$ with $x \to \pm\infty$ we get:

$$\int_{\mathbb{R}} \mathrm{d}x f(x)\partial_t p(x,t) = \int_{\mathbb{R}} \mathrm{d}x f(x)\left[-\partial_x(A(x,t)p(x,t)) + \frac{1}{2}\partial_x^2\left(B^2(x,t)p(x,t)\right)\right] \tag{B.8}$$

Since $f(x)$ is arbitrary we can write:

$$\partial_t p(x,t) = -\partial_x(A(x,t)p(x,t)) + \frac{1}{2}\partial_x^2\left(B^2(x,t)p(x,t)\right) \tag{B.9}$$

which is the Fokker-Plank equation.

B.2. Closed and non-closed form solution

Closed form of $\mathrm{e}^{-\frac{\Delta t}{2}\hat{L}_\gamma}$ integrator

First of all let us show that the propagator $\mathrm{e}^{-\frac{\Delta t}{2}\hat{L}_\gamma}$ can be integrated analytically[1]. This factor appears in the formal solution to the following Fokker-Plank equation:

$$\frac{\partial P}{\partial t} = \hat{L}_\gamma P$$

[1] which means that the differential equations that involve this propagator in their formal solutions can be solved analytically

where P is the probability density we have introduced in the chapter of the relevant theory[2].

By knowing that

$$\hat{L}_\gamma = -\gamma\left(p\,\partial_p + \frac{m}{\beta}\,\partial_p^2\right).$$

The corresponding forward Fokker–Planck contribution for the momentum density $P(p,t)$[3] is[4]

$$\frac{\partial P}{\partial t} = -\frac{\partial}{\partial p}[\,(-\gamma p)\,P] + \gamma\frac{m}{\beta}\,\frac{\partial^2 P}{\partial p^2},$$

so the associated Itô stochastic differential equation is

$$\mathrm{d}p(t) = -\gamma\,p(t)\,\mathrm{d}t + \sqrt{\frac{2m\gamma}{\beta}}\,\mathrm{d}W(t), \tag{A}$$

with $W(t)$ a standard Wiener process. Equation (A) is called as Ornstein–Uhlenbeck equation.

To solve (A) over a finite step Δt we now introduce the integrating factor $\mathrm{e}^{\gamma t}$ and set $M(t) = \mathrm{e}^{\gamma t}p(t)$[5]. Then by writing its differential we get:

$$\mathrm{d}M(t) = \mathrm{e}^{\gamma t}\,\mathrm{d}p(t) + \gamma\,\mathrm{e}^{\gamma t}p(t)\,\mathrm{d}t$$

From these two previous relations we can now isolate $p(t)$ and $dp(t)$:

$$p(t) = M(t)\mathrm{e}^{-\gamma t}$$

$$dp(t) = dM(t)\mathrm{e}^{-\gamma t} + \gamma p(t)$$

[2]Throughout the theory chapter the symbol $P(p,q,t)$ denoted the full phase–space probability density, a function of both the position q and the momentum p. In the present discussion we suppress the explicit q-dependence and write $P(p,t)$ for the momentum marginal alone. This simplification is legitimate because the operator under consideration, $\hat{L}_\gamma$, acts exclusively on the momentum coordinate; it contains no derivatives with respect to q. Consequently the Fokker–Planck equation separates,

$$\frac{\partial}{\partial t}P(p,q,t) = \hat{L}_\gamma P(p,q,t) \quad\Longrightarrow\quad P(p,q,t) = \rho(q,t)\,P(p,t),$$

where $\rho(q,t)$ evolves independently through the remaining part of the Liouvillian, while the factor $P(p,t)$ obeys the one–dimensional momentum equation derived on the preceding page. The position factor $\rho(q,t)$ can therefore retain any shape without affecting the solution for the momentum distribution.

[3]here is where we rename the distribution and use P to refer to the moment distribution only

[4]We know this is the corresponding equation by just comparing the shapes of the Fokker-Plank equation presented here and the one in the theoreme shown in the theory on duality of the stochastic equations and Fokker-Plank picture correspondance.

[5]this is the standard procedure to integrate Ito stochastic equations of this type

By substituting them into the equation (A)[6] we get an equation in terms of the new variable M:

$$dM = \sqrt{\frac{2m\gamma}{\beta}}\, \mathrm{e}^{\gamma t}\, \mathrm{d}W(t).$$

Integrating from t to $t + \Delta t$ gives

$$M(t+\Delta t) - M(t) = \sqrt{\frac{2m\gamma}{\beta}} \int_t^{t+\Delta t} \mathrm{e}^{\gamma(s)}\, \mathrm{d}W(s)$$

by re-substituting the definition of M in terms of p and making some simplifications we get:

$$\mathrm{e}^{\gamma \Delta t} p_{t+\Delta t} - p_t = \sqrt{\frac{2m\gamma}{\beta}} \int_t^{t+\Delta t} \mathrm{e}^{\gamma(s-t)}\, \mathrm{d}W(s).$$

Defining $u = s - t$ and solving for $p_{t+\Delta t}$ yields

$$p_{t+\Delta t} = p_t\, \mathrm{e}^{-\gamma \Delta t} + \sqrt{\frac{2m\gamma}{\beta}}\, \mathrm{e}^{-\gamma \Delta t} \int_0^{\Delta t} \mathrm{e}^{\gamma u}\, \mathrm{d}W(u).$$

The stochastic integral

$$Z = \int_0^{\Delta t} \mathrm{e}^{\gamma u}\, \mathrm{d}W(u)$$

is Gaussian with mean 0 and variance[7]

$$\mathrm{Var}[Z] = \int_0^{\Delta t} \mathrm{e}^{2\gamma u}\, \mathrm{d}u = \frac{\mathrm{e}^{2\gamma \Delta t} - 1}{2\gamma}.$$

By applying the reparametrization trick[8], we can write $Z = \sqrt{\mathrm{Var}[Z]}\, \eta$ with $\eta \sim \mathcal{N}(0,1)$. Now, if we substitute this into the formula for the integration step of $p_{t+\Delta t}$ above, we get, after some simplifications, the explicit one–step map

$$p_{t+\Delta t} = p_t\, \mathrm{e}^{-\gamma \Delta t} + \sqrt{\frac{m}{\beta}\big(1 - \mathrm{e}^{-2\gamma \Delta t}\big)}\, \eta, \qquad \eta \sim \mathcal{N}(0,1).$$

This affine–Gaussian transformation is the exact action of the propagator $\mathrm{e}^{-\Delta t \hat{L}_\gamma}$ on the momentum. The position q is unaffected because $\hat{L}_\gamma$ contains no derivatives with respect

[6] after having substituted the first relation into the second to clear form the dependency of dp on p

[7] The whole integral is a gaussian since W is a Weiner process, which means that its increments (infinitesimal) are normally and independently distributed with 0 mean. Since the integral is a summation, summation of gaussian variables is a gaussian variable and in this case the resulting gaussian has still 0 mean

[8] in this case there is no mean therefore the reparametrization trick is just made of the std term

to q.

If the operator is integrating over half time step $\frac{\Delta t}{2}$, then the same formula applies but with time step halved.

Non-closed form of $e^{-\Delta t \hat{L}_{pq}}$ integrator

The operator

$$\hat{L}_{pq} = f(q)\,\partial_p + \frac{p}{m}\,\partial_q, \qquad f(q) = -\frac{\mathrm{d}U}{\mathrm{d}q},$$

generates the deterministic Hamiltonian flow associated with the one–dimensional Hamiltonian $H(q,p) = \frac{p^2}{2m} + U(q)$. In fact, if we look at its form, it is exactly the definition of the Liouvillian with the Hamiltonian written here before. In fact, if we apply this operator to q and p we exactly get the Hamilton's equations:

$$\dot{q}(t) = \frac{p(t)}{m}, \qquad \dot{p}(t) = f\big(q(t)\big).$$

Thus the propagator $\exp(-\Delta t\, \hat{L}_{pq})$ moves a point (q,p) to $(Q(\Delta t), P(\Delta t))$ obtained from the solution of

$$\ddot{Q}(t) = \frac{f\big(Q(t)\big)}{m}, \qquad P(t) = m\dot{Q}(t), \qquad Q(0) = q,\ P(0) = p.$$

A closed form for the propagator would require explicit formulas for $Q(\Delta t)$ and $P(\Delta t)$ that hold for an arbitrary potential $U(q)$. Of course not for all the potentials an analytical solution exists, as we know from Analytical Mechanics course, but it is useful to remind how this can be shown in two different ways of reasoning:

Exponential-series argument For any analytic G the series

$$e^{-\Delta t \hat{L}_{pq}} G = \sum_{n=0}^{\infty} \frac{(-\Delta t)^n}{n!}\, \hat{L}_{pq}^{\,n} G$$

terminates after finitely many terms only if $\hat{L}_{pq}^{\,n} G = 0$ for some n. Repeated application of $\hat{L}_{pq}$ gives

$$\hat{L}_{pq} q = \frac{p}{m}, \qquad \hat{L}_{pq}^{2} q = \frac{f(q)}{m}, \qquad \hat{L}_{pq}^{3} q = \frac{f'(q)p}{m^2}, \dots$$

The sequence closes, and the series truncates, only when $f(q)$ is linear, that is, when $U(q)$ is at most quadratic. For any nonlinear force the series is infinite and cannot be summed to an elementary expression.

Quadrature argument

Energy conservation $H\big(Q(t),P(t)\big)=H(q,p)=E$ implies

$$t=\int_{q}^{Q(t)}\frac{\mathrm{d}\xi}{\sqrt{\frac{2}{m}\big(E-U(\xi)\big)}}.$$

For generic U the integral on the right is an elliptic or higher transcendental function; for example, with the quartic potential $U(q)=\frac{1}{4}kq^4$ it becomes an incomplete elliptic integral. Such integrals cannot be written with elementary functions, so no universal closed-form map $(q,p)\mapsto(Q(\Delta t),P(\Delta t))$ exists.

Because the exact flow generated by $\hat{L}_{pq}$ lacks a universal analytic expression, the exponential $\exp(-\Delta t\,\hat{L}_{pq})$ can be written in closed form only for the special cases of free motion $\big(U=\text{const}\big)$ and the harmonic oscillator $\big(U=\frac{1}{2}kq^2\big)$. For a general potential, it must be approximated numerically, for instance with the velocity–Verlet splitting

$$\exp\Big(-\tfrac{\Delta t}{2}\hat{L}_p\Big)\exp\big(-\Delta t\,\hat{L}_q\big)\exp\Big(-\tfrac{\Delta t}{2}\hat{L}_p\Big).$$

Closed form of $\mathrm{e}^{-\Delta t\hat{L}_q}$ integrator

In this case, we proceed exactly in the same way we have done for the study case of L_γ. Since the definition of L_q is simply:

$$\hat{L_q}=\frac{p}{m}\frac{\partial}{\partial q}$$

this is going to act on the position space only. Again, by looking at the Fokker-Plank equation which this is linked to, we can find the corresponding differential equation for the position (which in this case will not be affected by any noise or friction term) which simply is[9]:

$$\dot{q}=\frac{p}{m}$$

which integrated for a time interval Δt gives:

$$q_{t+\Delta t}=q_t+\frac{p}{m}\Delta t$$

[9]as we would expect it is just the first of the two Hamilton's equations

Closed form of $e^{-\frac{\Delta t}{2}\hat{L}_p}$ integrator

Proceeding as shown before, since $\hat{L}_p = f(q)\frac{\partial}{\partial p}$, it acts only on the momentum space, and yields to the equation for the momentum:

$$\dot{p} = f(q)$$

which, again, is the second equation of Hamilton, since $f(q) = -\frac{\partial U}{\partial q} = -\frac{\partial H}{\partial q}$ where, with H refers to the non-modified Hamiltonian.

Then the integrated step looks like:

$$p_{t+\Delta t} = p_t + f(q)\Delta t$$

B.3. Friction step preserves the gaussian nature of p

Although we have already seen that the term $e^{-\frac{\Delta t}{2}\hat{L}_\gamma}$ preserves the Boltzmann distribution, it is useful to show that with the definition of c_2, that naturally arises from the application of the propagator, preserves the gaussian distribution of the momenta.

What we aim to show is that, if p_{old} is distributed as a gaussian with 0 mean and $\sigma = mk_BT$ (as expected if the system is in thermal equilibrium) then p_{new} is still distributed in the same way.

In order to do that, we write the expression of p_{new} in terms of p_{old} as we have seen in the theory:

$$p_{new} = c_1 p_{old} + c_2 R$$

where R is a random variable following the normal distribution $N(0, 1)$. Then, p_{new} is a sum of gaussian variables and therefore it is as well normally distirbuted.

If we take the expected value of p_{new} we get, from linearity of the expectation value operator:

$$E(p_{new}) = c_1 E(p_{old}) + c_2 E(R) = 0$$

and if we compute the variance we get:

$$Var(p_{new}) = c_1^2 Var(p_{old}) + c_2^2 Var(R) = c_1^2 \frac{m}{\beta} + c_2^2 = c_1^2 \frac{m}{\beta} + \frac{m}{\beta}(1 - c_1^2) = \frac{m}{\beta}$$

where we have used the definition of c_2.

Then as we wanted, p_{new} is distributed as p_{old}.

C | Modeling a Heat Bath Appendix

C.1. Green's Functions

As said in relative chapter, assuming $x(t)$ is known, let us find the expression of q_α which satisfies the following system:

$$\begin{cases} m_\alpha \dot{q}_\alpha \;=\; p_\alpha, \\ \dot{p}_\alpha \;=\; -\,m_\alpha\,\omega_\alpha^2\,q_\alpha \;+\; c_\alpha\,x(t), \end{cases} \tag{3}$$

we can combine the two equation to get a single differential equation for q_α as follows.

Since $\dot{p}_\alpha = m_\alpha \ddot{q}_\alpha$, the second equation becomes

$$m_\alpha\,\ddot{q}_\alpha \;=\; -\,m_\alpha\,\omega_\alpha^2\,q_\alpha \;+\; c_\alpha\,x(t). \tag{C.1}$$

Dividing through by m_α:

$$\ddot{q}_\alpha(t) + \omega_\alpha^2\,q_\alpha(t) \;=\; \frac{c_\alpha}{m_\alpha}\,x(t). \tag{C.2}$$

Hence, we have the standard inhomogeneous harmonic-oscillator equation:

$$\ddot{q}_\alpha(t) \;+\; \omega_\alpha^2\,q_\alpha(t) \;=\; \left(\tfrac{c_\alpha}{m_\alpha}\right)x(t). \tag{C.3}$$

Let us first solve the homogeneous equation by ignoring the forcing term $\frac{c_\alpha}{m_\alpha}\,x(t)$:

$$\ddot{q}_\alpha^{(h)}(t) + \omega_\alpha^2\,q_\alpha^{(h)}(t) \;=\; 0. \tag{C.4}$$

The general solution is by writing:

$$q_\alpha^{(h)}(t) \;=\; A\,\cos\!\big(\omega_\alpha t\big) \;+\; B\,\sin\!\big(\omega_\alpha t\big), \tag{C.5}$$

for constants A and B. However, we require initial conditions specified at $t = t_0$. A convenient way to incorporate those initial data is:

$$q_\alpha^{(h)}(t) \;=\; q_\alpha(t_0)\,\cos\big[\omega_\alpha\,(t-t_0)\big] \;+\; \frac{\dot q_\alpha(t_0)}{\omega_\alpha}\,\sin\big[\omega_\alpha\,(t-t_0)\big]. \tag{C.6}$$

Since $\dot q_\alpha(t_0) = \frac{p_\alpha(t_0)}{m_\alpha}$, we can write

$$q_\alpha^{(h)}(t) \;=\; q_\alpha(t_0)\,\cos\big[\omega_\alpha\,(t-t_0)\big] \;+\; \frac{p_\alpha(t_0)}{m_\alpha\,\omega_\alpha}\,\sin\big[\omega_\alpha\,(t-t_0)\big]. \tag{C.7}$$

We now look for a particular solution of the full non-homogeneous equation:

$$\ddot q_\alpha(t) + \omega_\alpha^2\,q_\alpha(t) \;=\; \frac{c_\alpha}{m_\alpha}\,x(t). \tag{C.8}$$

A standard way to solve this is by using the Green's function for the operator $\frac{d^2}{dt^2} + \omega_\alpha^2$. Concretely:

- The Green's function $G(t-s)$ satisfies

$$\Big[\tfrac{d^2}{dt^2} + \omega_\alpha^2\Big]\,G(t-s) \;=\; \delta(t-s), \tag{C.9}$$

  with $G(t-s) = 0$ for $t < s$.

- For the harmonic oscillator, one finds

$$G(t-s) \;=\; \theta(t-s)\,\frac{\sin\big[\omega_\alpha\,(t-s)\big]}{\omega_\alpha}, \tag{C.10}$$

  where $\theta(\cdot)$ is the Heaviside step function.

Thus the particular solution is

$$q_\alpha^{(p)}(t) \;=\; \int_{-\infty}^{+\infty} ds\;\; G(t-s)\,\big[\tfrac{c_\alpha}{m_\alpha}\,x(s)\big]. \tag{C.11}$$

If we assume the system is unforced before t_0, we typically take s from t_0 to t. Then

$$q_\alpha^{(p)}(t) \;=\; \int_{t_0}^{t} ds\;\frac{\sin\big[\omega_\alpha\,(t-s)\big]}{\omega_\alpha}\;\frac{c_\alpha}{m_\alpha}\,x(s). \tag{C.12}$$

We can pull out constants:

$$q_\alpha^{(p)}(t) \;=\; \frac{c_\alpha}{m_\alpha\,\omega_\alpha}\int_{t_0}^{t} ds\;\sin\big[\omega_\alpha\,(t-s)\big]\;x(s). \tag{C.13}$$

The general solution of the inhomogeneous equation is

$$q_\alpha(t) \;=\; q_\alpha^{(h)}(t) \;+\; q_\alpha^{(p)}(t). \tag{C.14}$$

Then, substituiting the two pieces:

$$q_\alpha^{(h)}(t) \;=\; q_\alpha(t_0)\,\cos\big[\omega_\alpha\,(t-t_0)\big] \;+\; \frac{p_\alpha(t_0)}{m_\alpha\,\omega_\alpha}\,\sin\big[\omega_\alpha\,(t-t_0)\big], \tag{C.15}$$

$$q_\alpha^{(p)}(t) \;=\; \frac{c_\alpha}{m_\alpha\,\omega_\alpha}\int_{t_0}^{t} ds\;\sin\big[\omega_\alpha\,(t-s)\big]\;x(s). \tag{C.16}$$

Hence,

$$q_\alpha(t) \;=\; q_\alpha(t_0)\,\cos\big[\omega_\alpha\,(t-t_0)\big] \;+\; \frac{p_\alpha(t_0)}{m_\alpha\,\omega_\alpha}\,\sin\big[\omega_\alpha\,(t-t_0)\big] \;+\; \frac{c_\alpha}{m_\alpha\,\omega_\alpha}\int_{t_0}^{t} ds\;\sin\big[\omega_\alpha\,(t-s)\big]\;x(s). \tag{4}$$

C.2. F is a colored gaussian fluctuating force

We now want to prove the gaussian nature of the stochastic force $F(t)$. Let's assume that at t_0, the bath is in equilibrium and therefore is distributed according to

$$\rho_B \;=\; \frac{1}{Z}\,\exp\Big[-\beta\sum_\alpha\Big(\tfrac{p_\alpha^2}{2\,m_\alpha}+\tfrac{1}{2}\,m_\alpha\,\omega_\alpha^2\,q_\alpha^2\Big)\Big]. \tag{C.17}$$

Since the bath Hamiltonian is quadratic[1] in all the $\{p_\alpha,\,q_\alpha\}$, the distribution factorizes into a product of exponentials for each α. In other words, each pair $\big(q_\alpha(t_0),\,p_\alpha(t_0)\big)$ is distributed independently with respect to all the other pairs and with a Gaussian form.

Concretely, for each α,

$$\rho_\alpha(q_\alpha,\,p_\alpha) \;\propto\; \exp\Big[-\beta\Big(\tfrac{p_\alpha^2}{2\,m_\alpha} \;+\; \tfrac{1}{2}\,m_\alpha\,\omega_\alpha^2\,q_\alpha^2\Big)\Big]. \tag{C.18}$$

[1] We are referring to the bath Hamiltonian without the coupling with the system

This is precisely the form of a 2D Gaussian distribution in the variables $\big(q_\alpha,\, p_\alpha\big)$. By standard properties of the canonical ensemble for a harmonic oscillator:

- The mean of each coordinate and momentum is zero:

$$\langle q_\alpha(t_0)\rangle_{\rho_B} \;=\; 0, \quad \langle p_\alpha(t_0)\rangle_{\rho_B} \;=\; 0. \tag{C.19}$$

- The variances are:

$$\langle q_\alpha^2(t_0)\rangle_{\rho_B} \;=\; \frac{k_B T}{m_\alpha\,\omega_\alpha^2}, \quad \langle p_\alpha^2(t_0)\rangle_{\rho_B} \;=\; m_\alpha\, k_B T. \tag{C.20}$$

- The cross-correlation between q_α and p_α is zero:

$$\langle q_\alpha(t_0)\, p_\alpha(t_0)\rangle_{\rho_B} \;=\; 0. \tag{C.21}$$

- For $\alpha \neq \beta$, the random variables $\big(q_\alpha,\, p_\alpha\big)$ and $\big(q_\beta,\, p_\beta\big)$ are independent.

Hence each α-oscillator's initial condition $\big(q_\alpha(t_0),\, p_\alpha(t_0)\big)$ is a zero-mean Gaussian in 2D phase space, independent of the other $\beta \neq \alpha$.

We now notice that $F(t)$ is linear combination of gaussian variables in the form:

$$F(t) \;=\; \sum_\alpha \Big[A_\alpha(t)\, q_\alpha(t_0) \;+\; B_\alpha(t)\, p_\alpha(t_0)\Big], \tag{C.22}$$

where

$$A_\alpha(t) \;=\; \cos\big(\omega_\alpha\,(t-t_0)\big), \quad B_\alpha(t) \;=\; \frac{1}{m_\alpha\,\omega_\alpha}\,\sin\big(\omega_\alpha\,(t-t_0)\big). \tag{C.23}$$

Because each $q_\alpha(t_0)$ and $p_\alpha(t_0)$ is Gaussian and $F(t)$ is a finite linear combination of these Gaussian random variables, $F(t)$ itself must be a Gaussian random variable, since a linear combination of normally distributed variables is still distributed as a Gaussian.

Moreover, since $F(t)$ is given by a summation of random variables, when the number of degrees of freedom of the bath tends to infinity, even if the initial conditions are not distributed according to the Boltzmann distribution, provided they are still all equally distributed with finite variance, then by the Central Limit Theorem, $F(t)$ is distributed as a Gaussian.

We now want to prove that $F(t)$ respects the Fluctuation Dissipation theorem of the

second kind (shown in the same section) when the system is in thermal equilibrium. We start by proving that the mean of $F(t)$ is vanishing, and then we proceed to calculate its autocorrelation function, and show how it is linked to the friction memory kernel.

From the definition,

$$F(t) \;=\; \sum_{\alpha}\Big[A_\alpha(t)\,q_\alpha(t_0) \;+\; B_\alpha(t)\,p_\alpha(t_0)\Big]. \tag{C.24}$$

Taking the ensemble average under ρ_B, we have

$$\langle F(t)\rangle_{\rho_B} \;=\; \sum_{\alpha}\Big[A_\alpha(t)\,\langle q_\alpha(t_0)\rangle_{\rho_B} \;+\; B_\alpha(t)\,\langle p_\alpha(t_0)\rangle_{\rho_B}\Big]. \tag{C.25}$$

But as noted above, $\langle q_\alpha(t_0)\rangle_{\rho_B} = 0$ and $\langle p_\alpha(t_0)\rangle_{\rho_B} = 0$. Hence, each term in the sum vanishes, giving

$$\boxed{\langle F(t)\rangle_{\rho_B} \;=\; 0.} \tag{C.26}$$

We now compute the Correlation Function $\langle F(t)\,F(s)\rangle_{\rho_B}$:

$$\langle F(t)\,F(s)\rangle_{\rho_B} \;=\; \Big\langle\Big[\sum_{\alpha}\big(A_\alpha(t)\,q_\alpha + B_\alpha(t)\,p_\alpha\big)\Big]\Big[\sum_{\beta}\big(A_\beta(s)\,q_\beta + B_\beta(s)\,p_\beta\big)\Big]\Big\rangle_{\rho_B}, \tag{C.27}$$

where we abbreviate $q_\alpha(t_0) \to q_\alpha$ and $p_\alpha(t_0) \to p_\alpha$ for clarity. Expanding the product:

$$\langle F(t)\,F(s)\rangle_{\rho_B} \;=\; \sum_{\alpha,\beta}\Big\langle\big(A_\alpha(t)\,q_\alpha + B_\alpha(t)\,p_\alpha\big)\,\big(A_\beta(s)\,q_\beta + B_\beta(s)\,p_\beta\big)\Big\rangle_{\rho_B}. \tag{C.28}$$

Distributing the terms of the products:

$$\begin{aligned}= \sum_{\alpha,\beta}\Big[&A_\alpha(t)\,A_\beta(s)\,\langle q_\alpha\,q_\beta\rangle_{\rho_B} + A_\alpha(t)\,B_\beta(s)\,\langle q_\alpha\,p_\beta\rangle_{\rho_B}\\ &+ B_\alpha(t)\,A_\beta(s)\,\langle p_\alpha\,q_\beta\rangle_{\rho_B} + B_\alpha(t)\,B_\beta(s)\,\langle p_\alpha\,p_\beta\rangle_{\rho_B}\Big].\end{aligned} \tag{C.29}$$

Because $\{q_\alpha,\, p_\alpha\}$ if $\alpha \neq \beta$, we have

$$\langle q_\alpha\,q_\beta\rangle_{\rho_B} \;=\; 0, \quad \langle p_\alpha\,p_\beta\rangle_{\rho_B} \;=\; 0, \quad \langle q_\alpha\,p_\beta\rangle_{\rho_B} \;=\; 0. \tag{C.30}$$

Hence, only terms with $\alpha = \beta$ survive. Thus, the sum over β collapses to $\beta = \alpha$. We then get:

$$\langle F(t)\,F(s)\rangle_{\rho_B} \;=\; \sum_{\alpha}\Big[A_\alpha(t)\,A_\alpha(s)\,\langle q_\alpha^2\rangle_{\rho_B} \;+\; B_\alpha(t)\,B_\alpha(s)\,\langle p_\alpha^2\rangle_{\rho_B}\Big]. \tag{C.31}$$

where we have considered $\langle q_\alpha\,p_\alpha\rangle_{\rho_B} \;=\; 0$, since q and p are independent with resect to one another (even if they are about the same particle), and their single mean is null.

Also by recalling:

$$\langle q_\alpha^2\rangle_{\rho_B} \;=\; \frac{k_B T}{m_\alpha\,\omega_\alpha^2}, \quad \langle p_\alpha^2\rangle_{\rho_B} \;=\; m_\alpha\,k_B T, \quad \langle q_\alpha\,p_\alpha\rangle_{\rho_B} \;=\; 0. \tag{C.32}$$

and substituting the known variances, one gets:

$$=\; \sum_{\alpha}\Big[A_\alpha(t)\,A_\alpha(s)\,\frac{k_B T}{m_\alpha\,\omega_\alpha^2} \;+\; B_\alpha(t)\,B_\alpha(s)\,\big(m_\alpha\,k_B T\big)\Big]. \tag{C.33}$$

Furthermore, by recalling

$$A_\alpha(t) \;=\; \cos\big(\omega_\alpha\,(t-t_0)\big), \qquad B_\alpha(t) \;=\; \frac{1}{m_\alpha\,\omega_\alpha}\sin\big(\omega_\alpha\,(t-t_0)\big), \tag{C.34}$$

we have

$$A_\alpha(t)\,A_\alpha(s) = \;\cos\big(\omega_\alpha(t-t_0)\big)\;\cos\big(\omega_\alpha(s-t_0)\big), \tag{C.35}$$

$$B_\alpha(t)\,B_\alpha(s)\,m_\alpha = \;\frac{1}{m_\alpha\,\omega_\alpha^2}\;\sin\big(\omega_\alpha(t-t_0)\big)\;\sin\big(\omega_\alpha(s-t_0)\big). \tag{C.36}$$

Putting it all together:

$$\begin{aligned}\langle F(t)\,F(s)\rangle_{\rho_B} = k_B T\sum_{\alpha}\frac{1}{m_\alpha\,\omega_\alpha^2}\Big[&\cos\big(\omega_\alpha(t-t_0)\big)\;\cos\big(\omega_\alpha(s-t_0)\big)\\ &+\;\sin\big(\omega_\alpha(t-t_0)\big)\;\sin\big(\omega_\alpha(s-t_0)\big)\Big].\end{aligned} \tag{C.37}$$

Using the trigonometric identity $\cos x\,\cos y + \sin x\,\sin y = \cos(x-y)$, we get

$$\langle F(t)\,F(s)\rangle_{\rho_B} \;=\; k_B T\sum_{\alpha}\frac{1}{m_\alpha\,\omega_\alpha^2}\cos\big(\omega_\alpha\,\big[(t-t_0)-(s-t_0)\big]\big) \;=\; k_B T\sum_{\alpha}\frac{1}{m_\alpha\,\omega_\alpha^2}\cos\big(\omega_\alpha(t-s)\big). \tag{C.38}$$

We see that $\langle F(t)\,F(s)\rangle_{\rho_B}$ depends only on the time difference $t-s$ (which is typical for

stationary processes). If we now recall the expression of the friction memory kernel:

$$\gamma(t-s) \;:=\; \sum_{\alpha} \frac{1}{m_\alpha\,\omega_\alpha^2}\cos\big(\omega_\alpha\,(t-s)\big), \tag{C.39}$$

and if we call M some effective mass (or simply keep it as a factor, depending on conventions for the generalized Langevin equation), then we can write

$$\boxed{\langle F(t)\,F(s)\rangle_{\rho_B} \;=\; M\,k_B T\,\gamma(t-s).} \tag{C.40}$$

D | Markovian and non Markovian dyanmics Appendix

D.1. Markovian example calculations

Let's consider the equations of motion of the system exposed in the theory.

$$\begin{cases} \dfrac{dx}{dt} = \dfrac{p}{m}, \\ \dfrac{dp}{dt} = -m\,\omega_0^2\,x - \xi\,p + F(t), \end{cases} \tag{D.1}$$

For completeness, we consider the following boundary condition $p(-\infty) = 0$.

Let's consider the second equation:

$$\frac{dp}{dt} = -m\,\omega_0^2\,x(t) - \xi\,p(t) + F(t), \tag{D.2}$$

we rearrange it to the standard form

$$\frac{dp}{dt} + \xi\,p(t) = -m\,\omega_0^2\,x(t) + F(t). \tag{D.3}$$

Define the right-hand side as

$$\Phi(t) := -m\,\omega_0^2\,x(t) + F(t). \tag{D.4}$$

Hence the ODE becomes

$$\frac{dp}{dt} + \xi\,p(t) = \Phi(t). \tag{D.5}$$

We now consider the function $e^{\xi t}$. Multiply the entire ODE by $e^{\xi t}$[1]:

$$e^{\xi t}\,\frac{dp}{dt} \;+\; \xi\, e^{\xi t}\, p(t) \;=\; e^{\xi t}\,\Phi(t). \tag{D.6}$$

Notice that the left-hand side is precisely the time derivative of $e^{\xi t}\, p(t)$. Hence, our equation becomes

$$\frac{d}{dt}\big[e^{\xi t}\, p(t)\big] \;=\; e^{\xi t}\,\Phi(t). \tag{D.7}$$

Integrate both sides with respect to t from $-\infty$ up to t:

$$\big[e^{\xi t}\, p(t)\big] \;-\; \lim_{u\to-\infty}\big[e^{\xi u}\, p(u)\big] \;=\; \int_{-\infty}^{t} ds\,\big[e^{\xi s}\,\Phi(s)\big]. \tag{D.8}$$

We are told $p(-\infty) = 0$ and for $\xi > 0$, $e^{\xi u} \to 0$ as $u \to -\infty$[2].

Hence the left-hand side becomes simply $e^{\xi t}\, p(t)$. Thus we get

$$e^{\xi t}\, p(t) \;=\; \int_{-\infty}^{t} ds\,\Big[e^{\xi s}\,\Phi(s)\Big]. \tag{D.9}$$

Then by rearranging:

$$p(t) \;=\; e^{-\xi t}\int_{-\infty}^{t} ds\, e^{\xi s}\,\Phi(s). \tag{D.10}$$

Recall $\Phi(s) = -\,m\,\omega_0^2\, x(s) + F(s)$. Thus

$$p(t) \;=\; e^{-\xi t}\int_{-\infty}^{t} ds\, e^{\xi s}\,\Big[-\,m\,\omega_0^2\, x(s) \;+\; F(s)\Big]. \tag{D.11}$$

It is often more convenient to factor out $e^{-\xi t}$ as $e^{-\xi(t-s)}$. In other words,

$$p(t) \;=\; \int_{-\infty}^{t} ds\; e^{-\xi\,(t-s)}\Big[-\,m\,\omega_0^2\, x(s) \;+\; F(s)\Big]. \tag{D.12}$$

From the first equation we also have

$$\frac{dx}{dt} \;=\; \frac{p(t)}{m}. \tag{D.13}$$

[1] integrating factor method

[2] Note that requiring that p vanishes at $-\infty$ is not necessary, since the exponential term would cancel anyway given ξ is positive (friction coefficient)

Hence, by substituting the expression of $p(t)$:

$$\frac{dx}{dt} \;=\; \frac{1}{m}\int_{-\infty}^{t} ds\; e^{-\xi\,(t-s)}\Big[-\,m\,\omega_0^2\,x(s)\;+\;F(s)\Big]. \tag{D.14}$$

by splitting the integrals:

$$\frac{dx}{dt} \;=\; -\,\omega_0^2\int_{-\infty}^{t} ds\; e^{-\xi\,(t-s)}\,x(s)\;+\;\frac{1}{m}\int_{-\infty}^{t} ds\; e^{-\xi\,(t-s)}\,F(s). \tag{D.15}$$

If we define a memory kernel and an effective noise term as:

$$K(t-s) \;=\; \omega_0^2\,e^{-\xi\,(t-s)}, \quad F_{\text{eff}}(t) \;=\; \frac{1}{m}\int_{-\infty}^{t} ds\; e^{-\xi\,(t-s)}\,F(s).$$

then

$$\frac{dx}{dt} \;=\; -\int_{-\infty}^{t} ds\; K(t-s)\,x(s)\;+\;F_{\text{eff}}(t),$$

which is a generalized Langevin-type equation with memory.

D.2. Continuous Superposition of Exponentials

In the case where the kernel is represented by a continuous superposition,

$$K(t) = \int d\alpha\, c(\alpha)\, e^{-\lambda(\alpha)\,t}, \tag{D.16}$$

one can define a family of auxiliary variables

$$y(\alpha,t) := \int_0^t e^{-\lambda(\alpha)\,(t-s)}\,x(s)\,ds, \tag{D.17}$$

so that the memory integral becomes

$$\int_0^t K(t-s)\,x(s)\,ds = \int d\alpha\, c(\alpha)\,y(\alpha,t). \tag{D.18}$$

Differentiation as before yields

$$\frac{\partial}{\partial t}y(\alpha,t) = -\lambda(\alpha)\,y(\alpha,t) + x(t), \quad y(\alpha,0)=0. \tag{D.19}$$

Thus the original non-Markovian equation can be recast as an extended Markovian system in the infinite-dimensional state space spanned by $x(t)$ and $y(\alpha,t)$.

Acknowledgements

This thesis marks the culmination of one journey, and the beginning of another.

I would like to express my deepest gratitude to all who have accompanied me along the way, to those whose unwavering patience, kindness, and encouragement sustained me through both the most challenging days and the moments of greatest joy—no names need be listed here; those who know, know. I would say so much more, but my thoughts would not fit on this page.

This work is dedicated to us and to the bright future that lies ahead.